Fossil Record 25 (1) 2022, 99–145 | DOI 10.3897/fr.25.83781

PENSOFT

MUSEUM FÜR NATURKUNDE BERLIN

Amphibian and reptilian fauna from the early Miocene of Echzell, Germany

Davit Vasilyan[1,2], Andrej Čerňanský[3], Zbigniew Szyndlar[4], Thomas Mörs[5,6]

1 *JURASSICA Museum, Route de Fontenais 21. 2900 Porrentruy, Switzerland*
2 *Department of Geosciences, University of Fribourg, Chemin du musée 6, 1700, Fribourg, Switzerland*
3 *Department of Ecology, Laboratory of Evolutionary Biology, Faculty of Natural Sciences, Comenius University in Bratislava, Mlynská dolina, Ilkovičova 6, 842 15 Bratislava, Slovakia*
4 *Institute of Systematics and Evolution of Animals, Polish Academy of Sciences, Slawkowska 17, 31-016 Kraków, Poland*
5 *Department of Palaeobiology, Swedish Museum of Natural History, P.O. Box 50007, 104 05 Stockholm, Sweden*
6 *Bolin Centre for Climate Research, Stockholm University, Stockholm, Sweden*

http://zoobank.org/7A16698D-4F18-48D2-9D96-51A6E0CC15AC

Corresponding author: Davit Vasilyan (davit.vasilyan@jurassica.ch)

Academic editor: Florian Witzmann ♦ **Received** 13 October 2021 ♦ **Accepted** 3 May 2022 ♦ **Published** 10 May 2022

Abstract

The present study describes a rich amphibian and reptilian assemblage from the early Miocene locality Echzell, Germany. It consists of one allocaudate, five salamander, five frog, one gecko, chamaeleonids, anguine lizards, one lacertid, one skink and five snake taxa. The entire herpetofauna of Echzell is represented by genera and/or families very broadly known from the early Miocene of Europe. Contrary to other early Miocene herpetofaunas, the Echzell assemblage includes surprisingly only one form of crocodile-newts (*Chelotriton*). The Echzell *Palaeobatrachus robustus* represents the youngest record of the species and extends its stratigraphic range to the late early Miocene. Regarding chameleons, the frontal is partly preserved, but represents the first described frontal of the extinct species *Chamaeleo andrusovi*. The only anguine lizard that can be identified in the assemblage is represented by a new genus and species *Smithosaurus echzellensis*. Our phylogenetic analyses consistently recovered it as the sister taxon to either [*Ophisauriscus quadrupes* + *Ophisaurus holeci*] + [*Anguis* + *Ophisaurus*] (in the first analysis) or [*Anguis* + *Ophisaurus*] (in the second analysis). However, the results are based on limited fossil material – the parietal – and the support for the clade is very low. Thus, the interpretation of the *Smithosaurus* relationship among anguines needs to be taken with caution and has to be tested in further studies. Among snakes, *Natrix longivertebrata* represents the oldest record of the species and extends the stratigraphic range of this fossil snake back to the early Miocene. In addition, we provide here a broader comparison of the Echzell amphibian and reptilian assemblage with their European records for the MN3 and MN4 biostratigraphical units. Besides that, the entire herpetofauna of Echzell includes very broadly known early Miocene European forms. Remains of other groups of the same period such as Bufonidae, Hylidae, Pelodytidae, Amphisbaenia, Varanidae, Cordylidae, *Pseudopus*, are not found in the material available to us. We also conclude that the amphibian and reptilian fossil record across MN3–MN4 is significantly biased by taphonomic and/or environmental conditions. The amphibian and reptilian assemblage of Echzell is rich in forms living in humid and warm environments with forested areas, permanent water bodies and also some open habitats. The following climatic parameters can be reconstructed based on the herpetofauna: a mean annual temperature of 17.4–28.8 °C, minimal warm month temperature 18–28.3 °C, minimal cold month temperature 8–22.2 °C, and mean annual precipitation with a value of 791±254 mm.

Key Words

early Miocene, frogs, Germany, lizards, salamanders, snakes

Introduction

The early Miocene of the European continent is characterised by a number of faunistic changes, which in turn are caused by palaeogeographic and climatic reorganisations (Rössner and Heissig 1999; Steinthorsdottir et al. 2021). While the mammalian record is better studied, the fossil record of other tetrapod groups, such as amphibians, reptiles and birds, has received less attention. During recent years, research focussed on the early Miocene herpetofauna has been intensified and a number of studies documented so far poorly known fossil records of amphibians and reptiles (Ivanov 2008; Čerňanský et al. 2015; Čerňanský 2016; Villa et al. 2021). A better understanding of the faunistic evolution of those groups through time can be provided, taking into account the known fossil record. In the present study, we aim to describe amphibian and reptilian fossil material from the Echzell locality, which is so far known for its mammalian fauna (Fig. 1, see references below). Further, we aim also to provide a faunistic comparison of the studied groups across the MN3–MN4 zones.

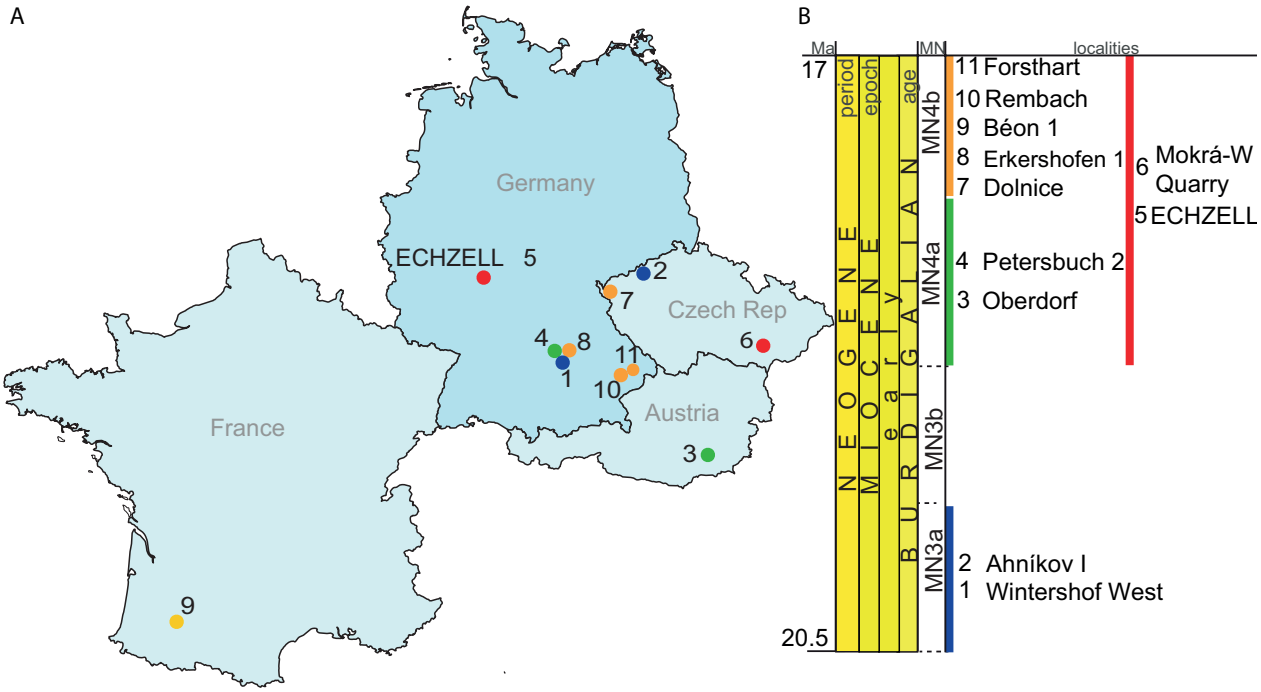

Figure 1. A. Partial map of Europe indicating Burdigalian (MN3–MN4) localities with well-represented amphibian and reptilian faunas including the Echzell locality. The colour of the circles indicating the localities corresponds to the vertical balks in (**B**); **B.** Temporal and biochronologic assignments of the fossil localities, the vertical balks in different colour correspond to MN (sub) zones (e.g. the localities Echzell and Mokrá-W Quarry belong to the MN4 zone where the former is located biochronologically older than the latter withing the same MN4 zone).

Echzell locality and biostratigraphic setting

Echzell is located approximately 30 km NNE of Frankfurt am Main at the eastern edge of the Horloff Graben, which cuts into the southwestern part of the basaltic Vogelsberg volcanic complex. The Vogelsberg was active during the entire Miocene and covered an area of 2,500 km^2. Some diatomitic maar lake deposits and reworked basaltic ashes produced Miocene vertebrate remains (for references, see Mörs 2010), but the disintegrated volcanic tuffs of the Echzell locality are most fossiliferous (Tobien 1954, 1982; Pineker and Mörs 2011; Mörs and Flink 2018; Jovells Vaqué and Mörs 2022). The Echzell fauna is dominated by small mammals (Table 1). Additionally, Tobien (1954, 1982) reported among large mammals *Gomphotherium angustidens*, *Bunolistriodon*, small ruminants, a rhinocerotid and a large amphicyonid.

Tobien (1954, 1982) also mentioned shell plates of testudinid tortoises, osteoderms of the anguine *Ophisaurus*, and metapodials of anurans. Unfortunately, the turtle material is missing, but we can add here a single tooth fragment of the alligator *Diplocynodon* and bone fragments of passeriform songbirds. Echzell represents an early Miocene, more specific a middle Orleanian fauna that can be correlated with the Mammalian Neogene unit MN4. The biostratigraphic setting is framed by taxa that have in Central Europe their last appearance datum (LAD) or first appearance datum (FAD) in MN4: *Pseudotheridomys parvulus* (LAD), *Ligerimys florancei* (LAD), *Democricetodon franconicus* (FAD), *Eumyarion weinfurteri* (FAD), *Melissiodon dominans* (LAD), *Neocometes similis* (FAD). *Anomalomys minor* (FAD) and *Gomphotherium angustidens* (FAD). Additionally, the evolutionary stage of *N. similis* is

Table 1. The Miocene small mammal fauna of Echzell.

MARSUPIALIA
Herpetotheriidae: *Amphiperatherium frequens*
LIPOTYPHLA
Erinaceidae: *Galerix* sp.
Talpidae: *Proscapanus* sp., *Mygalea antiqua*
Dimylidae: *Plesiodimylus hürzeleri*, *Chainodus intercedens*, *Lacrimodon vandermeuleni*, Dimylidae indet.
Soricidae: "*Sorex*" sp.
Heterosoricidae: *Dinosorex* sp., *Heterosorex neumeyrianus*
CHIROPTERA
Megadermatidae: *Megaderma franconica*
RODENTIA
Sciuridae: *Miopetaurist dehmi*, *Heteroxerus hürzeleri*, *Spermophilinus bredai*, *Palaeosciurus sutteri*
Gliridae: *Myoglis antecedens*, *Glirudinus undosus*, *G. gracilis*, *Glirulus diremptus*, *Peridyromys murinus*, *Bransatoglis cadeoti*, *Miodyromys aegercii*, *Microdyromys koenigswaldi*
Eomyidae: *Pseudotheridomys parvulus*, *Ligerimys florancei*, *Apeomys oldrichi*, *Megapeomys lindsayi*
Cricetidae: *Democricetodon franconicus*, *Eumyarion weinfurteri*, *Melissiodon dominans*
Platacanthomyidae: *Neocometes similis*
Anomalomyidae: *Anomalomys minor*
LAGOMORPHA
Ochotonidae: *Prolagus* sp.

very similar to the material from the MN4 locality Erkertshofen 2 (Fejfar 1999; Fejfar and Kalthoff 1999; Pineker and Mörs 2011; Steinthorsdottir et al. 2021), and the derived evolutionary stage of *Apeomys oldrichi* and *Megapeomys lindsayi* is very similar to material from the MN4 localities Dolnice 1 and Petersbuch 2 (Mörs and Flink 2018).

Material and methods

The vertebrate remains have been obtained from disintegrated volcanic tuffs by screen washing (Tobien 1954). Two fossiliferous layers, one at 2.20 m depth which yielded remains of both large and small mammals, and one at 11.0 m depth which produced the majority of the small mammals, were excavated by the Geological Department of the Hessisches Landesmuseum, Darmstadt, HLMD in September 1953 (Tobien 1954).

The fossil material has been photographed using a Hitachi S-4300 field emission scanning-electron microscope at the Swedish Museum of Natural History (Stockholm) and a Keyence VHX970 digital light microscope at the JURASSICA Museum (Porrentruy). Most photographs of fossil lizards from Echzell (except Gekkota and a parietal from Gratkorn) were taken using a Leica M205 C binocular microscope with an axially mounted DFC 290 HD camera at the Comenius University in Bratislava; software: LAS (Leica Application Suite) 4.1.0 (build 1264). For comparisons, the osteological collections of amphibians and reptiles at the JURASSICA Museum (MJSN), and specimens of extant species of chameleons deposited in the collections of the Department of Ecology, Comenius University in Bratislava, Faculty of Natural Sciences have been used.

The reconstruction of the climatic parameters follows the actualistic approach (Mörs et al. 2020). Temperature values have been reconstructed based on the climatic spaces of given reptilian taxa according to Haller-Probst (1997). The palaeoprecipitation value has been estimated using the herpetofaunistic assemblage of the locality according to Böhme et al. (2006). The ecophysiological indices for each taxon are given in Table 2. The present-day value of the nearest climatic station has been taken from Wetter und Klima – Deutscher Wetterdienst (www.dws.de). Standard anatomical orientation system is used throughout this paper, and terminology for describing individual bone structures is based on Rage and Augé (2010) and Čerňanský (2010, for acrodont lizards). For amphibians, terminology is directly indicated in the description.

This published work and the containing nomenclatural acts have been registered in ZooBank (www.zoobank.org) on https://doi.org/10.5194/fr-24-1-202 and under LSID number urn:lsid:zoobank.org:act:7A16698D-4F18-48D2-9D96-51A6E0CC15AC.

Phylogenetic analysis for the new anguine taxon

A morphological data matrix (see Suppl. material 1: Appendix S1) was developed and modified using characters taken primarily from Klembara et al. (2019). We added four characters of relevance for Anguimorpha (see Suppl. material 2: Appendix S2).

The matrix comprises 40 characters scored for 6 extant (*Ophisaurus harti*, *O. koellikerii*, *O. ventralis*, *Pseudopus apodus*, *Anguis fragilis*, *Xenosaurus grandis*) and 8 extinct (*Odaxosaurus piger*, *Ophisauriscus quadrupes*, *Ophisaurus holeci*, *Ophisaurus roqueprunensis*, *Pseudopus pannonicus*, *P. laurillardi*, *P. ahnikoviensis* and *Peltosaurus granulosus*) anguimorph taxa in addition to the new fossil anguine taxon described here. *Shinisaurus crocodilurus* was used as an outgroup taxon. The principal goal of this analysis is to understand the relationship of the new Miocene

Table 2. Overview of amphibian and reptilian faunas from MN3–MN4 sites. Each large taxonomic group is highlighted in different color. The herpetofaunistic record follows for: Wintershof West – Böhme and Ilg (2003); Ahníkov 1 (= Merkur North) – Čerňanský (2010a), Čerňanský and Bauer (2010), Čerňanský et al. (2015), Klembara et al. (2010), Villa and Delfino (2019a, b); Oberdorf – Čerňanský (2016), Čerňanský et al. (2020b), Sanchíz (1998), Szyndlar (1998), Villa and Delfino (2019a); Petersbuch 2 – Čerňanský (2011), Ivanov (2001), Klembara et al. (2010), Szyndlar and Schleich (1993), Szyndlar and Rage (2002), Szyndlar and Rage (2003), Villa and Delfino (2019a), Villa et al. (2018); Echzell – present study; Mokrá-W Q 1/2001 and Mokrá-W Q 2/ 2001 – Ivanov (2008), Ivanov et al. (2020); Dolnice – Böhme and Ilg (2003), Čerňanský (2010b), Fejfar and Roček (1986), Klembara (2015), Szyndlar (1987), Villa and Delfino (2019a); Erkertshofen 1 – Klembara et al. (2010); Beon 1 – Rage and Bailon (2005); Rembach – Klembara et al. (2010); Forsthart – Klembara et al. (2010). The ecophysiological indices for Echzell assemblage are given for each taxon as well as the calculated precipitation values and errors are calculated according to Böhme et al. (2006).

		taxon	Wintershof West	Ahníkov 1 (=Merkur North)	Oberdorf	Petersbuch 2	Echzell	Mokrá-W Q 1/2001	Mokrá-W Q 2/2001	Dolnice	Erkertshofen 1	Béon 1	Rembach	Forsthart
			MN3a	MN 3a	MN4	MN4a	MN4	MN4	MN4	MN 4b	MN 4b	MN 4b	MN 4b	MN 4b
Allocaudata	Albanerpetonidae	*Albanerpeton inexpectatum*	+	cf.	+	+	**0.0917**				+			
Urodela	Cryptobranchidae	*Andrias scheuchzeri*		+										
	Proteidae	*Mioproteus* sp.							+					
	Salamandridae	*Salamandrina* sp.				+								
		Chioglossa meini				+			+		+			
		Chioglossa sp.			+		**0.9768**							
		Mertensiella mera							+					
		Mertensiella sp.	+	+		+	**0.9768**		+					
		Salamandra sansaniensis	+		+	+					+			
		Salamandra sp.					**0.3918**							
		Chelotriton paradoxus	+			+								
		Chelotriton aff. *pliocaenicus*				+								
		Chelotriton sp.	+	+	+		**0.3918**				+	cf.		
		Chelotriton sp. 1						+	+					
		Chelotriton sp. 2						+	+					
		Triturus cf. *marmoratus*						+	+			+		
		Triturus ex. gr. *cristatus*							+					
		Triturus (*marmoratus* group) sp.				+								
		Lissotriton cf. *helveticus*				+						+		
		Lissotriton roehsi			+			+	+					
		Lissotriton aff. *roehsi*						+						
		Lissotriton sp.					**0.3918**							
		Triturus/Lissotriton sp.		+										
		Triturus aff. *vittatus*				+								
		Ichthyosaura alpestris												
		Ichthyosaura wintershofi	+											
Anura	Alytidae	*Latonia gigantea*								+				
		Latonia ragei	+	+	+	+								
		Latonia cf. *ragei*	+									+		
		Latonia sp.					**0.3918**							
	Palaeobatrachidae	*Palaeobatrachus robustus*					**1**							
		Palaeobatrachus sp.		+	+									
		Palaeobatrachidae sp. 1				+								
		Palaeobatrachidae sp. 2				+								
	Bufonidae	*Bufo* sp.							+					
		Bufotes (cf.) *viridis*				+					+			
	Ranidae	*Pelophylax* sync *esculenta*						+	+					
		Pelophylax sp.		+	+	+	**0.513**			+	+	+		
		Rana sp.	+				**0.3918**							+
	Pelodytidae	*Pelodytes* sp.	+	+	+						+			
	Pelobatidae	*Eopelobates* sp.	+	+						+				
		Pelobates sanchizi			+		**0.0917**	+	+					
		Pelobates sp.			+	+					+			+
		Pelobates sp. nov.				+								
	Hylidae	*Hyla* sp.			+					+				
Crocodylia		*Diplocynodon* sp.		+						+		+		
Testudines		*Ptychogaster* sp.	+			+				+	+	+		
		Ptychogaster buechelbergense		+						cf.				
		Testudo rectangularis												+
		Testudo sp.				+				+	+	+		+
		Geochelone/*Ergilemys* sp.				+						+		
		aff. *Clemmydopsis* sp.											+	
Serpentes	Colubridae	*Natrix longivertebrata*					+					cf.		
		Natrix merkurensis		+								aff.		

		taxon	Wintershof West	Ahníkov 1 (=Merkur North)	Oberdorf	Petersbuch 2	Echzell	Mokrá-W Q 1/2001	Mokrá-W Q 2/2001	Dolnice	Erkertshofen 1	Béon 1	Rembach	Forsthart
			MN3a	MN 3a	MN4	MN4a	MN4	MN4	MN4	MN 4b	MN 4b	MN 4b	MN 4b	MN 4b
Serpentes	Colubridae	*Natrix sansaniensis*		+		+						+		
		Natrix sp.						+	+					
		cf. *Neonatrix* sp.			+	+								
		Palaeonatrix lehmani				+				+		aff.		
		Neonatrix nova								+				
		Neonatrix europaea										+		
		Neonatrix natricoides										+		
		Palaeonatrix sp.			+									
		Natricinae indet.		+		+		+	+					
		Coluber caspioides		+	cf.	+								
		Coluber dolnicensis		+						+				
		Coluber pouchetii										+		
		Coluber suevicus		+										
		Coluber sp.						+	+					
		Texasophis meini										+		
		Texasophis bohemicus								+				
		Elaphe sp.		+										
		Colubrinae indet.		+			+							
		Colubrinae indet. 1						+	+					
		Colubrinae indet.	+						+					
		Colubrinae indet. A			+									
		Colubrinae indet. B			+									
		Colubridae indet.		+				+	+					
		Colubroidea indet.					+							
	Viperidae	*Vipera antiqua*				+				+				
		Vipera platyspondyla				+				+				
		Vipera aspis complex										+		
		Daboia/oriental *Vipera* complex										+		
		Viper sp.		+	+				+					
		Viperidae indet.						+	+					
		Viperinae indet.						+	+					
	Elapidae	*Naja romani*				+								
		Naja cf. *romani*					+							
		Micrurus gallicus				+						+		
		Elapidae indet.		+				+				+		
		Elapidae/Natricinae indet.			+									
	Boidae	*Bavarioboa hermi*				+		+		+				
		Bavarioboa cf. *hermi*					0.0917	+						
		Bavarioboa sp.		+										
		cf. *Bavarioboa* sp.			+									
		Pyton europaeus										+		
		Pyton sp.						+						
		Falseryx petersbuchi				+								
		Bransateryx septentrionalis				+				+				
		Bransateryx sp.												
		Scolecophidia indet.										+		
	Aniliidae	*Eoanilus* sp.				+								
		Serpentes indet.	+	+										
Iguania	Chamaeleonidae	*Chamaeleo* sp.				+							+	
		Chamaeleo andrusovi					0.0917			+				
		Chamaeleo caroliquarti	+							+	+			
		Chamaeleonidae indet.		+	?	+	+							
Gekkota	Gekkonidae	*Euleptes gallica*		+										
		Gekkota indet.	+	+	+		0.0917					+	+	
Amphisbaenia	Blanidae	*Blanus* sp.								+			+	
		Blanus thomaskelleri		+										
	Amphisbaenidae	Amphisbaenidae indet.									+	+		
		Amphisbaenia indet.							+					
Lacertiformata	Lacertidae	*Lacerta* cf. *L. poncenatensis*			+									
		Lacerta ex. gr. *L. viridis*								+				
		Lacerta sp.		+	+	+				+	+		+	
		Lacerta sp. 1	+											+
		Lacerta sp. 2	+											+
		Miolacerta tenuis								+				
		Miolacerta sp.				+							+	
		Janoskia sp.				+								
		Ambyolacerta dolnicensis								+				

		taxon	Wintershof West	Ahnikov 1 (=Merkur North)	Oberdorf	Petersbuch 2	Echzell	Mokrá-W Q 1/2001	Mokrá-W Q 2/2001	Dolnice	Erkertshofen 1	Béon 1	Rembach	Forsthart
			MN3a	MN 3a	MN4	MN4a	MN4	MN4	MN4	MN 4b	MN 4b	MN 4b	MN 4b	MN 4b
Lacertiformata	Lacertidae	*Ambyolacerta* sp.									+			
		Lacertidae indet.		+	+		**0**	+	+	+		+		+
		Lacertidae indet. 1										+		
		Lacertidae indet. 2										+		
		Lacertoidea indet.							+					
Scinciformata	Scincidae	*Eumeces* sp.									+			
		Bavariascincus mabuyaformis				+							+	+
		Chalcides augei			+									
		cf. *Chalcides* sp.					**0**							
		Scincidae indet.				+	+			+	+			
	Cordylidae	*Palaeocodylus bohemicus*								+				
		aff. *Palaeocodylus bohemicus*		+										
		Cordylidae indet.		?	+	+								
		Scincoidea indet.			+				+					
Anguimorpha	Varanidae	*Varanus mokrensis*						+	+					
		Varanus hofmanni				+								
		Varanus sp.									+	+		
		cf. *Varanus* sp.				+								
	Shinisauridae	*Merkurosaurus ornatus*		+										
		Shinisauridae indet.	+											
	Anguidae	*Pseudopus laurillardi*				+		+	+		+	+		
		Pseudopus confertus		+										
		Pseudopus ahnikoviensis		+						+				
		Pseudopus sp.	+					+	+	+			+	+
		Smithosaurus echzellensis					+							
		Anguis sp.								+				
		Ophisaurus fejfari				+				+				
		Ophisaurus cf. *O. fejfari*	+											
		Ophisaurus spinari		+						+				
		Ophisaurus cf. *O. spinari*			+									
		Ophisaurus robustus								+				
		Ophisaurus aff. *O. robustus*									+			
		Ophisaurus holeci		+						+				
		Ophisaurus sp.		+	+	+		+		+		+		+
		Ophisaurus sp. 1		+						+			+	
		Ophisaurus sp. 2		+						+			+	
		Anguinae indet.					+	+	+					
		Anguidae indet.			+	+	+						+	
		Squamata indet.					+							
		Squamata indet. 1			+									
		Squamata indet. 2			+									
		Squamata indet. 3			+									
		average ecophysiological index					0.344							
		MAP					791							
		recent MAP (in mm)					630							
		95 % prediction interval - error (in mm)					254							
		(near) city/town of the value or recent MAP					Frankfurt a. M.							
		MAP/MAPrecent (in %)					125.5036157							

taxon described here among Anguinae. The data matrix was analysed using maximum parsimony as an optimality criterion in the program TNT and the NT (New Technology) search (with ratchet) and 1000 iterations (Goloboff et al. 2008). All characters were treated as unordered and were equally weighted. Support was estimated through Bremer support indices (Bremer 1994). Mesquite v.2.75 was used to visualize all trees (build 566; Maddison and Maddison, D. R. et al. 2011). In the second analysis, the heuristic traditional search in TNT was also used to observe and compare the potential results.

Systematic Paleontology

Lissamphibia Haeckel, 1866
Allocaudata Fox & Naylor, 1982
Albanerpetontidae Fox & Naylor, 1982
***Albanerpeton* Estes & Hoffstetter, 1976**

***Albanerpeton inexpectatum* Estes & Hoffstetter, 1976**
Fig. 2

Material and horizon. One frontal HLMD-Ez 2004, four praemaxillae HLMD-Ez 2005–2008, nine maxillae

HLMD-Ez 2009–2016, ten dentaries HLMD-Ez 2017–2027, one vertebra HLMD-Ez 2028.

Description. Frontal: Frontal is partly preserved. It is triangular in shape and as wide as long (Fig. 2A). The entire preserved dorsal surface of the bone is covered by moderately deep polygonal pits limited from each other by rather low ridges. The anterolateral processes are missing. The anteriorly-projecting internasal is rather narrow and elongated. In ventral view, its spike-like outline is more evident (Fig. 2B). Only the anteromedial slot is preserved. It is long, low and not deep. In ventral view, the ventrolateral crest is broad, concave and in transverse view, triangular in outline. It starts at the base of the preserved portion of the anterolateral process and projects posterolaterally, reaching the posterior lateral tips of the frontal. The crest becomes thinner laterally. The ventral surface of the frontal, between the posterolateral crests, is flat.

Praemaxilla: Available four praemaxillae show different preservation and are not fused. The medial surface of the bone, where two praemaxillae connect with each other, possesses grooves and flanges (Fig. 2G). The width of the bone, measured along the tooth row, ranges from 1–1.5 mm. The pars dorsalis is elongated and long. In lateral view, it is curved. The laterodorsal notch is weakly developed. The pars dorsalis at its middle part extends slightly laterally, which in large-sized bones is stronger developed than in the small-sized ones. The labial surface of the bone is covered by different structures (Fig. 2C, F). The ventral portion, corresponding to the pars dentalis, is nearly smooth. The middle part of the surface, making the most of the pars dorsalis, is pierced by nutrition foramina. The tip of the pars dorsalis possesses the boss. Pustular structures and polygonal-shaped pits cover it. In labial view, the maxillary process of praemaxilla projects laterally behind the pars dorsalis. In lingual view, the well-developed suprapalatal pit at the medial base of the pars dorsalis is present (Fig. 2D, H). It has an elongate outline and reopens ventrally as a palatal foramen in the ventral surface of the pars palatinum. In medial view, the pars palatinum is curved. Distinct vomerine and maxillary processes are visible on the pars palatinum. The maxillary process is stronger developed than the vomerine one. Six to seven pleurodont teeth are attached to the pars dentalis.

Maxilla: In total, eight maxillae with different preservation are available. The pars dentalis in most well-preserved specimens possesses 13–14 teeth or tooth bases. In lingual view, the pars dentalis is high anteriorly and reduces in height posteriorly (Fig. 2J, M, P). The pars palatinum is well-developed and curved. In the middle part of the bone, it reaches its most width. The anterior tip of the pars palatinum extends anteromedially and forms a distinct process (Fig. 2J, P). The premaxillary process is well developed (Fig. 2M, P). The distinct nasal process projects anterodorsally (Fig. 2J, M). Both the dorsal and labial surfaces of the maxillae are pierced by short rows of up to three nutrition foramina, which are limited to the area around the nasal process (Fig. 2N, L, Q).

Dentary: All eleven dentaries are only partially preserved. No dentary with a fully preserved tooth row (pars dentalis) is available in the material to count the tooth number. The teeth reduce in height posteriorly. The Meckelian groove is closed and form a canal. The dental shelf is moderately broad, and its lingual margin is angular (Fig. 2R, V). The symphyseal articulation surfaces are flat and vertical. Lingually, it possesses two distinct prongs (Fig. 2R, S). The dorsal prong is long and oriented anterodorsally. The ventral one is smaller and anteroventrally oriented. The ventral prong and the main symphyseal surface are separated with a moderately deep depression, which is pierced by the anterior opening of the Meckelian groove. The latter opens posteriorly with two large ventral and small dorsal ("opening for an unnamed canal" sensu Szentesi et al. (2015); fig. 8) openings. Taking into account the "natural" cross-sections of the bones (Fig. 2U, X, Z), the split of the Meckelian canal into two branches already at the sixth tooth position can be stated. The small dorsal branch runs below the tooth row, whereas the large ventral one is enclosed in the ventral portion of the bone. The labial surface of the dentary is smooth. A row of labial foramina of different sizes is arranged along the midline of the dentary (Fig. 2T, W, Y).

Dentition: The teeth on premaxillae, maxillae. and dentary have similar morphology. All teeth are pleurodont and closely located. The tip of teeth is tricuspid with a main central large cuspid and two lateral small cuspids, which are sometimes nearly absent. The tooth pedicles are compressed anterodorsally. The tooth tip is round in cross-section. They reduce in size posteriorly.

Remarks. The fossil remains can be assigned to the genus *Albanerpeton* considering the presence of the following autapomorphies (Venczel and Gardner 2005): 1) dorsal/ventral outlines of fused frontals are triangular (Character state 21(1) in Venczel and Gardner (2005)); 2) ratio of midline length of fused frontals to the width across posterior edge of bone, between lateral edge of the ventrolateral crest, is as wide as long (1:1) (Character state 22(1) in Venczel and Gardner (2005)); 3) path followed by canal through pars palatinum in praemaxillae, between dorsal and ventral openings of palatal foramen, is vertical (Character 27(1) in Venczel and Gardner (2005)). Among the species of the genus, two apomorphies of *A. inexpectatum* are such as; 1) the pustular ornament pattern of labial surface of premaxillary (Character 8(1) in Venczel and Gardner (2005)) and 2) form of ventrolateral crest on large, fused frontals wide and triangular in transverse view, with strongly concave ventral surface (Character 24(2) in Venczel and Gardner (2005)). Further, two character states [16(1), 17(1)] of Venczel and Gardner (2005) cannot be observed due to poor preservation of the material. The Echzell remains can be clearly distinguished from the second available European Tertiary albanerpetontid species *Albanerpeton pannonicum* by: 1) lack of

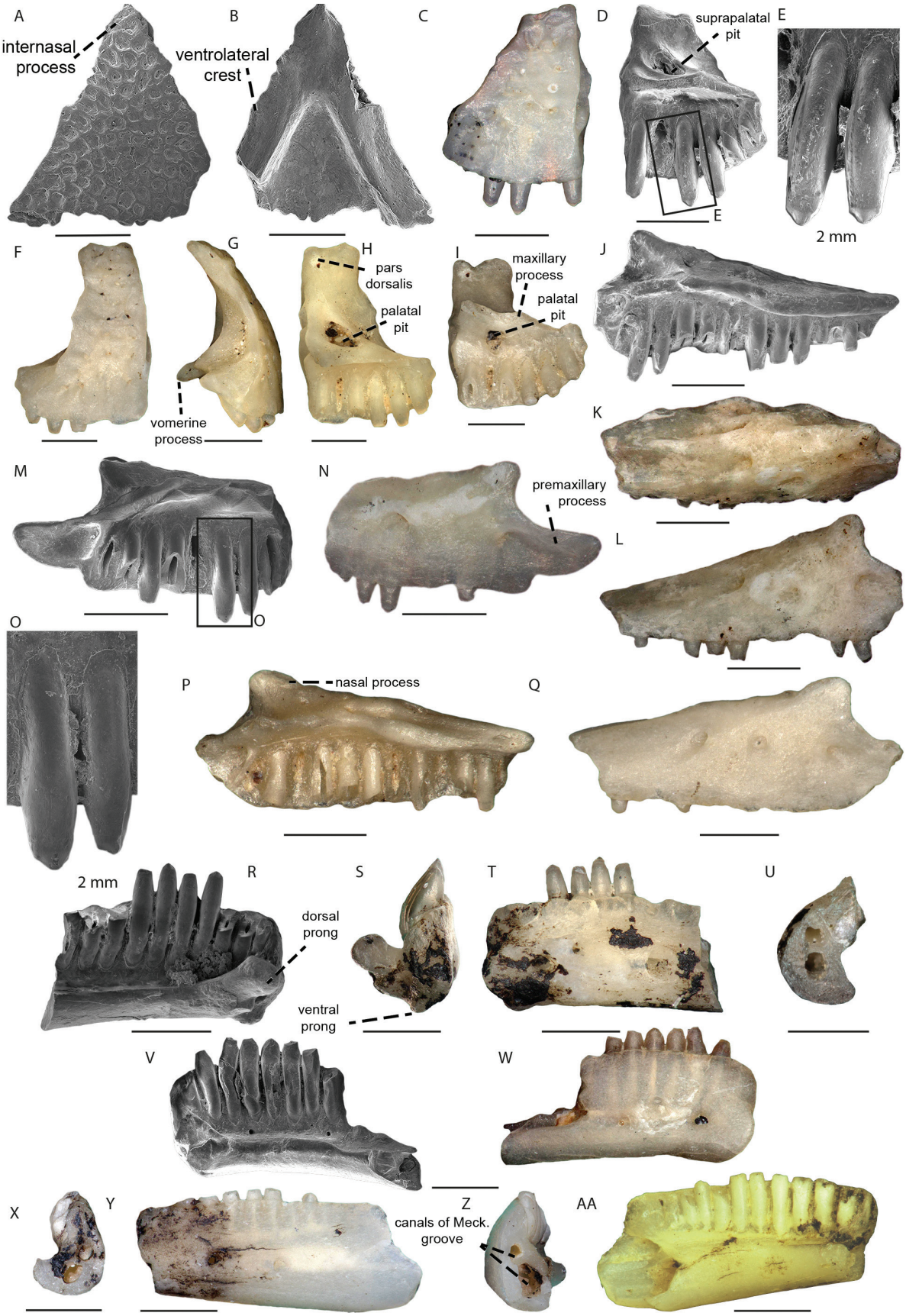

Figure 2. *Albanerpeton inexpectatum* from the Echzell locality. Frontal (**A, B.** HLMD-Ez 2004). Premaxillae (**C–E.** HLMD-Ez 2161; **F–I.** HLMD-Ez 2005). Maxillae (**J–L.** HLMD-Ez 2009; **M–O.** HLMD-Ez 2010; **P, Q.** HLMD-Ez 2012). The bones are figured in (**A, K**) dorsal, (**B**) ventral, (**C, F, L, N, Q, T, W, Y**) labial, (**D, E, H, J, M, O, P, R, V, AA**) lingual, (**I**) ventroposterior, (**S, X**) medial, (**G, U, Z**) posterior views. Where not indicated, the scale bar equals 5 mm.

the ventromedial keel on frontals (vs. present in *A. pannonicum*); 2) labial pustulate ornament on premaxilla is not restricted to the boss but also cover the surface of the bone ventrally from the boss. The presence of boss on praemaxilla has been suggested as a characteristic for *A. pannonicum* and should be absent in *A. inexpectatum* (e.g., Venczel and Gardner 2005; Szentesi et al. 2015). The structures on the dorsolabial surface of the pars dorsalis on the studied material is interpreted as boss and most probably, suggesting the character to be shared between two species.

Urodela Duméril, 1806
Caudata Scopoli, 1777
Salamandridae Goldfuss, 1820
***Mertensiella* Wolterstorff, 1925**

***Mertensiella* sp.**
Fig. 3A–G

Material. Five trunk vertebrae, HLMD-Ez 2039–2041.

Description. The vertebrae are elongated and have opistocoelous centra (Fig. 3B, C). The pre- and postzygapophyses are elliptical and extended anteriorly. The condyle is rounded and has a clear constriction at its base. The cotyle is larger in diameter than the condyle. The neural arch is moderately high. In anterior view, the neural canal is slightly dorsoventrally flattened. The neural spine is high (observable in the rather well-preserved specimen (Fig. 3B)). The anterior tip of the neural spine is located behind the posterior margin of the prezygapophyses. Posteriorly the neural spine does not reach the posterior margin of the pterygapophysis. The zygapophyseal crest is absent (four vertebrae) or extremely poorly developed. The transverse processes are poorly preserved; however, distinct dia- and parapophysis can be observed (Fig. 3B, C). The anterior and posterior alar processes (anterior and posterior ventral crests sensu Venczel and Hír (2013)) connecting the parapophysis with the centrum are rather well developed.

Remarks. See the remarks in *Chioglossa* sp.

Chioglossa Bocage, 1864

***Chioglossa* sp.**
Fig. 3H–I

Material. Ten trunk vertebrae, HLMD-Ez 2042–2045.

Description and remarks. The vertebra morphology is nearly identical to *Mertensiella* sp. The following differences from it can be observed on the available material: 1) the lack or extremely poor development of the posterior alar process (vs. rather well-developed in *Mertensiella*); 2) the anterior zygapophyseal crest is well developed (vs. absent in *Mertensiella*) (Sanchíz and Młynarski 1979; Hodrová 1984; Ivanov 2008). The orientation of the dia- and parapophysis, the shape of the pterygapophyses have been mentioned as further characters allowing to distinguish these two genera (Hodrová 1984; Sanchíz 1998). However, due to poor preservation of the material, neither these characters can be evaluated nor any further identification at the species level can be done.

***Lissotriton* Bell, 1839**

***Lissotriton* sp.**
Fig. 4

Material. Six vertebrae, HLMD-Ez 2047–2050.

Description. The preserved small-sized trunk vertebrae have opistocoelous centra measuring up to 2 mm in length. The condyle is shorter and slightly smaller than the cotyle. The pericondylar constriction is well pronounced. The anteriorly oriented prezygapophyses have an oval outline. In dorsal view, the neural arch has a weakly-pronounced sandglass shape, where the narrowest part is located behind the prezygapophyses. The posterior margin of the neural arch is either flat or slightly bifurcated. The posterior notch is well preserved and visible on HLMD-Ez 2047 (Fig. 4E). The neural spine starts behind the anterior margin of the neural arch and reaches the posterior tip of the latter (Fig. 4B, G). The neural spine is always missing; however, where it is preserved, no ornamentation can be observed on it, and its rather large height can be suggested. The pre- and postzygapophyses are connected by a well-pronounced (nearly) horizontal interzygapophyseal crest, which covers slightly the proximal part of the transverse process (Fig. 4B). The transverse process is composed of the dia- and parapophysis, which in turn are connected by an osseous lamina along their length. In ventral view, the anterior and poster processes form a distinct ventral lamina of triangular to irregular rhomboidal shape (Fig. 4C, H). It is pierced by two smaller subcentral foramina near the center of the vertebra centrum. The anterior alar process is larger than the posterior one. The opening of the spinal nerve is visible behind the transverse process at the base of the neural arch. In anterior view, the neural canal is large (larger than the diameter of the condyle) and has a round or slightly expressed pentagonal outline (Fig. 4D, I). In posterior view, the neural canal is also large and has a round or slightly elliptical outline (Fig. 4E, J).

Remarks. The remains can be clearly assigned to the genus *Lissotriton* considering their small sizes; the lack of the dorsal widening or any structures on the neural spine; the presence of a well-pronounced rhomboid/triangular ventral lamina on the vertebral centrum (Ivanov 2008; Georgalis et al. 2019). On the one hand, poor and partial preservation of vertebrae and, on the other hand, not adequate knowledge of the osteology of the *Lissotriton* genus does not allow any further allocation at species or species group levels.

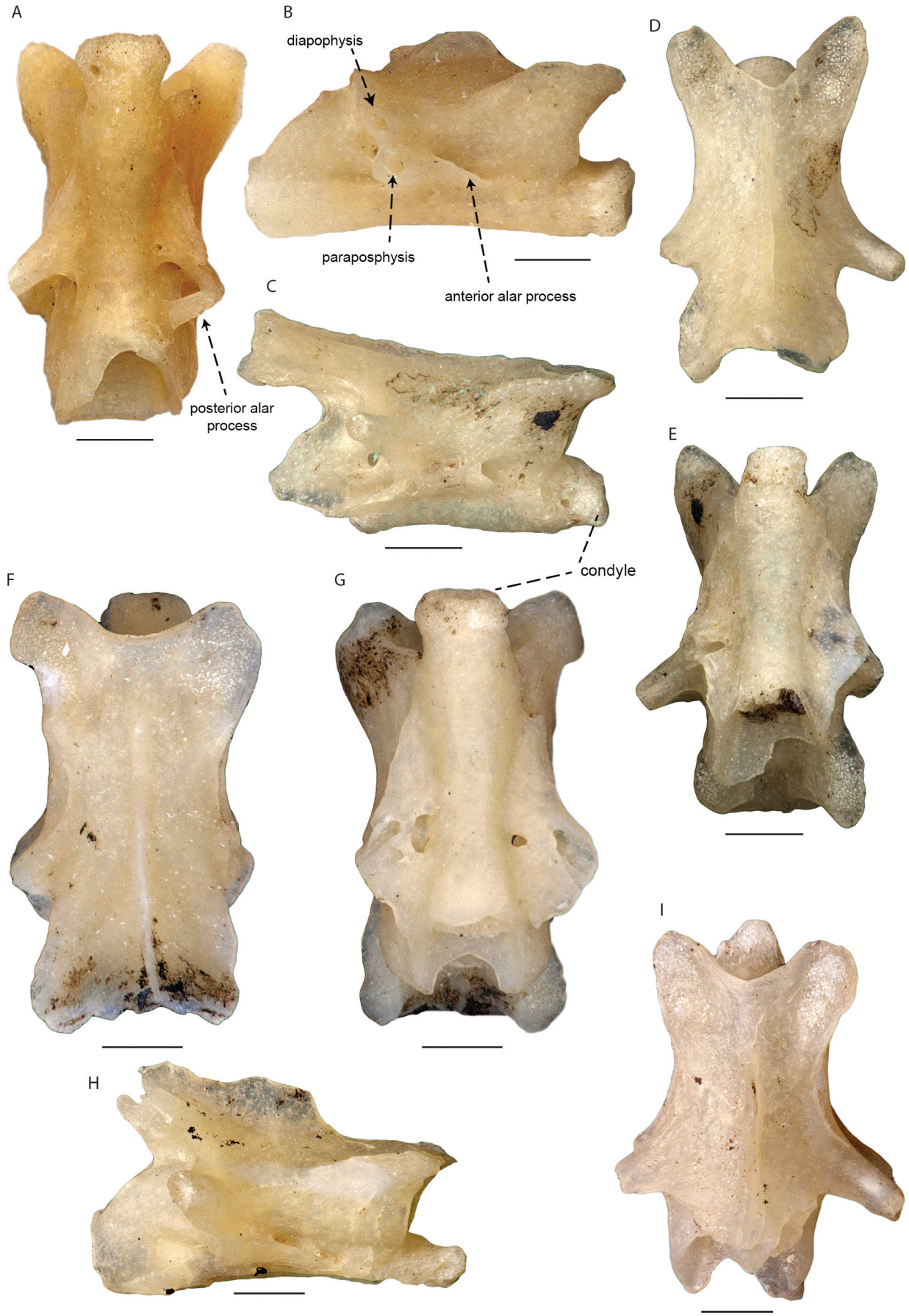

Figure 3. Vertebrae of *Chioglossa* sp. (**A, B.** HLMD-Ez 2042; **C, D.** HLMD-Ez 2043; **F, G.** HLMD-Ez 2044; **E.** HLMD-Ez 2043) and *Mertensiella* sp. (**H, I.** HLDM-Ez 2039) from the Echzell locality in (**A, C, E, H**) dorsal, (**B, D, F**) lateral and (**D, G, I**) ventral views. Scale bars: 0.5 mm.

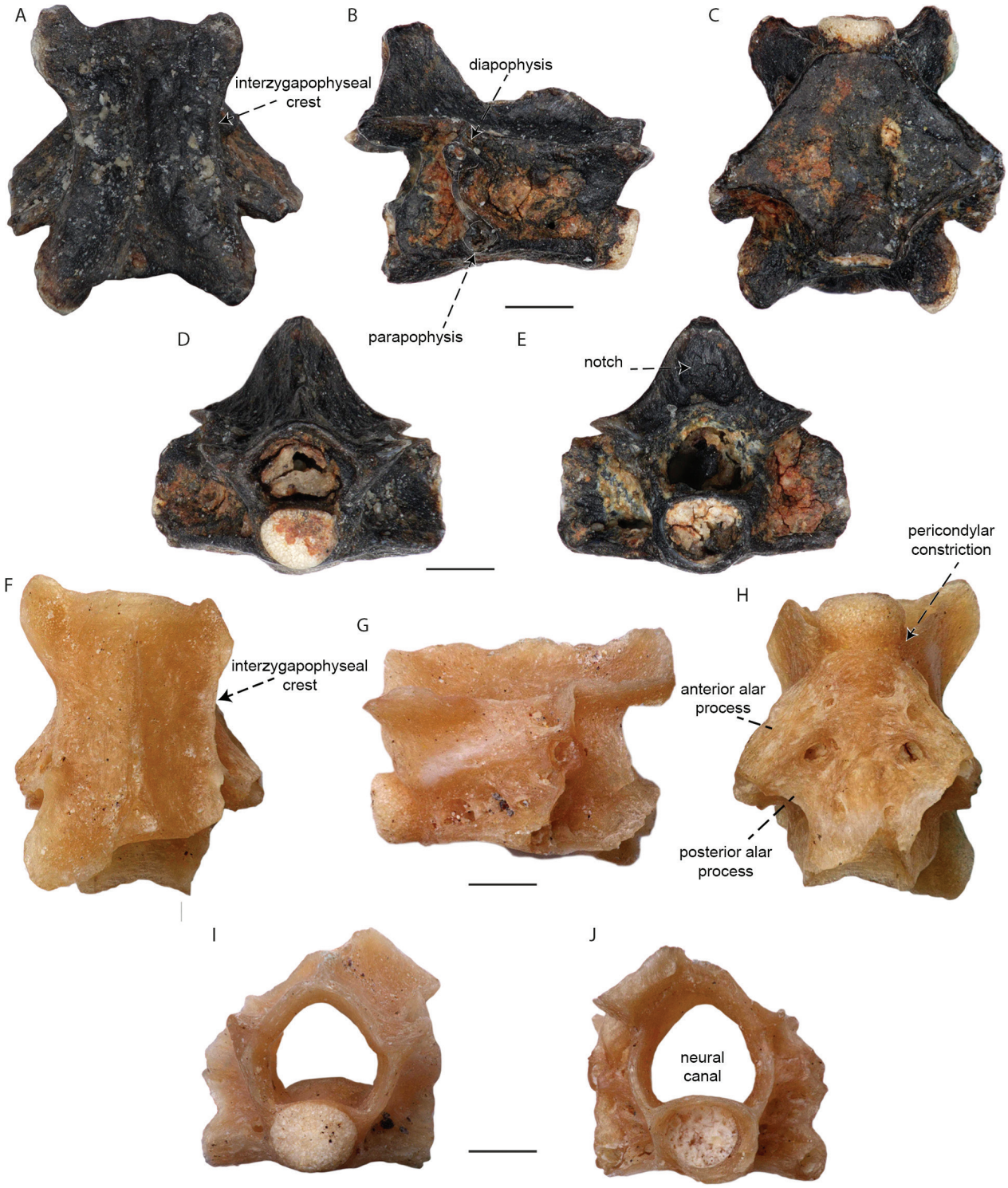

Figure 4. Vertebrae of *Lissotriton* sp. (**A–E.** HLDM-Ez 2047; **F–J.** HLDM-Ez 2048) from the Echzell locality in (**A, F**) dorsal, (**B, G**) lateral, (**C, H**) ventral, (**D, I**) anterior and (**E, J**) posterior views. Scale bars: 0.5 mm.

Salamandra Garsault et al., 1764

Salamandra sp.

Fig. 5A–F

Material. Five trunk vertebrae, HLMD-Ez 2029–2033.

Description. The vertebrae are opistocoelous and dorsoventrally flattened. They are large in size (5–7 mm). In dorsal view, the neural arch is broad and has an outline of a rectangle (HLMD-Ez 2029, Fig. 5A) or square (HLMD-Ez 2031, Fig. 5F). The prezygapophyses have round outlines and project anterolaterally. The neural arch between the prezygapophysese is flat. The neural spine starts behind this short flat surface and posteriorly does not reach the posterior tip of the pterygapophysis. In lateral view, the neural spine is low. It is highest at its middle point. The posterior margin of the pterygapophysis can be bifurcated. Its posterior surface possesses two distinct notches of

variable sizes and dimensions. In anterior view, the neural canal is dorsoventrally flattened. In HLMD-Ez 2029, the bases of the prezygapophyses are pierced by the subzygapophyseal (sensu Vasilyan et al. 2017) or anterior (sensu Tissier et al. 2015) foramen. Other vertebrae do not have this character. The arterial canal with large and/or smaller openings runs across the base of the transverse process. The latter is fully preserved only in HLMD-Ez 2029. It projects posterolaterally and is composed of dia- and parapophysis, which are connected with a thin lamina at their medial half (Fig. 5B); otherwise, they are free laterally. Additionally, the parapophysis is connected with the centrum anteriorly and posteriorly by anterior and posterior alar processes, respectively. They build a triangular-shaped lamina (Fig. 5C). In lateral view, a well-pronounced horizontal interzygapophyseal ridge connects the prezygapophysis with diapophysis, whereas the horizontal dorsal lamina connects the diapophysis with postzygapophysis. The centrum is flattened dorsoventrally and arched.

Remark. The general morphology and large size of remains, including the dorsoventrally compressed ophistocoelous vertebrae, broad and low neural arch as well as arched vertebra centrum allow assigning the remains to the genus *Salamandra* (Estes and Hoffstetter 1976). HLMD-Ez 2029 shows a slightly different morphology (presence of subprezygaphyseal foramen vs. its lack; square outline of the vertebra in dorsal view vs. rectangular outline) than the other available vertebrate. Comparable morphology is observable in the second vertebrae of *Salamandra salamandra* (see the morphosource link https://www.morphosource.org/concern/parent/000S44906/media/000165871). Thus, the HLMD-Ez 2029 can interpreted as an anterior vertebra.

Chelotriton Pomel, 1853

Chelotriton sp.

Figs 5G–6M

Material. Four frontals HLMD-Ez 2070–2073, four prefrontals HLMD-Ez 2068–2069, one nasal HLMD-Ez 2058, seven maxillae HLMD-Ez 2063–2065, two squamosals HLMD-Ez 2066–2067, one dentary HLMD-Ez 2057, five trunk vertebrae HLMD-Ez 2059–2061, ten ribs HLMD-Ez 2053–2056.

Description. Frontal: All four frontals are fragmentarily preserved. They represent individuals of different sizes. The frontal is widest at its most complete posterior portion. Its dorsal surface is covered by dermal ornamentation (Fig. 5G, I, K). The bone is slightly bent along its midline between the fronto-squamosal arch (sensu Ivanov 2008) and the rest of the bone. The fronto-squamosal arch projects posteriorly behind the main part of the bone. In ventral view, the partes contactae are reduced and run parallel along the anteroposterior axis of the bone. The braincase roof, located medially from the pars contacta, is delimited by a low crest of a semilunar outline (Fig. 5H, J, L).

Prefrontal: The prefrontals are wing-shaped bones, anteriorly broad and posteriorly narrowing to a sharp tip (Fig. 5M–N). The lateral margin (margo orbitalis) of the bone forms the anterodorsal wall of the orbit. The anterior corner of the margo orbitalis is pierced by the foramina of the V nerve. In ventral view, the ventral vertical wall separates the margo orbitalis from the rest of the bone. The articulation surface with the frontal bone, located at the posterolateral margin of the bone, is massive and more strongly developed than any other margin of the bone.

Nasal: The nasal bone has a nearly rectangular outline (Fig. 5O–P). All its margins are flat, without any concave outlines. Its dorsal surface is slightly rounded and possesses dermal ornamentation. In ventral view, parallel to the medial margin of the bone a ridge for articulation with the premaxillae is present.

Maxilla: only the posterior portions of the bone without dentition are present in the material. In dorsal view, the bone is narrow and a thin-walled horizontal pterygoid process projects lingually (Fig. 5S, U). In lateral view, the bone surface is covered by dermal ornamentation made of a dense network of small pits and pustules. Posteriorly the bone increase in height. In lingual view, the bone surface is smooth (Fig. 5R, T). The articulation surface with the quadratojugal bone is located on the posterodorsal surface of the bone. The size and dimensions of the articulation surface vary among available maxillae.

Squamosal: Two squamosals are partially preserved. In dorsal view, the HLMD-Ez 2066 is nearly semilunar in outline (Fig. 5V). The frontal process is curved slightly medially and possesses a vertical and almost flat articulation surface with the frontal. The lateral margin of the bone is rounded. The dorsal surface of the bone is somewhat horizontal and is covered by dermal ornamentation similar to other skull bones. The parietal process (in HLMD-Ez 2067, Fig. 5X) has a horizontal surface. It is slightly shorter but broader than the frontal process. In ventral view, a medioposteriorly oriented ridge, corresponding to the base of the ventral process of the bone, is visible. Posteriorly from the ridge, the bone surface is moderately concave.

Dentary: The fragmentary-preserved dentary is 1.7 mm in height. In lingual view, it shows a very low dental shelf with traces of the tooth pedicles. The preserved portion of the Meckelian groove is narrow and rather shallow (Fig. 5Z). Another but smaller groove is observable below the posterior half of the Meckelian groove, resembling most probably the articulation surface with the coronoid. In lateral view, the dentary is heavily ornamented by pits and pustules (Fig. 5Y). A remarkable concave surface separates the portion of the dental shelf from the rest of the bone.

Trunk vertebrae: the vertebrae are robust. The opistocoelous vertebra centrum is massive and slightly dorsoventrally flattened. The neural crest is nearly as high as the vertebra centrum (Fig. 6B, I). In dorsal view, its dorsal surface possesses a flat and (elongate) triangular

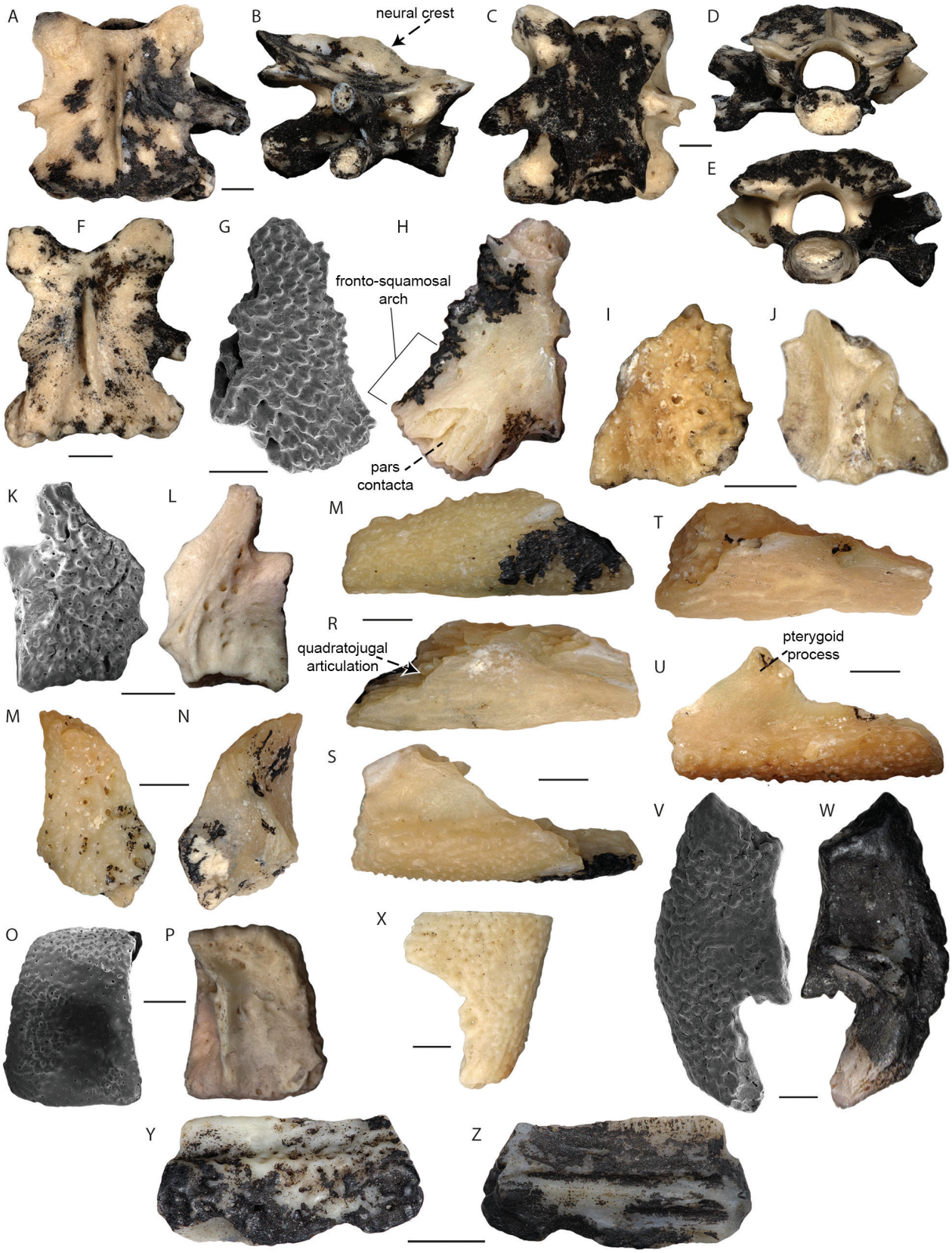

Figure 5. Vertebrae of *Salamandra* sp. (**A–E.** HLDM-Ez 2029; **F.** HLDM-Ez 2031) and (**G–Z**) cranial bones of *Chelotriton* sp. from the Echzell, including frontals (**G, H.** HLDM-Ez 2070; **I–J.** HLDM-Ez 2071; **K, L.** HLDM-Ez 2072), prefrontal (**M, N.** HLDM-Ez 2068), nasal (**O, P.** HLDM-Ez 2058), maxillae (**Q–S.** HLDM-Ez 2063; **T–U.** HLDM-Ez 2064), squamosals (**X.** HLDM-Ez 2067; **V, W.** HLDM-Ez 2066) and dentary (**Y, Z.** HLDM-Ez 2057). The bones are figures in dorsal (**A, F, G, I, K, M, O, S, X, V**) dorsal, (**B**) lateral, (**C, H, J, L, N, P, W**) ventral, (**D**) anterior, (**E**) posterior, (**Q, Y**) labial and (**R, T, Z**) lingual views. Scale bars: 1 mm.

Figure 6. Vertebrae (**A–E.** HLDM-Ez 2059; **F–J.** HLDM-Ez 2060) and ribs (**K.** HLDM-Ez 2054; **L.** HLDM-Ez 2053; **M.** HLDM-Ez 2055) of *Chelotriton* sp. Frontal (**N, O.** HLDM-Ez 2038) and ribs (**P, Q.** HLDM-Ez 2036; **R, S.** HLDM-Ez 2037) remains of Salamandridae indet. from Echzell. Bones in (**A, H, N**) dorsal, (**B, I**) lateral, (**C, J, O**) ventral, (**D, F**) anterior, (**E, G**) posterior, (**K, L, M, P, S**) posterior/anterior and (**Q, R**) medial views. Scale bars: 1 mm.

in outline plate, which is covered by a dermal ornamentation made of deep pits and low pustules (Fig. 5A, H). This place can be well developed and projects over the neural arch. Anteriorly, the neural crest does not reach the anterior tip of the neural arch (Fig. 6D, F). The pre- and postzygapophyses are round or elongated and project (latero-)anteriorly. The neural arch between the anterior half of the prezygapophyses has a smooth and convex surface. In anterior view, the neural canal is rounded or nearly triangular in outline (Fig. 6F). The condyle has a dorsoventrally flattened oval shape.

Small subprezygapophyseal foramina (sensu Vasilyan et al. 2017) can be present at the basis of the prezygapophyses. In lateral view, the transverse process is connected with the postzygapophysis by a clearly visible dorsal lamina (Fig. 6B, I). The posterior alar process connecting the parapophysis with the cotyle is smaller than the dorsal lamina. The prezygapophysis is connected with the parapophysis by a well-developed accessory alar process. A very thin anterior alar process connects the base of the prezygapophysis with the parapophysis of the transverse process. In ventral view, rather large-sized subcentral foramina and

rather smaller foramina are visible on the ventral surface of vertebrae. The transverse process consists of para- and diapophysis, which, though located close to each other, are separated by a thin lamina (Fig. 6B). In posterior view, the pterygapophysis possesses two distinct notches.

Ribs: All ribs are fragmentarily preserved. The articulation joints with the transverse process of the vertebrae are bicapitate. Both articulation heads are rounded and connected with a thin bone lamina (HLMD-Ez 2053, Fig. 6L). The dorsal surface of all ribs possesses two (HLMD-Ez 2054, Fig. 6K) to five (HLMD-Ez 2055, Fig. 6M) spines of different sizes and orientations.

Remarks. Based on the combination of the following characters, the described fossil remains can be attributed to the genus *Chelotriton*, broadly known from the Cenozoic deposits of Europe: 1) the presence of the characteristic dorsal ornamentation on skull bones and the horizontal plate of the neural spine of vertebrae; 2) the pterygoid process of the maxillae connected with the pterygoid; 3) the presence of spines on the ribs and 4) general morphology and dimensions of the bones (Ivanov 2008; Schoch et al. 2015; Vasilyan 2020). The remains cannot be clearly assigned to any known species of the genus due to the lack of a comprehensive understanding of the taxonomic diversity within the *Chelotriton* genus. However, some comparative remarks can be given below. The described skull bones differ significantly from all so far known *Chelotriton* records. For example, the frontal shows an intermediate morphology observable in *Chelotriton* sp 1. and sp. 2 from Mokrá-Western Quarry, Czech Republic, early Miocene (Ivanov 2008) and *Chelotriton paradoxus* from the Enspel Maar, Germany, late Oligocene, and Randecker Maar, Germany, early Miocene (Schoch et al. 2015). The shape of the squamosal in the Echzell material can be found only in *Chelotriton* sp. from Orsberg, Germany, late Oligocene (Marjanović and Witzmann 2015), where a bone of a similar shape is named as a quadratojugal-quadrate bone. The nasal from Echzell (nearly rectangular in outline) can be clearly distinguished from that of all known forms in which the form varies from irregular-shaped one (e.g. in *Chelotriton paradoxus* from Enspel, Roček and Wuttke 2010) to trapezoid-shaped in *Chelotriton* sp. form Orsberg (Marjanović and Witzmann 2015). Most probable, the suggested high variability of the skull bone (Schoch et al. 2015) can be explained by uncovered high specific diversity of *Chelotriton*. Thus, at this stage of knowledge, we describe the fossil remains of *Chelotriton* with an open nomenclature.

Salamandridae indet.

Fig. 6N–S

Material. One frontal, HLMD-Ez 2038, seven trunk vertebrae, HLMD-Ez 2034, 20 caudal vertebrae, HLMD-Ez 2035, nine vertebrae, HLMD-Ez 2051, 2052, 2062, two ribs HLMD-Ez 2036, HLMD-Ez 2037, two extremity bones HLMD-Ez 2052.

Description and remarks. A single frontal, with a length of 6 mm, displays a flat dorsal surface (Fig. 6N). In dorsal view, the most anterior portion of the bone possesses an articulation facet with the parietal that is covered by parallel to each other ridges. Comparison with recent similar-sized species shows most similarities with *Salamandra salamandra* (MJSN-OS 806). However, due to the lack of comprehensive studies of the skull bones among salamandrids, an allocation of the bone to the family Salamandridae is more appropriate.

The vertebrae are poorly preserved. They show ophistocoelous morphology partially with complex structures of haemal and neural processes, characteristic of the caudal region of the vertebral column (Duellman and Trueb 1994). On the one hand, the poor preservation and, on the other hand, the poor knowledge on osteological differences of the caudal region in *Chelotriton* and *Salamandra* genera (both present in the fossil locality) make it at the moment impossible to identify the vertebrae correctly.

Nine small-sized opistocoelous vertebrae are available in the material. They have variable preservation; however, a large number of structures/characters are missing for further identification. Considering the vertebra sizes as well as available similar-sized salamander taxa present in the material, most probably, they represent remains of *Lissotriton*, *Mertensiella* or *Chioglossa*. The juvenile and most distal caudal vertebra of *Salamandra* and *Chelotriton* can be excluded because in the former form the juvenile vertebrae are not fully ossified, whereas in the latter the dorsal tip of the neural crest possesses a ornamented surface, which is missing here.

Two bicapitate rips are present (Fig. 6P–S). Their lateral portion does not possess any process, which allows to exclude them from *Chelotriton*. Most probable, they should belong to the genus *Salamandra*, which has a similar rib morphology and is represented in the material by large-sized individuals as well.

Anura Fischer, 1813
Pelobatidae Bonaparte, 1850
Pelobates Wagler, 1830

Pelobates sanchizi Venczel, 2004

Fig. 7

Material. Four frontoparietals HLMD-Ez 2107–2110, 13 squamosals HLMD-Ez 2104–2106, one premaxilla HLMD-Ez 2098, 48 maxillae HLMD-Ez 2095–2097, 38 fragments of skull bones HLMD-Ez 2103, three presacral HLMD-Ez 2098, 2099, 2102 and two sacral vertebrae HLMD-Ez 2100, 2101, 11 ilia HLMD-Ez 2111–2115.

Description. Frontoparietals: Fragmentarily preserved remains are covered dorsally with the characteristic pit-and-ridge style sculpture as well as low spines (Fig. 7A, H). The tectum supraorbitale is moderately broad. In dorsal view, the lateral superior process is longer than broad. The articulation surface with the squamosal is well-developed, concave and oriented fully laterally (Fig. 7A). Neither incrassation

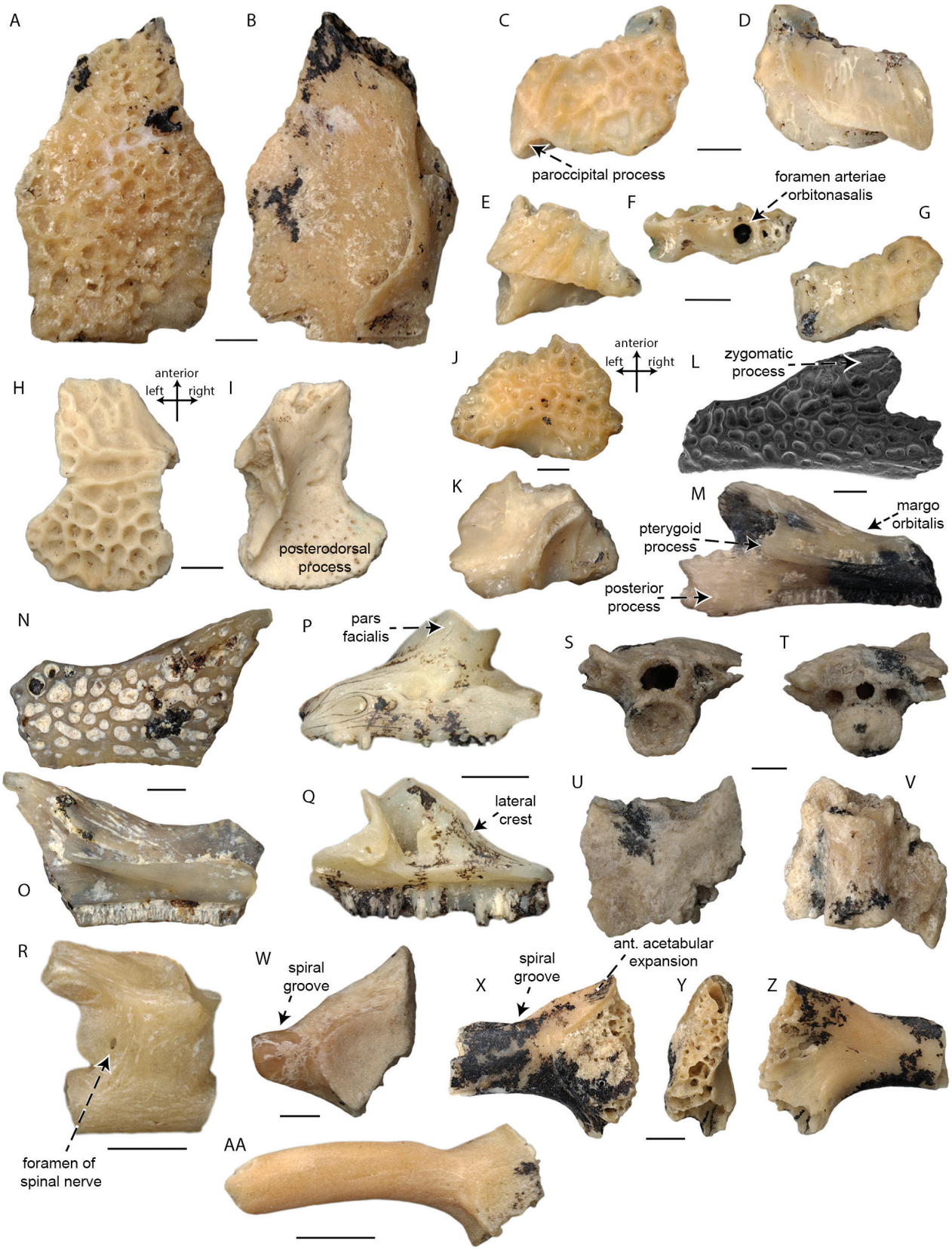

Figure 7. *Pelobates sanchizi* from the Echzell locality. Frontoparietals HLDM-Ez 2109 (**A, B**), HLDM-Ez 2107 (**C, D**), HLDM-Ez 2108 (**E–G**). Squamosals HLDM-Ez 2105 (**H, I**), HLDM-Ez 2106 (**J, K**). Maxillae HLDM-Ez 2077 (**L, M**), HLDM-Ez 2097 (**N, O**). Premaxilla HLDM-Ez 2098 (**P, Q**). Vertebrae HLDM-Ez 2101 (**S–V**), HLDM-EZ 2099 (r). Ilia HLDM-Ez 2113 (**W**), HLDM-Ez 2111 (**X–Z**), HLDM-Ez 2112 (**AA**). Bones figures in (**A, C, E, G, H, J, U**) dorsal, (**B, D, I, K, V**) ventral, (**F, T, Y**) posterior, (**L, N, P**) labial, (**M, O, Q**) lingual, (**S**) anterior, (**R, W, X, AA**) lateral and (**z**) medial views. Scale bars: 1 mm.

frontoparietalis nor the margins are preserved/observable in the remains. The paroccipital process is reduced, but its dorsal surface possesses a distinct crest. The medial base of the paroccipital process is pierced by the occipital arterial foramen, which is covered dorsally by the posterior margin of the frontoparietal and, thus, not visible in dorsal view (Fig. 7E). The fragmentarily preserved parts of the inferior superior process suggest that it was not longer than the lateral superior process. However, its lateral and slightly ventrally bending can be assumed. The arteria orbitonasalis opens ventrally on the supraorbital tectum (Fig. 7F).

Squamosals: The dorsal surface is covered by a similar to frontoparietal pit-and-ridge sculpture. The bone remains are fragmentarily preserved. Only in HLMD-Ez 2105 (Fig. 7H, I), an intact posterodorsal process lamina is present, and shows rounded posterior margin. The dorsal and zygomatic processes are broken. However, considering the presence of intact and concave bone margins between the preserved bases of these processes, we can suggest that they were delimited from each other. In ventral view, lamellar structures at the base of the posterolateral processes are observable (Fig. 7I, K). However, they are incomplete for any further description.

Maxillae: The labial surface of the bone is covered by a dense network of moderately deep to deep pits-and-ridge sculpture. The distinct zygomatic process extends posterodorsally and has a rounded posterior tip (Fig. 5L). The posterior process projects backwards. It is separated clearly from the zygomatic process by a deep concavity and projects much posteriorly. The orbital margin is concave. In lingual view, the pterygoid process projects posteromedially (Fig. 7M, O). Anteriorly, it is connected with the dorsally oriented lamella above the horizontal lamina.

Premaxilla: In anterior view, the pars dentalis is low but broad. Its surface is covered by rugose structures (Fig. 7P), which recalls the pit-and-ridge sculpture of, e.g., frontoparietal and maxilla. The pars facialis is broken, but its preserved base suggests a L-shaped form. Medially from this process, another shorter and posteromedially oriented process is present. The lateral crest (sensu Venczel 2004) is moderately developed. The dental crest possesses 15 tooth pedicles (Fig. 7Q).

Vertebrae: three presacral and two sacral vertebrae are present. The vertebra centrum is procoelous (four vertebrae, HLMD-Ez 2098, 2100–2102) or amphicoelous (one vertebra, HLMD-Ez 2099, Fig. 7R). The HLMD-Ez 2099 represents a small-sized individual that, most probably, does not have fully ossified joints. In presacral vertebrae, the neural arch is high; and the neural canal is large. The foramina for the spinal nerve are present slightly above the posterior bases of the neural arch. In presacral vertebrae, they are visible in lateral view, whereas in sacral ones – in posterior views (Fig. 7T). The sacral vertebrae have a broad and flattened transverse process.

Ilium: Though all ilia are very fragmentarily preserved, the following characters can be observed on the material: the acetabular region triangular; the acetabulum itself has round outline; the dorsal prominence low and covered by rare irregular structures; the dorsal protuberance absent; the moderately deep spiral groove extends from ventrolateral to dorsomedial direction in the region of the fusion of iliac shaft and acetabulum (Fig. 7W–AA); in medial view, the ilioischiatic juncture is covered by elongated striae (Fig. 7Z); the dorsal acetabular expansion larger than the ventral one.

Remarks. The described remains can be assigned to the genus *Pelobates* based on the following combination of characters: 1) azygous frontoparietals articulating with the squamosals; 2) well-pronounced pit-and-ridge style sculpture with pustular structures on frontoparietal, squamosal and maxillae; 3) the presence of the spinal nerve foramina in vertebrae; 4) the presence of the moderately deep spiral groove on ilium, etc. (e.g., Venczel 2004; Roček et al. 2014). The fossil material of *Pelobates* can be allocated to the species *P. sanchizi* considering: 1) the presence of moderately broad tectum supraorbitale; 2) the occipital arterial foramen not visible in dorsal view; 3) the arteria orbitonasalis opening ventrally on the supraorbital tectum; 4) delimited posterior and posterodorsal processes of squamosal (Venczel 2004)

Comparison of our material with other fossil species of *Pelobates* (Böhme et al. 1982; Khozatskiy 1985; Böhme 2010; Roček et al. 2014) allowed to suggest further diagnostic features for *P. sanchizi* such as: 1) the lateral superior process of the frontoparietal is longer than broad; 2) articulation surface on frontoparieals with squamosal well-developed, concave and oriented fully laterally.

The single premaxilla from Echzell shows a remarkable feature: ornamented on the anterior surface of the bone, recalling the pit-and-ridge sculpture of, e.g., frontoparietal and squamosal. Comparable ornamentation has not been ever described for the genus *Pelobates* and in *P. sanchizi* from other Miocene localities. Only for *Eopelobates deani* (Roček et al. 2014), a moderated rugose outer surface has been mentioned.

Alytidae Fitzinger, 1843
Latonia von Meyer, 1843

Latonia sp.

Fig. 8

Material. 76 maxillae HLMD-Ez 2130–2135, seven frontoparietals HLMD-Ez 2141–2144, one prooticoccipital HLMD-Ez 2127, six atlases HLMD-Ez 2116–2117, 23 presacral HLMD-Ez 2118–2120 and 22 sacral vertebrae HLMD-Ez 2121–2123, two costae (ribs) HLMD-Ez 2128, 23 urostyles 2124–2126, 58 ilia HLMD-Ez 2136–2140.

Description. Frontoparietals: All bones are very fragmentarily preserved, and all of them possess ornamentation made of a dense network of tubercles (Fig. 8A, C, E). In ventral view, a number of ridges and structures are visible (Fig. 8B, D, F); however, due to their preservation, any further description/anatomical identification is impossible.

Figure 8. *Latonia* sp. from Echzell. Frontoparietals HLMD-Ez 2141 (**A, B**), HLMD-Ez 2142 (**C, D**), HLMD-Ez 2143 (**E, F**). Maxilla HLMD-Ez 2133. Prooticoccipital HLMD-Ez 2127 (**I–L**). Atlas HLMD-Ez 2116 (**M, N**). Presacral vertebrae HLMD-Ez 2118 (**O, P**) and HLMD-Ez 2119 (**Q–T**). Sacral verterba HLMD-Ez 2122 (**W–Y**). Urostyle HLMD-Ez 2124 (**Z**) and HLMD-Ez 2125 (**AA**). Ilia HLMD-Ez2137 (**AB**), HLMD-Ez2138 (**AC–AE**), HLMD-Ez 2140 (**AF**) and HLMD-Ez2139 (**AG–AI**). Bones are figures in (**A, C, E, L, O, T, X, Z, AA**) dorsal, (**B, D, F, K, M, R**) ventral, (**G**) labial, (**H**) lingual, (**I, Q, Y, Ad, Ah**) posterior, (**J, N, P, S, W**) anterior and (**AB, AC, AE, AF, AG, AI**) lateral views. Scale bars: 1 mm.

Maxillae: All bones are fragmentarily preserved. Their labial surface is smooth and does not possess any ornamentation (Fig. 8G). Only in (HLMD-Ez 2132), the labial surface is covered by some irregularities. In lingual view, the horizontal lamina has a rounded surface and reduces height anteriorly (Fig. 8H). Posteriorly, it terminates with a medioposteriorly projecting pterygoid process. The posterior depression is moderately developed. The margo orbitalis is slightly concave.

Prooticoccipital: One preserved prooticoccipital (HLMD-Ez 2127) consists of both fused prootic and lateral occipital processes (Fig. 8I–L). It displays a distinct supracondylar depression. The prominentia ductus semicircularis posterioris is present as a distinct crest. It starts at the base of the lateral prootic process and projects medioanteriorly until the articulation surface with the frontoparietal. A foramen is present at the ventral base of the lateral prootic process. The sulcus venae jugularis is present as a horizontal groove. The fenestra ovalis is massive (Fig. 8K).

The atlas has a dorsoventrally flattened centrum (HLMD-Ez 2116, Fig. 8N). The neural arch is not preserved. The crista ventralis is well developed. The condyloid fossae are separated from each other by a notch. The opisthocoelous presacral vertebrae have massive, slightly dorsally compressed centrum. The transverse processes project laterally. The neural arch in a small-sized vertebra projects posterodorsally (HLMD-Ez 2118), and the neural spine is clearly visible (Fig. 8O, P). The sacral vertebrae have one anterior and two posterior condyles with very rounded external surfaces (Fig. 8X, Y). The neural arch is short. It measures as long as the bases of the transverse processes. The latter widens laterally and project lateroposteriorly. The prezygapophyses in both presacral and sacral vertebrae project laterodorsally (Fig. 8S, W).

The urostyle possesses two condyloid fossae and two lateroposteriorly bending transverse processes (Fig. 8Z, AA). The opening of the neural canal is rounded. The neural canal opens dorsally behind the transverse processes in the form of a narrow and long strip.

The preserved ilia have low or moderately developed dorsal prominence. The dorsal protuberance has a flat surface and shows high variation in shape and size. It can be very reduced in the form of a small protuberance (HLMD-Ez 2137, Fig. 8AB) or rather well-developed elongate (HLMD-Ez 2140, Fig. 8AF) or short drop-shaped (HLMD-Ez 2140–2141, Fig. 8AF) structure. It is connected with the lateromedially compressed iliac shaft by a thin lamina which reduces in height anteriorly behind the dorsal protuberance. The acetabular region is well developed. The dorsal acetabular expansion is well-developed and has a triangular outline. The ventral acetabular expansion is rather reduced and widens ventrally, expanding below the ventral margin of the acetabular crest. The ventral portion of the acetabular crest is well developed and projects ventrolaterally. The supraacetabular fossa is absent or, if present, weakly developed. A distinct tubercular fossa is visible in the corner between dorsal prominence and iliac shaft. In both medial (Fig. 8AE, AI) and posterior views (Fig. 8AH), a well-developed interiliac tubercle is visible. In posterior view, the ilioischiatic juncture can be clearly divided into a massive ventral and a slender dorsal portions, which are delimited in the medial surface by a deep groove.

Remarks. The herein described remains can be assigned to the genus *Latonia* based on the presence of the following features: 1) frontoparietal with the characteristic tubercular sculpture; 2) prooticooccipital bone with a distinct supracondylar depression; 3) atlas possessing ventral crest; 4) urostyle with lateroposteriorly projecting transverse processes; 5) the general morphology of ilium and presence of the interiliac tubercle etc. (Roček 1994). Due to the poor preservation of the material, any further taxonomic identification is impossible.

Ranidae Rafinesque, 1815
Pelophylax Fitzinger, 1843

Pelophylax sp.

Fig. 9A–D

Material. Four ilia HLMD-Ez 2088–2091.

Description. All ilia are fragmentary. The iliac shaft and most proximal portions are missing. The dorsal prominence is well developed; it is high, in lateral view projects anterodorsally, whereas in posterior view, it has a medially curved outline. The dorsal protuberance is massive, drop-shaped, with a rounded surface (Fig. 9D). The supraacetabular fossa is moderately developed and located posteriorly from the ventral base of the dorsal prominence. The acetabular ridge is ventrally significantly higher than dorsally (Fig. 9C, D). The iliac shaft is rather thin and round in cross-section. The iliac shaft and the dorsal prominence are connected by a high and thin bone lamina.

Remarks. See remarks of *Rana* sp.

Rana Linnaeus, 1758

Rana sp.

Fig. 9E–H

Material. Three ilia HLMD-Ez 2092–2094.

Description. The best-preserved ilium (HLMD-Ez 2094, Fig. 9G, H) shows a well-developed (rather narrow and high) dorsal acetabular expansion and a reduced (broad and low) ventral acetabular expansion. The dorsal prominence is not very high. It is oriented rather anteriorly than anterodorsally. The dorsal protuberance has an oval outline. Its surface is either smooth (HLMD-Ez 2094, Fig. 9G) or possesses muscle scars (HLMD-Ez 2093, Fig. 9E). The iliac shaft is rather thin and round in cross-section. A low and thin bone lamina connects the iliac shaft and the dorsal prominence. In posterior view, the dorsal prominence projects laterodorsally. The ilioischiatic juncture is narrow (Fig. 9H).

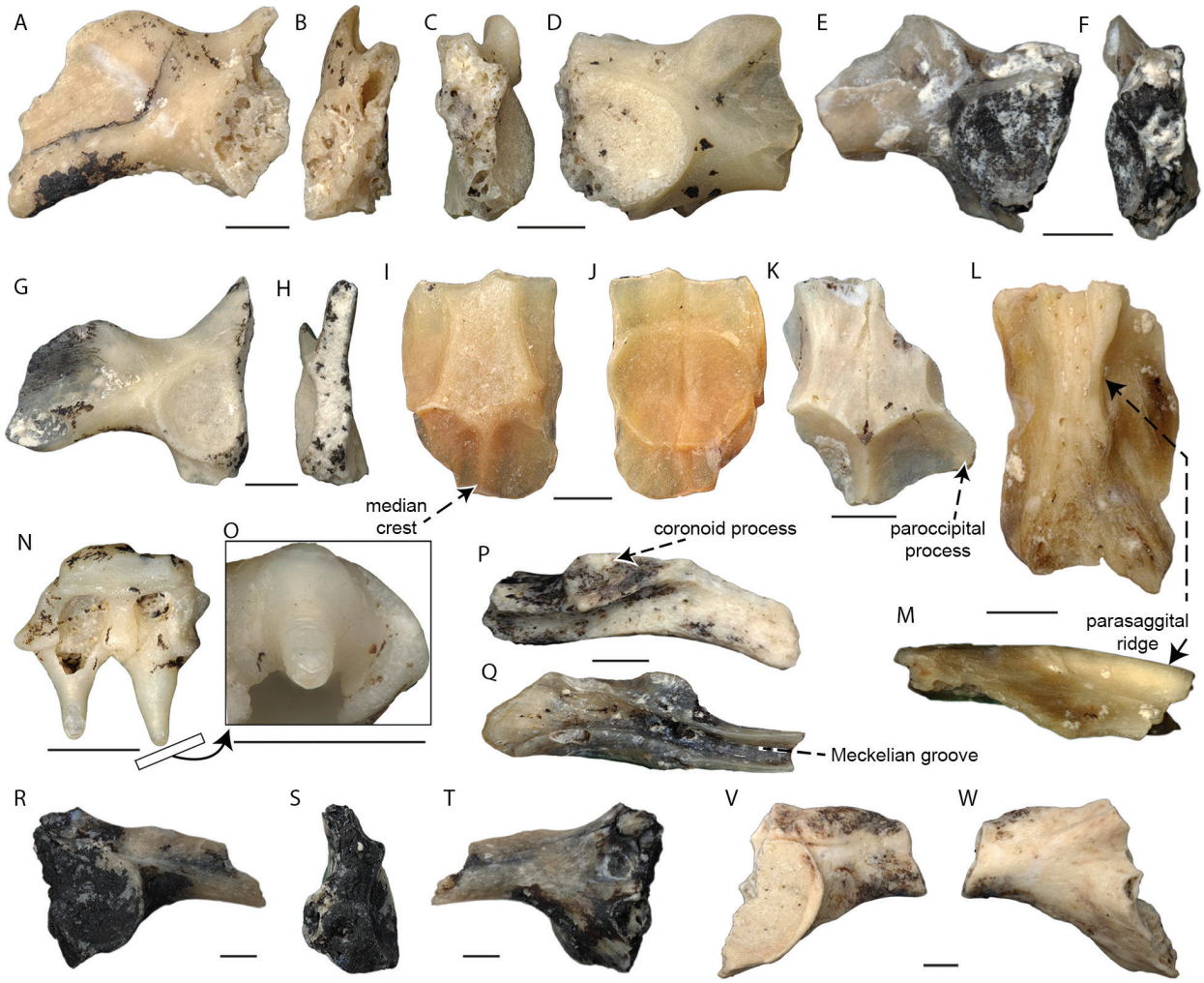

Figure 9. Frogs from Echzell locality. Ilia of *Pelophylax* sp. HLMD-Ez 2089 (**A, B**) and HLMD-Ez 2090 (**C, D**). Ilia of *Rana* sp. HLMD-Ez 2093 (**E, F**) and HLMD-Ez 2094 (**G, H**). *Palaeobatrachus robustus* (**I–W**). Frontoparietals HLMD-Ez 2077 (**I, J**), HLMD-Ez 2078 (**K**) and HLMD-Ez 2076 (**L, M**). Jaw bone HLMD-Ez 2084 (**N, O**). Angulars HLMD-Ez 2083 (**P**) and HLMD-Ez 2082 (**Q**). Ilia HLMD-Ez 2079 (**R–T**) and HLMD-Ez 2080 (**V, W**). Bones are figured in (**A, D, E, G, M, R, V**) lateral, (**B, C, F, H, S**) posterior, (**I, K, L, P, Q**) dorsal, (**J, O**) ventral, (**N**) labial and (**T, W**) medial views. Scale bars: 1 mm.

Remarks. Echzell frog ilia can be clearly assigned to green *Pelophylax* and brown *Rana* frogs based on the following characters. The genus *Pelophylax* is characterised by: anterodorsally oriented, high, large and dorsomedially curved dorsal prominence and protuberance; the dorsal protuberance has a smooth surface; whereas the genus *Rana* by in lateral view anterodorsally and in posterior view laterodorsally oriented, rather low and reduced dorsal prominence and protuberance, the dorsal protuberance has smooth or irregular surface (Böhme 1977; Blain et al. 2007).

Palaeobatrachidae Cope, 1865
Palaeobatrachus Tschudi, 1838 (sensu Wuttke et al. 2012)

Palaeobatrachus robustus Hossini & Rage, 2000

Fig. 9I–W

Material. Four frontoparietals HLMD-Ez 2076–2078, five ilia HLMD-Ez 2079–2081, two angulars HLMD-Ez 2082, 2083, five jaw bones HLMD-Ez 2084, 2085.

Description. Frontoparietals are flat and thin. They represent small-sized individuals. The parasagittal ridges are well-developed and build the limit between the flat dorsal surface of the bones and somewhat concave orbital margins. The parasagittal ridges are very closely located near the midpoint of the bone and form a sandglass shape at the dorsal surface of the bone. The dorsal surface of the bone between the parasagittal ridges is irregular and pierced by small foramina (pineal foramen sensu Villa et al. 2016) and pits (Fig. 9L). Posteriorly, the surface of the frontoparietal table is flat and rather smooth. The irregularities, if present, are weakly pronounced. The parasagittal ridges reach the paroccipital processes posteriorly (Fig. 9I, K). The latter are not fully preserved. Only their bases are observable, which in turn, possess a crest. A smaller posterior median crest is present along the anteroposterior axis of the bone which starts from the posterior margin of the frontoparietal table. The posterior margin of the bone between the median margin and paroccipital process is arched and forms a “bilobed” outline

(Fig. 9K). The median crest is lower than the paroccipital processes. Judging from the preserved portions of the paroccipital process and posterior median process, a shorter length of the former in comparison to the latter can be assumed. In ventral view, the frontoparietal incrassation, visible only in HLMD-Ez 2077 (Fig. 9J), representing the posterior portion of the bone, has a round outline with slightly prominent margins. No structure similar to the lanceolate area (sensu Roček et al. 2015) is observable on the available frontoparietals.

Premaxillae, maxillae, vomer: all three bones are fragmentarily preserved and do not allow any detailed description. The preserved teeth and tooth pedicles display diagnostic characters, such as the conical and slightly lingually bent ankylosed teeth. At the tooth basis, large and deep pits are preserved. The bicuspid tooth has a small labial and large apical cusps (Fig. 9N, O, HLMD-Ez 2084).

Angulars: in total, two angulars can be clearly assigned to this taxon. They are elongated and curved bones. The coronoid process is compact and can be oval to drop-shape (Fig. 9P, Q). Its surface is concave, rather smooth and can possess tubercles (muscle scars). The Meckelian groove behind the coronoid process is broad and opens dorsally, whereas anteriorly, it is open laterally or slightly dorsolaterally.

Ilium: The acetabular region of the ilium is robust. The dorsal prominence (sensu Gómez and Turazzini 2015) is not well-developed. The drop-shape dorsal protuberance (sensu Gómez and Turazzinin 2015) is large (Fig. 9R) and can be weakly to moderately developed (Fig. 9V). Its surface is rather smooth, and its small posterior portion is located above the anterior margin of the acetabular crest. The ventral acetabular expansion (also known as pars descendens) does not project ventrally, but it is massive in ventral/dorsal views (Fig. 9R). The dorsal acetabular expansion (also known as pars ascendens), even if only fragmentarily preserved, is moderately developed. The ventral half of the acetabular fossa is massive. The well-developed ventral portion of the acetabular crest projects laterally and contributes to the ventroanterior surface of the acetabular region of the ilia. In larger individuals (e.g. HLMD-Ez 2080), an oval knob-like flat surface is present in the lateroventral cornet between the iliac shaft and acetabulum (Fig. 9V). It represents most probably the attachment surface for the muscle iliacus internus (sensu Gómez and Turazzini 2015). In posterior view, the well-pronounced interiliac groove and laterally projecting acetabular crest are observable. The iliac shaft is moderately developed, lateromedially flattened and has a rather smooth surface.

Remarks. The fossil remains display characteristic features of the genus *Palaeobatrachus* as well as the family Palaeobatrachidae such as: 1) azygous frontoparietal with a flat dorsal surface; 2) angular coronoid process smooth and/or covered by muscle scars; 3) anteroventrally extending large acetabulum; 4) acetabular area strongly protruding; 5) well-pronounced interiliac groove (Wuttke et al. 2012) and 6) paroccipital processes do not extend probably beyond the level of posterior median process (Roček et al. 2015; see characters 12, table 2). Among the material available bones, only the frontoparietal can be used for the species-level identification since other elements such as ilium, angular do not contain sufficient diagnostic characters. The *Palaeobatrachus* frontoparietal from Echzell can be distinguished from other Miocene forms, e.g. *P. hiri* (locs. Bátraszölos and Sámsonhaza, Venczel 2004), and *P.* sp. A (loc. Rudabanya, Roček 2005) by the sculptured frontoparietal (vs. unsculptured in *P. hiri* and *P.* sp. A) and weakly developed frontoparietal incrassation (vs. strongly developed, in form of crests in *P. hiri* and *P.* sp. A). The Echzell frontoparietals strongly resemble the morphology of the *P. robustus* from the early Miocene (MN2) of France (loc. Laugnac, Hossini and Rage 2000), in having 1) a comparable sculpture on dorsal surface of the bone; 2) the skull table narrows in the midpoint of the bone, giving a sandglass shape; 3) weakly developed, rounded frontoparietal incrassation. We did not compare with *P. hauffianus* from Randecker Maar, Germany (middle Miocene) (Roček et al. 2006) which taxonomic status still needs revision.

Anura indet.

Material. Six angulars HLMD-Ez 2086, eight premaxillae HLMD-Ez 2129, 38 humeri HLMD-Ez 2087, a number of bone fragments HLMD-Ez 2145.

Remarks. The bones are either very fragmentarily preserved or do not possess characters useful for further identification.

Squamata Oppel, 1811
Gekkota Cuvier, 1816–1817

Gekkota indet.
Fig. 10

Material. One right dentary HLMD-Ez 1958, one vertebra HLMD-Ez 1959.

Description. Dentary: Only a fragment of the right mid-dentary region is preserved (Fig. 10A, B). It bears 16 tooth positions that are densely spaced. Unfortunately, all teeth are broken off and missing, except for two preserved tooth bases. The dentary is slender (note, however, that the alveolar crest is high). In medial view, it gradually widens posteriorly and Meckel`s groove is fully closed. The ventral margin of the dentary is slightly concave. Besides three labial foramina, the external surface of the bone is smooth.

Vertebra: Only one isolated dorsal vertebra is preserved (Fig. 10C–G). The vertebra is small, lightly built and anteroposteriorly elongated. It is amphicoelous with the centrum pierced by a notochordal canal. On the dorsal surface of the low neural arch, a straight dorsal and longitudinal, almost indistinct crest is present along the surface of the neural spine. The neural spine is weak, and

it does not rise dorsally. However, the posterior region of this area is damaged, and the right postzygapophysis is broken off. On the anterior side, a deep and wedge-shaped notch is present (note, that it is unclear how much its contour is a result of potential breakage and/or normal state). Both pre- and postzygapohyses are almost anteriorly and posteriorly directed. The neural canal is large and heart-shaped because of the rounded centrum that is located ventrally. In lateral view, there is an elliptical synapophysis. In this view, the centrum has a concave ventral margin. In ventral view, the lateral margins of the centrum are concave as well. In the central region, a short ridge is developed between the anterior and posterior portions of the centrum. Laterally from the ridge, the surface is pierced by a pair of subcentral foramina.

Remarks. In the European Miocene, the sphaerodactylid genus *Euleptes* is often present (see e.g., Daza et al. 2014; Čerňanský et al. 2018). Extinct genera of Gekkota are represented by *Gerandogekko*, which has been identified as closely related to *Euleptes* (Daza et al. 2014) and *Palaeogekko* (Schleich 1987). The material from Echzell is, however, too fragmentary for a generic assignment.

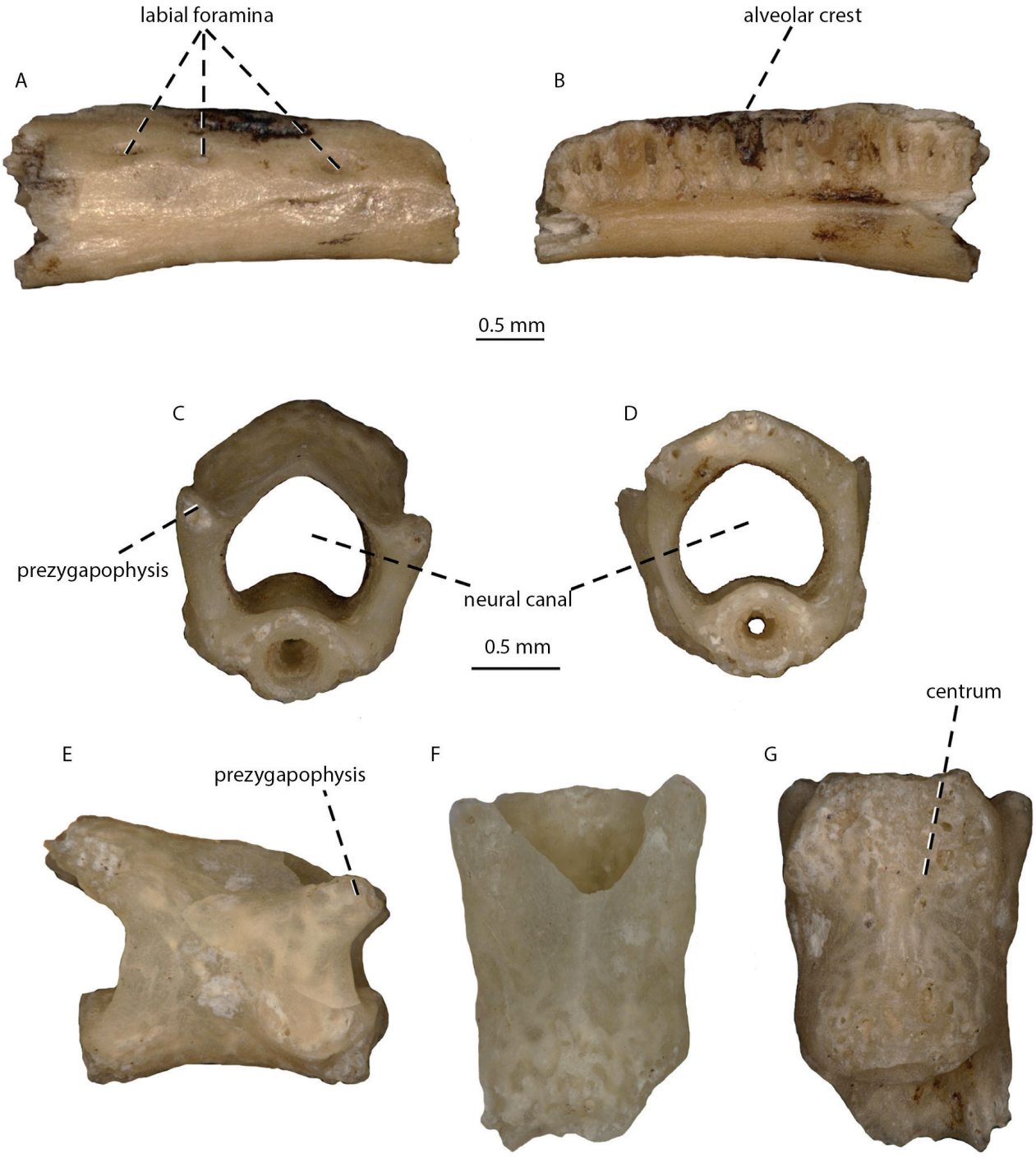

Figure 10. Gekkota indet. from the Echzell locality. right dentary HLMD-Ez 1958 in (**A**) lateral and (**B**) medial views. Vertebra HLMD-Ez 1959 in (**C**) anterior, (**D**) posterior, (**E**) lateral, (**F**) dorsal and (**G**) ventral views.

Iguania Cope, 1864
Acrodonta Cope, 1864
Chamaeleonidae Gray, 1825
***Chamaeleo* Linnaeus, 1758–1759**

***Chamaeleo andrusovi* Čerňanský, 2010b**
Fig. 11A, B

Material. One frontal HLMD-Ez 1960.

Description. Frontal: The frontal is partly preserved. Only its posterior region around the parietal foramen (sensu Gauthier et al. 2012: character 105) is available. The dorsal surface possesses well-developed ornamentation formed by large, robustly developed, and distinctly pustular protuberances (Fig. 11A). Only four are preserved (note, however, most of the dorsal surface of two of them is damaged). In the posterior region, the protuberances are large and somewhat anteroposteriorly elongated. They appear to be moderately spaced with a more-or-less complex structure (somehow resembling gomphothere molars). The internal surface of the frontal (Fig. 11B) is pierced by a small, elliptical foramen. It opens a canal that continues anterodorsally (note that the preserved dorsal surface is not pierced by it). Lateral to it, rounded, dorsally sloped ridges are well-developed. They form the border between the central, bulged region with its central shallow longitudinal depression and two additional distinct depressions located lateral to the central region. These lateral depressions become more distinct anteriorly, being gradually more recessed (in other words, the central region is deeper relative to the lateral areas). In the central region, another hole is preserved, which was most probably caused by damage.

Remarks. Similar depressions located laterally from the central area with a foramen and being more anteriorly recessed, whereas the foramen opens a canal which continues anterodorsally, can be observed in extant *Chamaeleo chamaeleon* as well. The typical ornamentation formed by distinctly developed and complicated pustular protuberances, which are moderately spaced and not arranged in a ridge here, allows allocation of this cranial bone to the European Miocene chameleon *Chamaeleo andrusovi* Čerňanský 2010b. This species was initially described from the early Miocene of the Czech Republic (Čerňanský 2010b) and later recognized from other areas of Europe (e.g., Georgalis et al. 2016; Čerňanský et al. 2017).

Chamaeleonidae indet.
Fig. 11C–M

Material. Two right maxillae HLMD-Ez 1961–1962, two left dentaries HLMD-Ez 1963–1964.

Description. Maxilla: The specimen HLMD-Ez 1961 (Fig. 11C–E) represents the anterior maxillary section. It bears five small teeth. The fragment is relatively massively built with a slight medial curvature at its anterior end. The bone rises dorsally, but only the base of the facial process is preserved. In medial view, the anterior internal dorsal margin has a rough surface. It can be most likely interpreted as a facet for the premaxilla. The supradental shelf is thin in medial view. However, this structure is well-expanded medially, being broad in ventral view. The external surface of the preserved section of the bone is smooth. The specimen HLMD-Ez 1962 (Fig. 11F, G) represents a posterior maxillary section – a part of the posteroventral process. It bears four teeth. In medial view, the supradental shelf is well-developed. Dorsally from this structure, the maxilla forms a longitudinal depression; a facet for the jugal is present here. The lateral surface of this fragment is smooth.

Dentary: Both dentaries are fragmentarily preserved. The specimen HLMD-Ez 1963 (Fig. 11H–J) represents the anterior portion of the left dentary. The anterior end of the dentary is curved medially, and a large elliptical symphysis is located here. This dentary fragment bears six teeth, although it should be noted that the anterior tooth is broken off. Ventrally to it, the dental groove is present, being shallow rather than deep. The well-developed and straight supra-alveolar ridge floors it. Most of the ventral portion of the Meckel`s groove is damaged. The external surface is pierced by a labial foramen located closed to the ventral margin. The specimen HLMD-Ez 1964 (Fig. 11K–M) bears only two teeth. Its lateral surface shows well-developed triangular interdental grooves (two are preserved), which incline anteroventrally.

Dentition: The tooth implantation is acrodont. Tooth size increases more-or-less posteriorly, but the dentary specimen HLMD-Ez 1964 and maxillary specimen HLMD-Ez 1962 show that at least the last posterior tooth is smaller than the adjacent anterior (probably penultimate) one. The teeth are triangular, with a low degree of tricuspidity – the central cusp is distinctly dominant. The teeth are compressed mediolaterally. The sizes of the inter-dental gaps are small in the anterior region and distinctly widen posteriorly. The large posterior teeth have wide interdental gaps. Thus, their bases are not in contact. On the posterior region of the maxilla, however, the size of the inter-dental gap between the last and the penultimate tooth is small.

Remarks. The absence of pleurodont dentition in the anterior section of the tooth row allows the allocation to Chamaeleonidae without doubts (Čerňanský 2010b; Čerňanský et al. 2020a). In contrast to chamaeleonids, agamids retain a trace of the primitive pleurodont condition in the anterior region (often in caniniform anterior teeth; Moody 1978).

Lacertoidea Estes, Queiroz & Gauthier, 1988
Lacertidae Oppel, 1811

Lacertidae indet.
Fig. 12A, B

Material. Right dentary HLMD-Ez 1992.

Description. Dentary: The description is based on a right dentary that represents the anterior section (Fig. 12A, B). The specimen bears 13 tooth positions with

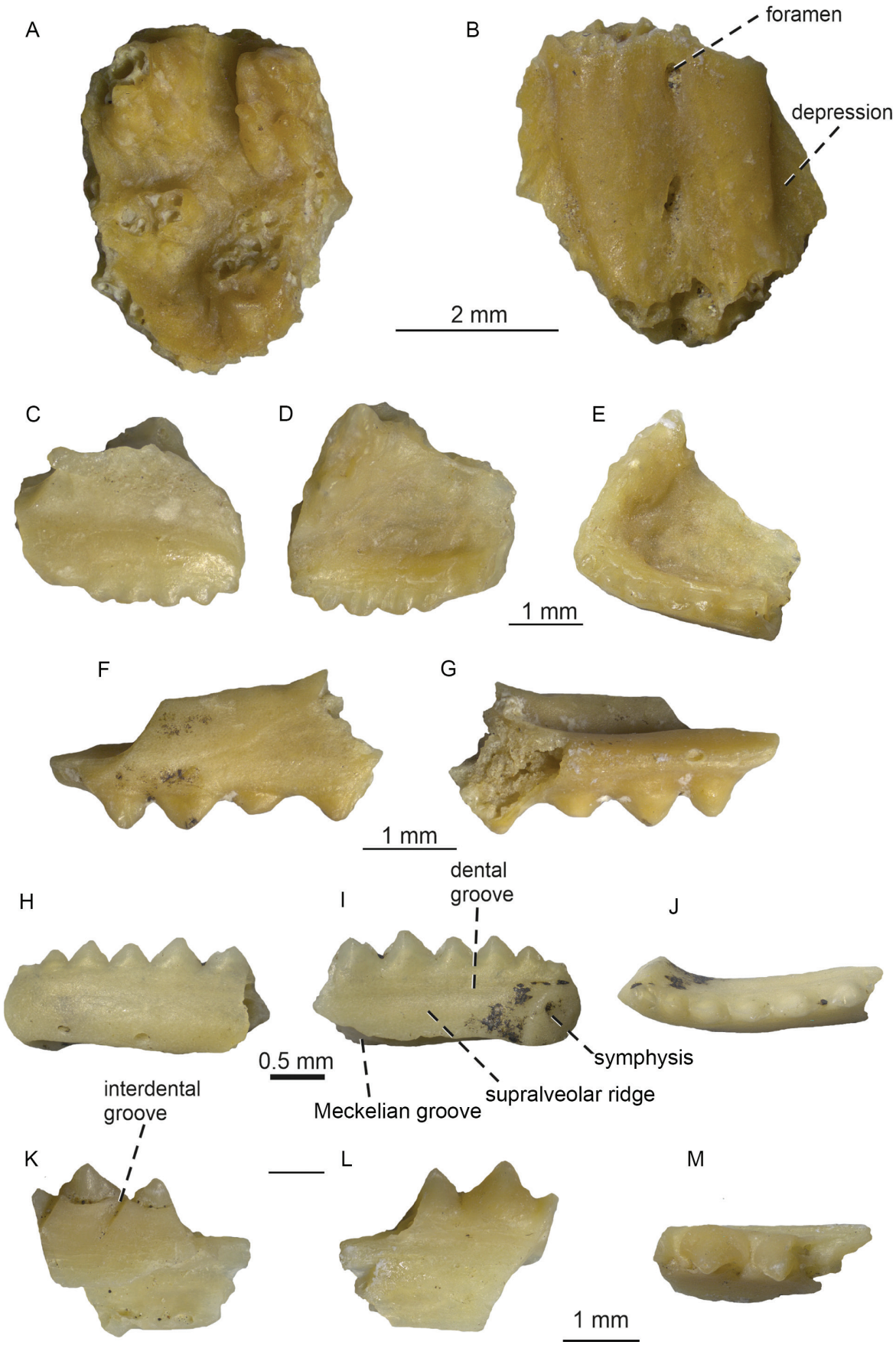

Figure 11. *Chamaeleo andrusovi* (**A, B**) and Chamaeleonidae indet. (**C–M**) from the Echzell locality. Frontal HLMD-Ez 1960 in (**A**) dorsal and (**B**) ventral views. Right maxilla HLMD-Ez 1961 in (**C**) lateral, (**D**) medial and (**E**) ventral views. Right maxilla HLMD-Ez 1962 in (**F**) lateral, and (**G**) medial views. Left dentary HLMD-Ez 1963 in (**H**) lateral, (**I**) medial, and (**J**) dorsal views. Left dentary HLMD-Ez 1964 in (**K**) lateral, (**L**) medial, and (**M**) dorsal views.

nine teeth still attached. However, its posterior region is broken off and the real tooth number is undoubtedly higher. The preserved portion of the dentary is more-or-less robust, anteroposteriorly elongated. The bone gradually narrows anteriorly. In dorsal view, its anterior portion has a small medial curvature. The otherwise smooth lateral surface is pierced by several labial foramina located in the mid-portion of the bone (five are preserved). In medial view, the Meckel`s groove is narrow, entirely open and gradually widens posteriorly. The subdental shelf is medially protruded and robust, especially in the anterior region. It narrows posteriorly because of the presence of the splenial articulation facet. The symphysis is rectangular.

Dentition. The tooth implantation is pleurodont. The teeth are conical and high. They are bicuspid with a dominant distal cusp and smaller accessory mesial cusp. However, the anteriormost dentary teeth are monocuspid, becoming bicuspid starting from the sixth to seventh tooth position. The lingual aspect of the tooth crowns has very fine vertical striations, and the tooth necks bulge slightly medially, with small interdental gaps.

Scinciformata Vidal & Hedges, 2005
Scincidae Gray, 1825
Chalcides Laurenti, 1768

cf. *Chalcides* sp.

Fig. 12C–H

Material. Right maxilla HLMD-Ez 1990, six right dentaries HLMD-Ez 1993–1998, one left dentary HLMD-Ez 1999.

Description. Maxilla: One fragment of a right maxilla is preserved. The specimen HLMD-Ez 1990 (Fig. 12C, D) represents the posterior region of the maxilla. The lateral surface of this specimen is completely smooth. This maxillary fragment bears eight tooth positions with five teeth still attached). The nasal process is partly preserved. Note, however, that the dorsoventral height of the posteriorly located posteroventral process of the maxilla is still significant. Thus, it forms the wall along the entire length of the process here rather than narrowing posteriorly into a tip. Moreover, the shallow notch is developed posteriorly between the dental crest supporting teeth and the dorsally located wall. Although the posterior portion of this dorsal wall is broken off, it can be estimated that, when completely preserved, it exceeds the dental part posteriorly. The dorsal margin of the posteroventral process is slightly damaged, but this portion has a thicker appearance than the ventrally located region possessing a longitudinal depression. This depression partly forms a jugal facet. The ventrally located supradental shelf is thin and expands laterally. It is dorsally convex, but only a small portion is completely preserved. No alveolar superior foramen is preserved here. This highlights a possible anterior position of this foramen.

Dentary: The description is based on several fragments (Fig. 12E–H), most of which represent more-or-less anterior sections. The most complete specimen bears 20 tooth positions; however, its posterior region is broken off. The real tooth number is undoubtedly slightly higher. The dentary is slender, anteroposteriorly elongated. The bone gradually narrows anteriorly. In dorsal view, its anterior portion has a small medial curvature. The otherwise smooth lateral surface is pierced by several labial foramina located in the mid-portion of the bone. In medial view, the Meckel`s groove is narrow, but entirely open. The subdental shelf is medially protruded and robust, especially in the anterior region. It narrows posteriorly because of the presence of the splenial articulation facet. The symphysis is small, rectangular and somewhat narrow.

Dentition: The tooth implantation is pleurodont. The teeth are conical and high. They are closely spaced with small interdental gaps. The tooth crowns are mediolaterally compressed. Thus, the necks have a slightly lingually enlarged appearance. The tooth crowns have blunt apices. In medial view, they have a labial and lingual cusp. The lingual side, bordered by the culmen lateralis posterior and anterior, has striation formed by apicobasal ridges. They are more-or-less parallel to each other and their number usually varies from around five to eight. The labial aspect of the teeth appears smooth. Resorption pits pierce the tooth bases of some teeth.

Remarks. All scincid elements here are assigned to one species based on the significant similarity in the dentition. Moreover, all elements are from the same locality and comparable in size. Besides tooth morphology (see Kosma 2004), the Echzell skink material can be allocated to the clade Scincidae (sensu Hedges 2014; Scincinae sensu Estes et al. 1988) based on the narrow but fully open Meckelian groove in the dentary. This is present in members of the Scincidae clade and in, e.g., *Ateuchosaurus*, whereas it is closed in members of Acontiidae, Sphenomorphidae, Eugongylidae, Lygosomidae, Egerniidae and Mabuyidae (see, e.g., Greer 1970, 1974; Evans 2008; Hutchinson and Scanlon 2009; Čerňanský et al. 2020b; Čerňanský and Syromyatnikova 2021).

The specimens resemble members of the genus *Chalcides*. The Miocene species of this taxon is represented by *Chalcides augei* (see Čerňanský et al. 2020b) and the Echzell material shows similarities to this taxon. Note that usually five striations are reported in *Ch. augei*, it can range from five to seven, and the small variation in the number of striae (from five to seven ot eight) can be seen in specimens from Austria as well (Čerňanský 2016). However, the limitation of the Echzell material does not allow alpha taxonomy and caution is needed here.

Anguimorpha Fürbinger, 1900
Anguidae Gray, 1825
Anguinae Gray, 1825

Smithosaurus gen. nov.

http://zoobank.org/4D22CE09-4ABF-438A-8870-230F484F5D5D

Fig. 13

Etymology. We name this genus in honour of American paleoherpetologist Krister T. Smith for his valuable contributions to vertebrate paleontology and particularly

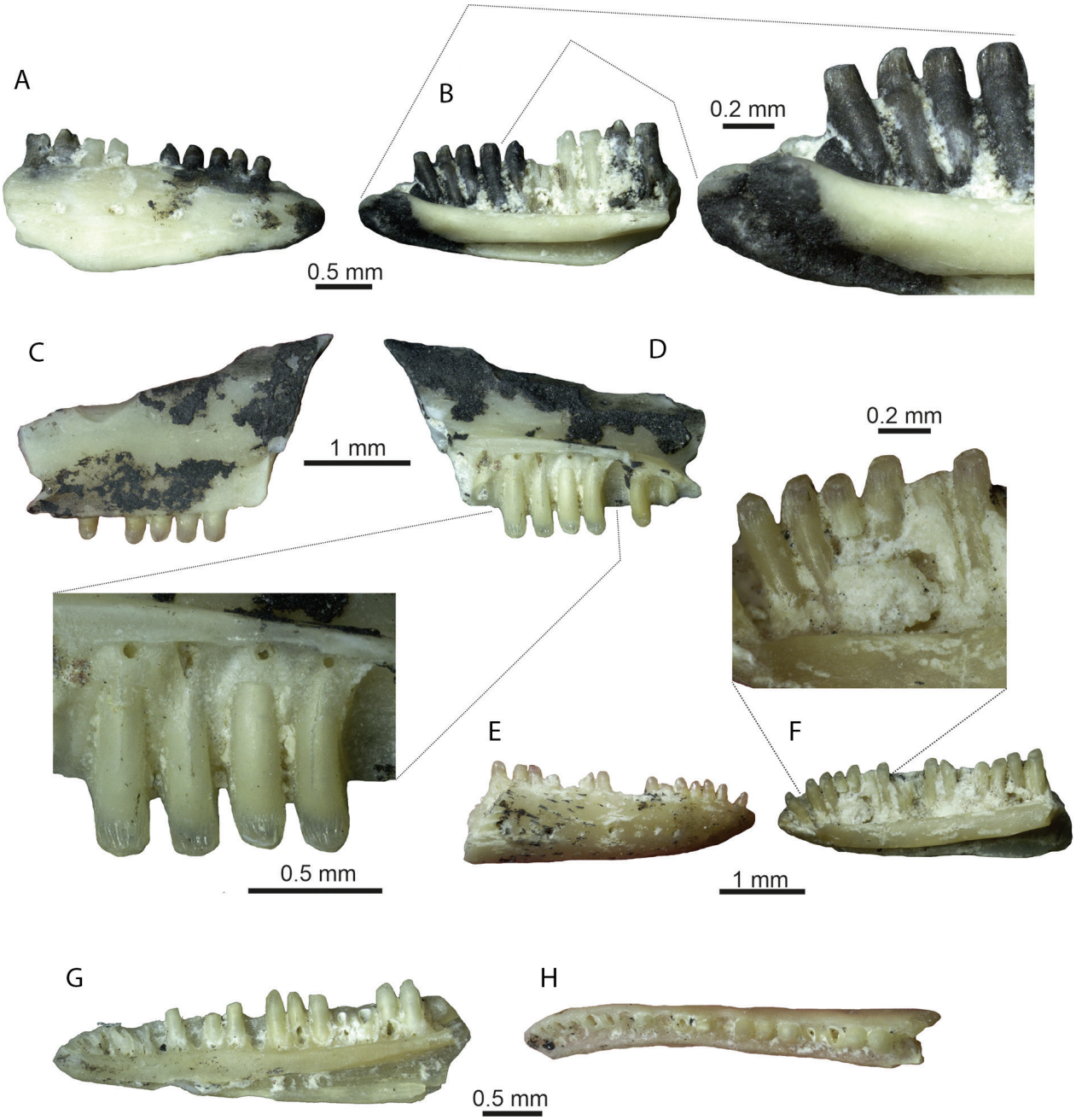

Figure 12. Lacertidae indet. (**A, B**) and cf. *Chalcides* sp. (**C–H**) from the Echzell locality. Right dentary HLMD-Ez 1992 in (**A**) lateral and (**B**) medial views with a detail of dentition. Right maxilla HLMD-Ez 1990 in (**C**) lateral and (**D**) medial views with a detail of dentition. Right dentary HLMD-Ez 1994 in (**E**) lateral and (**F**) medial views with a detail of dentition. Right dentary HLMD-Ez 1993 in (**G**) lateral, and (**H**) medial views.

to squamate morphology and evolution; and from Greek σαύρα [saura], lizard.

Diagnosis. As for *Smithosaurus echzellensis*, the only known species.

***Smithosaurus echzellensis* gen. et sp. nov.**

http://zoobank.org/ED8797D9-46FE-4462-BA43-A32D16934582

2014 *Ophisaurus spinari* – Böhme and Vasilyan: p. 29, fig. 3f.

Etymology. Based on the locality Echzell in Germany – one of two known localities, where this taxon occurred.

Holotype. One parietal UMJGP 204.749.

Paratype. One parietal HLMD-Ez 1965.

Range. Germany (Echzell), early Miocene; Austria (Gratkorn), late middle Miocene.

Remarks. Both parietals – HLMD-Ez 1965 from the early Miocene Echzell locality and UMJGP 204.749 from the late middle Miocene Gratkorn locality in Austria (see Böhme and Vasilyan 2014; fig. 3f), exhibit the same unique combination of features and can be placed to a single taxon without any doubts. Because the parietal UMJGP 204.749 (Fig. 13A, B) is better preserved than HLMD-Ez 1965 (Fig. 13C, F), it has been designated as the holotype for the new taxon.

Diagnosis. Anguine lizard distinguishable from *Anguis*, *Pseudopus* and *Ophisaurus* by two autapomorphic features:

(1) the parietal table gradually expands laterally in the anterior direction in an extreme way; thus, it appears to be distinctly constricted at the level of the parietal foramen or slightly posterior to it. The lateral margins of the table markedly diverge anterolaterally from this point, inclining at an angle of about 30° from the median plane. Posteriorly located lateral margins diverge gradually posterolaterally and continue to more-or-less straight supratemporal processes. Due to the lateral expansion of the parietal table, the anterolateral corner of the parietal table reaches further laterally than the supratemporal process. The ornamented surface on the dorsal side of the bone gradually widens anteriorly as well (in contrast to being rectangular);
(2) the parietal cranial crests diverge in the anterior direction to form a V that separates the cranial vault from the muscular surface laterally (the anteriormost section of the crests bents laterally rather than medially).

Besides these two autapomorphic features, this taxon is characterized by the unique combination of the following characters: (1) the occipital shield is large, its anteroposterior length is longer than the length of the posteriorly located smooth area; (2) a narrow muscular surface is present; (3) a short postfoveal crest is present; (4) anterior end of the ventrolateral ridge of the supratemporal process joins the parietal cranial crest at the level anterior to the posteromedial margin of the floor of the parietal fossa. The parietal crest is sharp in the area of the junction; (5) the virtual line, continuing from the ventrolateral ridge of the supratemporal process to the anterior margin of the parietal table, reaches the level as the lateral margin of the parietal foramen here; (6) the supratemporal process has a smooth ventrolateral surface, which fluently continues anteriorly to the muscular surface of the parietal table; and (7) the supratemporal process is straight.

Description. Parietal: The parietal UMJGP 204.749 (Fig. 13A, B) from Gratkorn is fairly preserved, whereas HLMD-Ez 1965 (Fig. 13C, D) from Echzell represents the posterior half of the parietal table, with the left supratemporal process being, however, only partly preserved. The description is therefore based mostly on the holotype UMJGP 204.749. The ornamented surface of several fused headshield osteoderms covers most of the parietal table. The ornamentation consists of well-developed foramina and pits of various sizes, being densely distributed. At the periphery of the ornamented surface, radiated grooves and ridges are developed. The interparietal shield is well recognized in both specimens. This region is pierced by the large anteroposteriorly elongated parietal foramen. Unfortunately, its anterior margin is not preserved. The occipital shield is very large. Its anteroposterior length is twice as long as the length of the posteriorly located smooth area. The parietal notch is well developed. The lateral (=parietal) shields are preserved (but note that the almost entire lateral margins of the parietal table in HLMD-Ez 1965 are damaged). The arcuate edge runs on the dorsal surface of the bases of the supratemporal processes and diminishes laterally. The right supratemporal process is almost completely preserved, being straight. The parietal table extremely widens anteriorly – so it appears to be distinctly constricted at the level of the parietal foramen or slightly posterior to it. Thus, the lateral margins of the table markedly diverge anterolaterally from this point, inclining at an angle of about 30° from the median plane. Due to the lateral expansion of the parietal table, the anterolateral corner of the parietal table reaches further laterally than the supratemporal process. The anterolateral corners protrude into anterolateral processes. The ornamented surface is not rectangular but gradually widens anteriorly as well. The anterior end of the interparietal sulcus lies medial to the anterolateral corner of the ornamented surface.

On the ventral surface, many diagnostic features can be recognized. The oval parietal fossa is small, located in the central posteriormost region of the parietal table. The short postfoveal crests are well developed. In ventral view, both cranial crests are preserved, especially the complete right one, including the anterior portions missing in the Echzell specimen. The cranial crests are sharp. They diverge anteriorly, forming a V-shaped outline that separates the cranial vault from the muscular surface laterally. The muscular surface is narrow, but present. The virtual line, continuing from the ventrolateral ridge of the supratemporal process to the anterior margin of the parietal table, reaches the level as the lateral margin of the parietal foramen here. The ventrolateral ridge of the supratemporal process is well developed and preserved on the right side in UMJGP 204.749 and left side in HLMD-Ez 1965. Its anterior end joins the parietal cranial crest at the level anterior to the posteromedial margin of the parietal fossa. The cranial crest is sharp in this region. The root portion of the supratemporal process is broad. The other distal portion distinctly narrows posteriorly. The ventrolateral ridge is well developed. The supratemporal articulation extends anteriorly, being well visible on the lateral surface of the supratemporal process. Anteriorly to it, between the most anterior portion of the ventrolateral ridge and the anterolateral margin of the supratemporal process, a short ventrolateral surface can be recognized. This surface lies posterior to the parietal cranial crest-supratemporal process junction (note that it is broadly damaged in the Echzell specimen).

Remarks. See the discussion part.

Phylogenetic analysis of *Smithosaurus echzellensis*. The phylogenetic trees presented here are based on limited fossil material – the parietal, and thus more complete fossil specimens of this taxon are needed to draw more robust conclusions. However, in both two analyses, *Smithosaurus echzellensis* is consistently recovered as the sister taxon to either [*Ophisauriscus quadrupes* + *Ophisaurus holeci*] + [*Anguis* + *Ophisaurus*] (in the first analysis) or [*Anguis* + *Ophisaurus*] (in the second analysis). In overall, the support for the clade is very low (no strict synapomorphy; the calculating Bremer supports

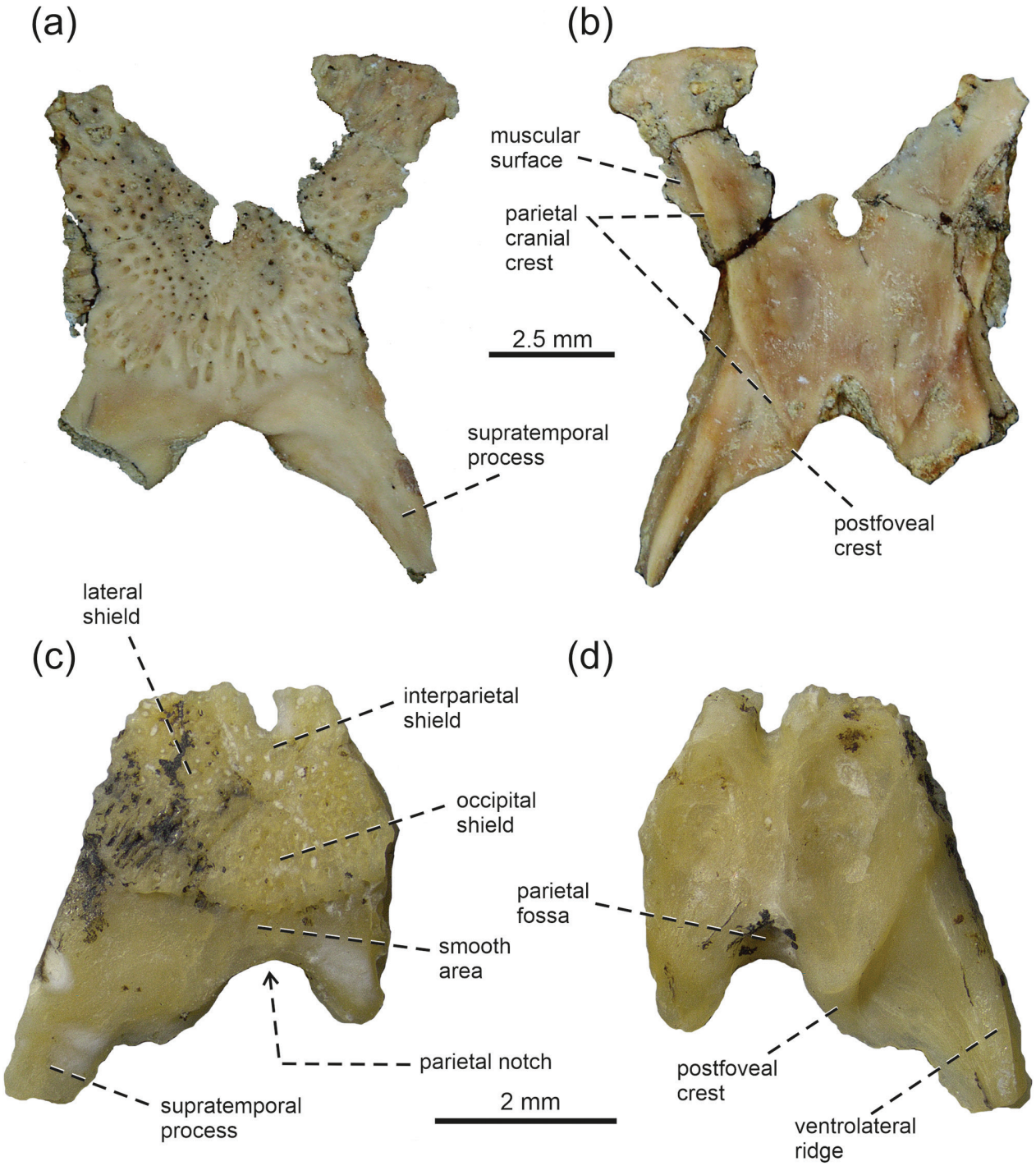

Figure 13. *Smithosaurus echzellensis* gen. et sp. nov. Holotypic parietal UMJGP 204.749 from the Gratkorn locality in (**A**) dorsal, and (**B**) ventral views. Paratypic parietal HLMD-Ez 1965 from the Echzell locality in (**C**) dorsal and (**D**) ventral views.

collapsed the node into polytomy, see below) and thus, the interpretation of the *Smithosaurus* relationship among anguines needs to be met with caution.

1. A New Technology (NT) search in TNT produced a single tree (Fig. 14A). The position of *Smithosaurus echzellensis* is recovered as being sister to the clade [[*Ophisauriscus quadrupes* + *Ophisaurus holeci*] + [*Anguis* + *Ophisaurus* (all others except of *O. holeci*)]]. The calculating Bremer supports collapsed the node (Bremer value 1, relative Bremer 25; Fig. 14B), with the relationship among *Smithosaurus echzellensis* and the clades [*Ophisauriscus quadrupes* + *Ophisaurus holeci*] (Bremer value 3, relative Bremer 50) and [*Anguis* + *Ophisaurus*] (Bremer 2, relative Bremer 50) being unresolved.
2. The heuristic search in TNT produced two equally parsimonious trees. In both,

Smithosaurus echzellensis is recovered as sister to [*Anguis* + *Ophisaurus* (all others except of *O. holeci*)], whereas *Ophisauriscus quadrupes* and *Ophisaurus holeci* are sister to the clade formed by *Smithosaurus*, *Anguis* and *Ophisaurus* (all others except of O. *holeci*). This is contrary to the results from the NT analysis (see above). In the strict consensus tree, however, the position of *Smithosaurus* is unresolved among [*Ophisauriscus quadrupes* + *Ophisaurus holeci*] and [*Anguis* + *Ophisaurus* (all others except of *O. holeci*)], although all these taxa together form a clade. Thus, the topology of examined taxa in this strict consensus tree is identical to that figured in Fig. 14B.

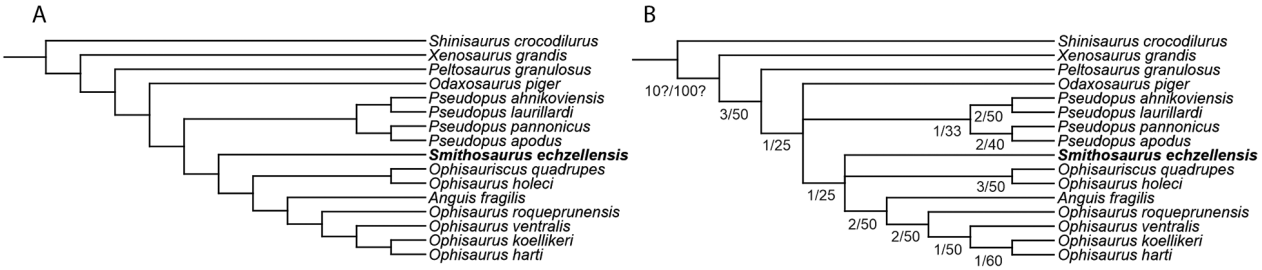

Figure 14. Phylogenetic position of *Smithosaurus echzellensis*. **A.** Single parsimonious tree recovered by TNT using NT (New Technology) search (with ratchet) and 1000 iterations; **B.** Tree showing Bremer / relative Bremer values at nodes recovered by TNT.

Anguinae indet.

Fig. 15

Material. One right maxilla HLMD-Ez 1966, one right and one left dentaries HLMD-Ez 1967–1968, 12 dorsal vertebrae HLMD-Ez 1969–1980.

Description. Maxilla: Only a fragment of the right maxilla is preserved (Fig. 15A, B). It represents the area around the superior alveolar foramen plus the section of the posteroventral process. This maxillary fragment bears eight tooth positions (one tooth is still attached). The otherwise smooth lateral surface is pierced by the labial foramina – three and a half are preserved. The medial side bears the well-developed supradental shelf. At the level of the fifth tooth position (counted from posterior), the shelf expands medially to form the palatine articulation. At this level, the superior alveolar foramen is located on the dorsal side of the shelf. Only the base of the nasal process is preserved; the rest of the bone is broken off. The posterior portion gradually narrows into the posteroventral process. Its dorsal margin smoothly decreases ventrally without being stepped.

Dentary**:** Two dentary fragments are preserved, both representing only the posterior portions (Fig. 15C–F). The right one (HLMD-Ez 1967) possesses five tooth positions, where the penultimate and fourth (counted from posterior) are still partly preserved. Except for two labial foramina, the lateral surface is smooth (only one foramen is preserved in HLMD-Ez 1968). The medial surface exhibits open Meckel`s groove, which narrows anteriorly. It is roofed by the concave, shallow subdental shelf. The position of the anterior inferior alveolar foramen between the dentary and a splenial can be recognized at the level of the fifth tooth position, but this area appears to be eroded. The alveolar foramen is located at the level of the third tooth position. The intramandibular septum, which separates the alveolar canal from Meckel`s groove, is completely fused with the body of the dentary (the free ventral portion is absent). The surangular spine is damaged, so only its root portion can be recognized. The angular process is broken off. The other posterior processes are damaged. The left dentary HLMD-Ez 1968 represents a specimen with four tooth positions – only one complete tooth and the base of another one are still preserved. The position of the anterior inferior alveolar foramen can be still recognized on the subdental shelf. The splenial spine is absent in both specimens. Due to poor preservation of this area, however, this appears to represent a postmortal damage only.

Dentition: The tooth implantation is shallowly pleurodont. The teeth are large, well exposed over the dorsal crest, which supports them laterally. They are conical and distinctly recurved. Their tips are pointed. The mesial and distal cutting edges are well developed. The tooth bases are broad, being pierced by resorption pits. In most cases, the pits are located slightly posterior to the tooth axis. The dentary teeth are smooth by weathering (or affected by digestive process of carnivores), the maxillary tooth crown possesses fine but dense striations on both labial and lingual sides.

Dorsal vertebra: The description is based on the well-preserved specimen HLMD-Ez 1969 (Fig. 15G–J). The vertebral centrum is anteroposteriorly elongated. The height of the vertebra gradually increases posteriorly. The neural spine is low, however, its dorsal portion is broken off. It forms a ridge running along almost the entire length of the dorsal section of the neural arch. In dorsal view, the ridge is thin, becoming less distinct in the anterior section. In the posterior third of its length, it is well defined and widens at its posterior end. The neural canal is high and well arched dorsally. The cotyle is depressed, being mediolaterally expanded and broader than the neural canal. However, the maximum height of the cotyle is

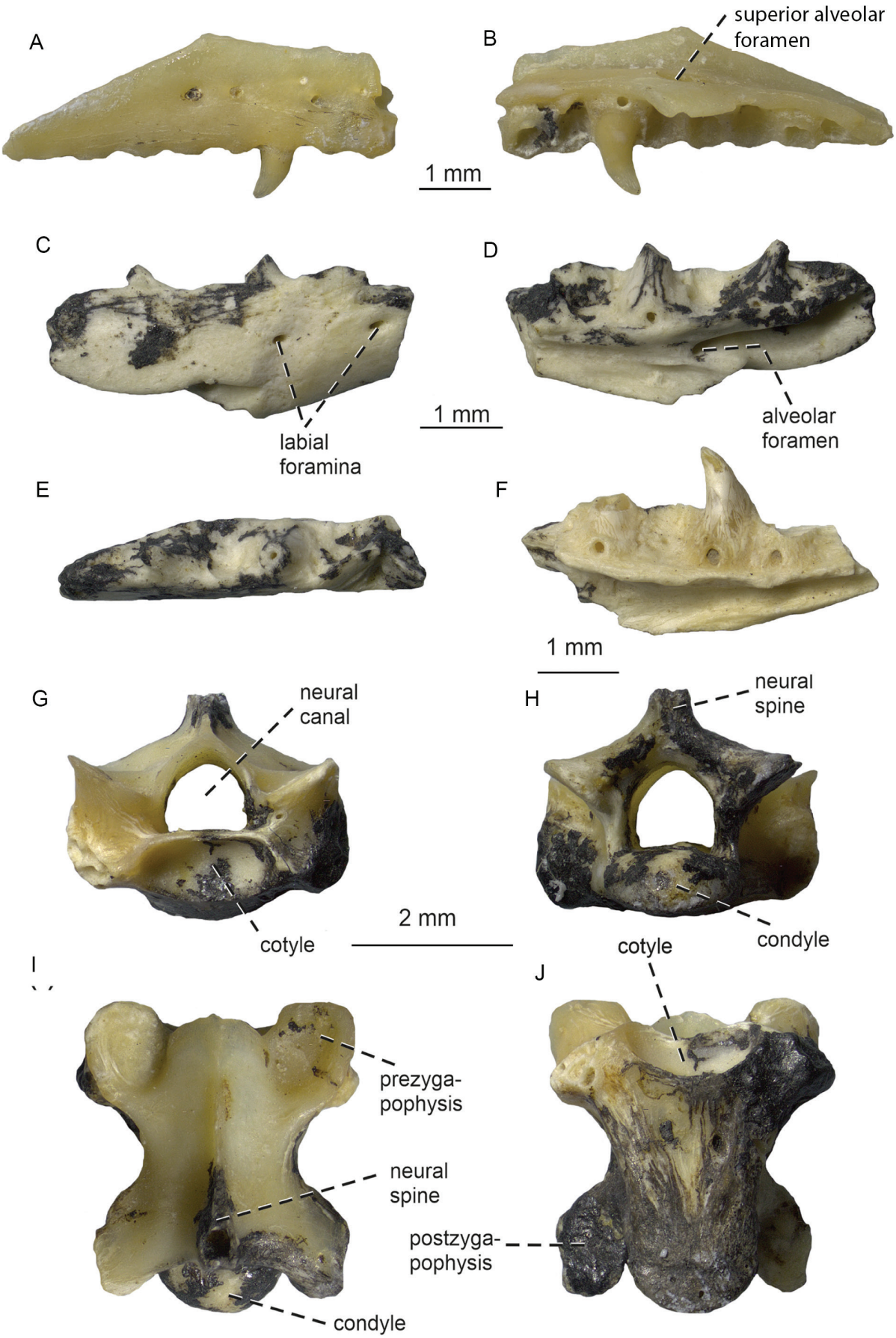

Figure 15. Anguinae indet. from the Echzell locality. Right maxilla HLMD-Ez 1966 in (**A**) lateral, and (**B**) medial views. Right dentary HLMD-Ez 1967 in (**C**) lateral, (**D**) medial and (**E**) dorsal views. Left dentary HLMD-Ez 1968 in (**F**) medial view. Dorsal vertebra HLMD-Ez 1969 in (**G**) anterior, (**H**) posterior, (**I**) dorsal and (**J**) ventral views.

lower than the maximum dorsoventral height of the neural canal. The pre- and postzygapophyses are well expanded laterally; a well-developed interzygapophyseal constriction is located between them. The pre- and postzygapophyses have elliptical articulation surfaces, oriented more or less anteroposteriorly. The prezygapophyses are inclined from the horizontal plane at an angle of approximately 30°. The synapophyses are protruding laterally, being square in shape. The condyle, which is well-protruded posteriorly, is markedly depressed as well as the above-mentioned cotyle. The ventral surface of the centrum is flat. It is pierced by two subcentral foramina in the anterior one-third of the centrum. The lateral margins of the centrum have a concave course, running more anterolaterally from the level of the subcentral foramina.

Remarks. Among extant anguine genera, the morphology of herein described vertebrae resembles that of *Ophisaurus* (Čerňanský et al. 2019). The maxilla with markedly recurved teeth and vertebrae similar to those from Echzell have been described also from Gratkorn (see Böhme and Vasilyan 2014). Such a distinct tooth curvature is not very typical among members of extant *Ophisaurus* (see Klembara et al. 2014), but can be found in fossil species, e.g. in *O. acuminatus* (see Klembara and Čerňanský 2020). However, it should be noted that some features in the dentary, such as the presence of a splenial spine, cannot be supported with confidence due to poor preservation. Moreover, another crucial reason exists why the allocation of this material to *Ophisaurus* might be problematic – the occurrence of a new taxon *Smithosaurus echzellensis* in both Echzell and Gratkorn localities. We cannot entirely exclude the very plausible option that some of those specimens (if not all) belong to this newly described taxon. For this reason, we allocated this material only as Anguinae indet. Caution is also needed in regards to interpretations of isolated jaw fragments and isolated vertebrae from other European Miocene localities, where such incomplete and fragmentary materials are often described as *Ophisaurus*. More complete and articulated material of *Smithosaurus echzellensis*, in which bones can be associated together to observe the anatomy of this taxon, is crucial to resolve this problem.

Anguidae indet.

Fig. 16

Material. Four caudal vertebrae HLMD-Ez 1981–1984, 73 osteoderms HLMD-Ez 1985–1987 (figured ones), HLMD-Ez 1988 (the remaining osteoderms).

Description. Caudal vertebra: The caudal vertebrae (Fig. 16A–E) are elongate and narrow. Both pre- and postzygapophyses are small; thus, there is a typical tendency toward the elongation of the centra in caudal vertebrae and a relative reduction of all processes. The cotyle and condyle are dorsoventrally depressed. The neural canal is a tunnel-like structure here. The haemapophyses are fused to the posterior portion of the centrum, but, unfortunately, their ends are broken off. Only the bases of the anteroventrally oriented transverse processes (pleurapophyses) are preserved, being dorsoventrally slightly flattened. They are pierced by a foramen. The distal portions are, however, broken off. The neural spine is posterodorsally oriented, rather slim and pointed. The transverse autotomic split is present.

Remarks. The presence of an autotomic split indicates that we can exclude *Pseudopus*, in which only autotomic foramina are developed (see Čerňanský et al. 2019). In contrast, the autotomic split is present in both *Anguis* and *Ophisaurus* (see Hoffstetter and Gasc 1969).

Osteoderm: A large number of osteoderms of several types are preserved in the material. The first type represents wide, rectangular osteoderms (e.g., HLMD-Ez 1985, Fig. 16G–F). There is a low medial ridge running along their central regions. However, the ridge is almost indistinctive and restricted only to the sculptured region. The anterior overlap surface is large and occupies about one-third of the external surface. The lateral bevel is the highest close to the overlap surface. The posterior portion of the external surface is ornamented. The ornamentation is formed by several tubercles, pits, long grooves, and ridges diverging from the central region. Three foramina pierce the central part of the internal surface. The second type (and the most common, as represented by HLMD-Ez 1986, Fig. 16H) includes slender osteoderms. In those, the medial ridge runs along the entire external surface, including both ornamented and anterior overlap surface. The third type (rare, HLMD-Ez 1987, Fig. 16I) is represented by a flat and wide osteoderm without a medial ridge.

The differences might very likely represent individual variability and a different body topology from where osteoderms originated (e.g., ventral vs. dorsal armour; see, e.g., Čerňanský and Klembara 2017). Their determination to the alpha taxonomy level is currently impossible. Nevertheless, they resemble osteoderms of *Ophisaurus*, but other taxa cannot be excluded.

Squamata indet.

Fig. 17A–F

Material. One premaxilla HLMD-Ez 1989, right quadrate HLMD-Ez 2002, left pterygoid HLMD-Ez 2003, two osteoderms HLMD-Ez 2000–2001.

Description. Premaxilla: Premaxilla HLMD-Ez 1989 (Fig. 17A–C) represents a small element, although with a more-or-less robust appearance. It is almost fully preserved. It is a single, unpaired T-shaped element (note, a groove or break is running through the midline, see remarks). The premaxilla bears seven-tooth positions with three teeth still attached to the dental parapet. The laterally extended maxillary processes are well developed. They are rather short than long. They possess an articulation facet for the maxilla on their dorsolateral surfaces. The fragmentarily preserved nasal process is wide, its external surface is flat. Here, a few small vestiges of osteoderms attached to the bone are present. In anterior and posterior views, the base of the nasal process

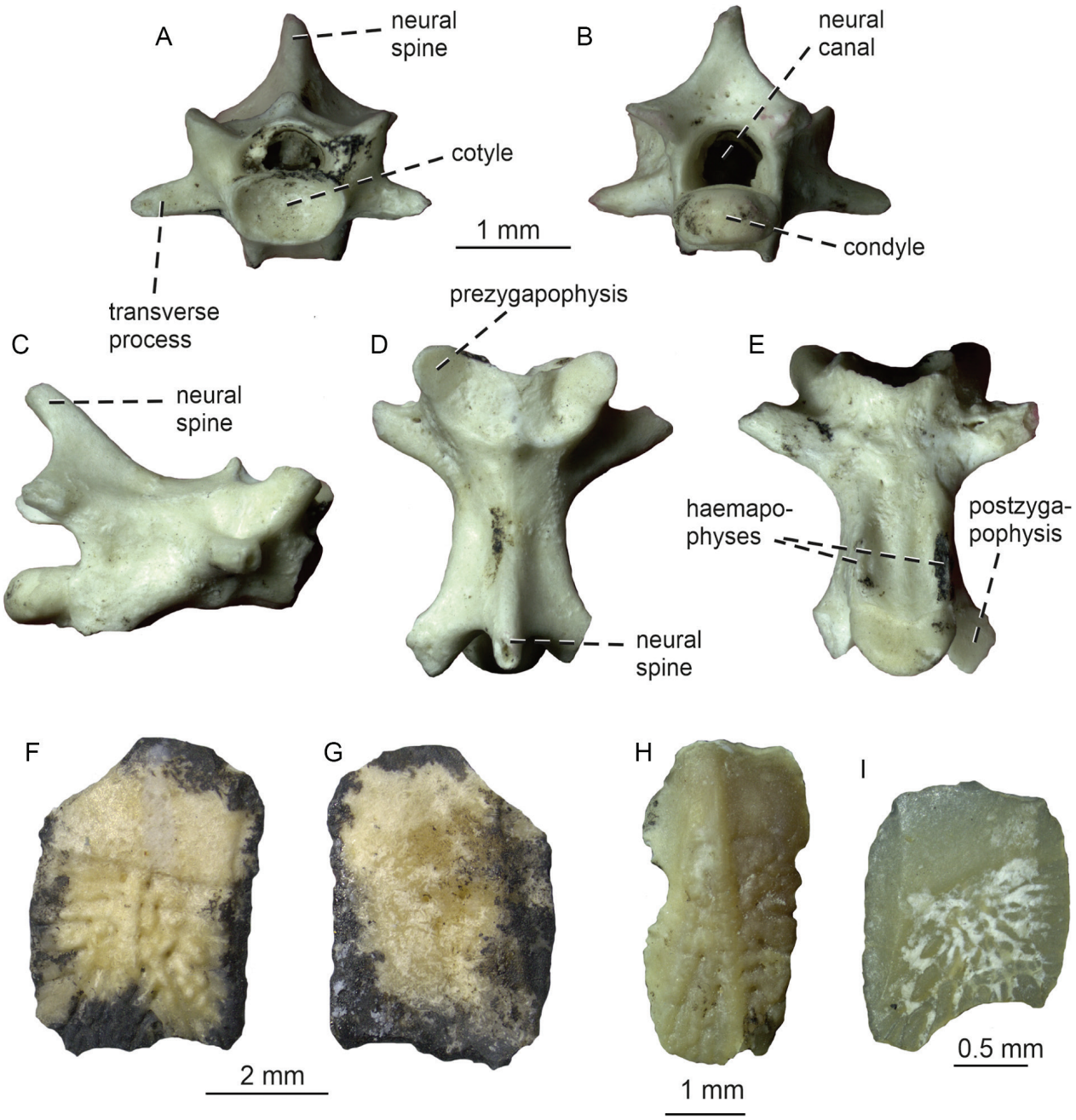

Figure 16. Anguidae indet. from the Echzell locality. Caudal vertebra HLMD-Ez 1981 in (**A**) anterior, (**B**) posterior, (**C**) lateral, (**D**) dorsal and (**E**) ventral views. Osteoderms HLMD-Ez 1985 (**G**), HLMD-Ez 1986 (**E**) and HLMD-Ez 1987 (**I**) in (**F, H, I**) external and (**G**) internal views.

is laterally constricted. Thus, the lateral margins in the lowest region of the process are rounded, having a cut-out like appearance. Dorsally, this region is wide, having more-or-less parallel lateral margins. The most dorsal preserved portion of the process narrows abruptly again, but the rest of the process – the posterodorsal portion with a termination - is broken off. On the internal side, there is a sagittal ridge running along the entire length of the preserved nasal process. It separates the facet for the nasals on both sides. On the lateral side, the ethmoidal foramen is located close to the base of the nasal process. The supradental shelf is formed by two segments, which are well expanded posteriorly. The dorsal side bears the vomerine process, which forms a small bulge. The short, weakly bilobed median incisive process is located ventral to the supradental shelf.

Remarks. Although the right and left premaxillae are fused, note that there is a fracture-like structure (or a tiny groove) running through the central portion of the element. However, it is unclear whether this is postmortal damage only or reflects the fusion of the right and left premaxillae during ontogeny. Even if it is only a fracture

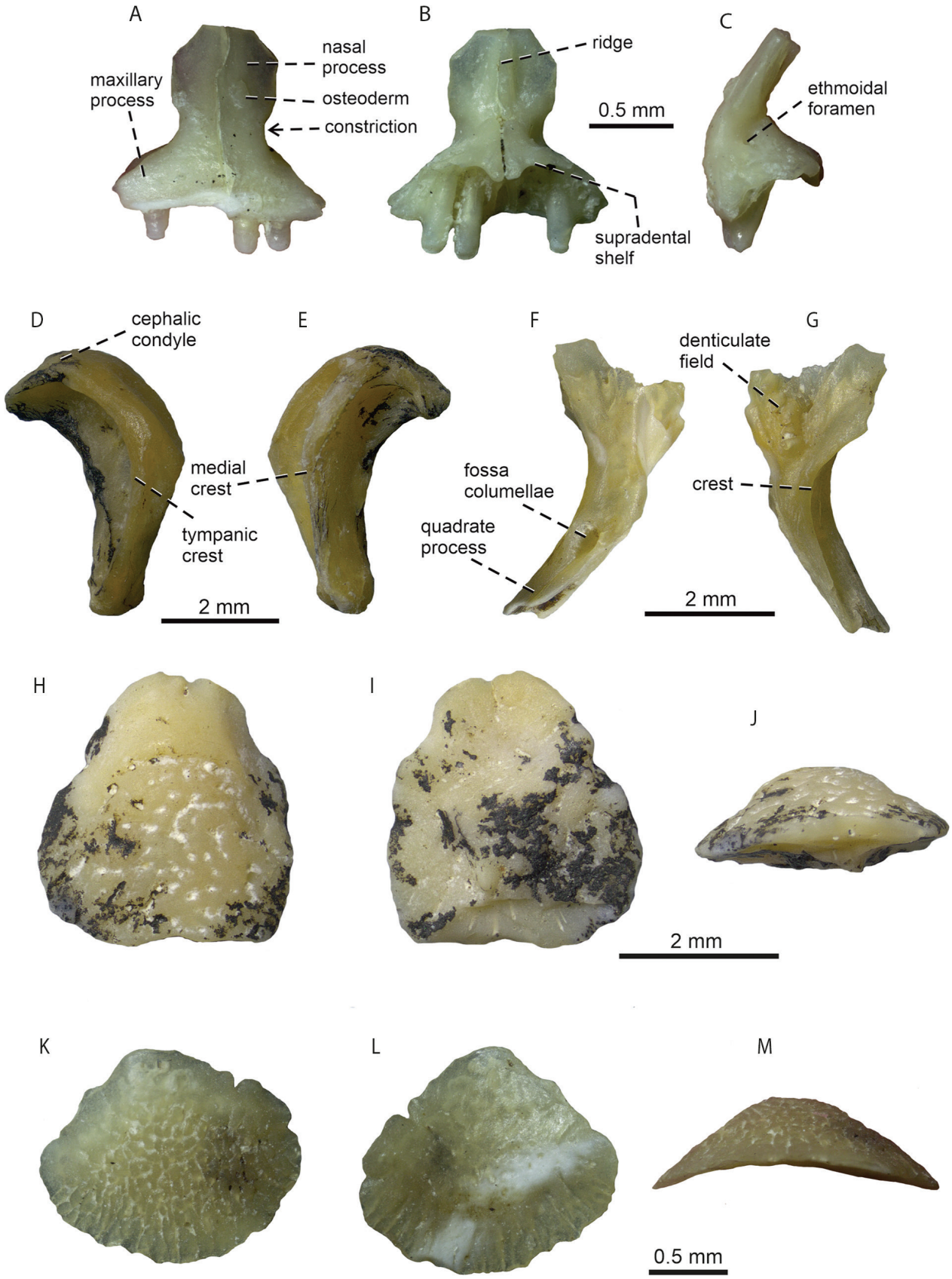

Figure 17. Squamata indet. from the Echzell locality. Premaxilla HLMD-Ez 1989 in (**A**) anterior, (**B**) posterior, and (**C**) lateral views. Right quadrate HLMD-Ez 2002 in (**D**) lateral, and (**E**) medial views. Left pterygoid HLMD-Ez 2003 in (**F**) dorsal and (**G**) ventral views. Osteoderms HLMD-Ez 2000 (**H–J**) and 2001 (**K–M**) in (**H, K**) external, (**I, L**) internal and (**J, M**) posterior views.

caused by damage, the central region might be weaker due to the late fusion and, thus, prone to breakage when pressure is applied. Among *Chalcides* species, a groove indicating a fusion is often present in various degrees (for *Ch. ocellatus*, see Digimorph.org 2002–2012; in some, e.g., *Ch. polylepis*, the right and left premaxillae are separated; see, e.g., Caputo (2004); pers. obs. of A.Č.). However, its lacertid affinity can not be excluded. The premaxilla of lacertids is formed by a single element (see, e.g., Čerňanský and Syromyatnikova 2019). If the specimen HLMD-Ez 1989 represents a lacertid, the present groove is caused by postmortal damage only. In any case, we decided to allocate this specimen to Squamata indet.

Quadrate: A right quadrate is available in the material (Fig. 17D, E). It is a slender, dorsoventrally elongated element. In lateral view, the quadrate is anteroposteriorly narrow, with an anteriorly expanded, rounded anterior margin. Here, the sharp and laterally expanded tympanic crest is present. This crest is continuous from the cephalic to the mandibular condyle. The crest is slightly angled approximately in the mid-region. Further dorsally, it fluently and gradually continues without being distinctly separated by a sharp angle from the portion formed by the cephalic condyle. The dorsal portion of the cephalic condyle protrudes slightly posteriorly. The ventral half of the quadrate narrows gradually ventrally. The ventral region ends with the saddle-shaped mandibular condyle. It is slightly smaller than the cephalic condyle. The medial surface possesses a distinct medial crest. Posterior to this crest, the bone is pierced by a quadrate foramen located in the ventral one-third of the dorsoventral height of the element.

Remarks. The morphology of the quadrate HLMD-Ez 2002 is similar to that of lacertids (see e.g., Čerňanský and Syromyatnikova 2019) rather than anguids. Note, however, that the general shape of the lacertid quadrate resembles that of scincids (see Villa and Delfino 2019b),

Pterygoid: The left pterygoid is incompletely preserved (Fig. 17F, G). It is a tri-radiate, Y-shaped element. Its ventral portion bears a distinct dentition located in the central region. Only the base of the ectopterygoid process is preserved, being broad. From its posterior region, a sharp crest runs to the quadrate process. Here, the crests border a fossa located laterally on the process. The quadrate process is long but note that its end is broken off. The fossa columellae (= epipterygoid fossa), which is present on the dorsal side, is large and elliptical.

Identification of isolated elements as pterygoids is problematic and caution is needed. However, the morphology of HLMD-Ez 2003, e.g., the absence of the obtuse process (ventromedial process sensu Conrad 2008), indicates that we can exclude Anguidae here. Its morphology, including the crests bordering a fossa located laterally on the quadrate process, resembles skinks. Although note that dentition is absent in e.g., *Chalcides occelatus*, but present in, e.g., *Plestiodon fasciatus* (see Caputo 2004; Digimorph.org 2002–2012).

Osteoderm: Two osteoderms are available in the material. The larger osteoderm HLMD-Ez 2000 (Fig. 17H–J) is roughly trapezoidal in shape. It is thick, with distinct external bulging. Its external surface expands in the anterior direction, being gradually more pronounced. This gives a convex appearance in cross-section. The whole osteoderm gradually narrows anteriorly. Here, the well-developed anterior overlap surface is located, forming one-third of the entire anteroposterior length of the osteoderm. Its anterior mid-region bears a short groove, which is present on the internal side as well. The region posterior to the overlap surface bears ornamentation. The ornamentation appears to be rather weak and not dense, being formed mostly by ridges and pits, connected by short grooves in some cases. The medial ridge is absent. The internal aspect of the osteoderm is not flat, but is rough. It has several irregularly distributed pits, foramina, and a few grooves near the posterior end.

The smaller specimen HLMD-Ez 2001 (Fig. 17K–M) is wide. Its width is slightly greater than its anteroposterior length. The anterior portion, which bears a narrow overlap surface, is triangular, whereas the posterior portion has a round margin. The osteoderm is thick, although note that it is narrower relative to its size if compared to the larger one. Here, the internal surface of the smaller osteoderms is slightly concave. The ornamentation of the external surface is formed by densely spaced ridges and grooves running from the ossification centre; those ones located on the periphery are prolonged.

The differences in these two osteoderms can be caused by ontogeny and different origins regarding the body topology. Overall, this type of osteoderms resembles the osteoderms described by Čerňanský (2016; fig. 11) as Squamata indet. 2 from the lower Miocene of the Austrian locality Oberdorf. They might very likely belong to skink.

Serpentes Linnaeus, 1758
Boidae Gray, 1825
Bavarioboa Szyndlar & Schleich, 1993
Bavarioboa hermi Szyndlar & Schleich, 1993

Bavarioboa cf. *hermi*

Fig. 18A–E

Material. Forty-two trunk vertebrae HLMD-Ez 2146–2148, one cloacal vertebra HLMD-Ez 2149, four caudal vertebrae HLMD-Ez 2150 and HLMD-Ez 2150a.

Description. Trunk vertebrae: All but one trunk vertebrae come from the middle trunk portion of the column. Some of them are preserved in relatively good condition, perhaps due to their robust morphology as characteristic of constrictors. In lateral view, these vertebrae are as high as long. In dorsal and ventral views, they are distinctly wider than long. In the largest and best-preserved vertebra HLMD-Ez 2148, the centrum length measures 5.7 mm, centrum width – 7.2 mm, centrum length/centrum

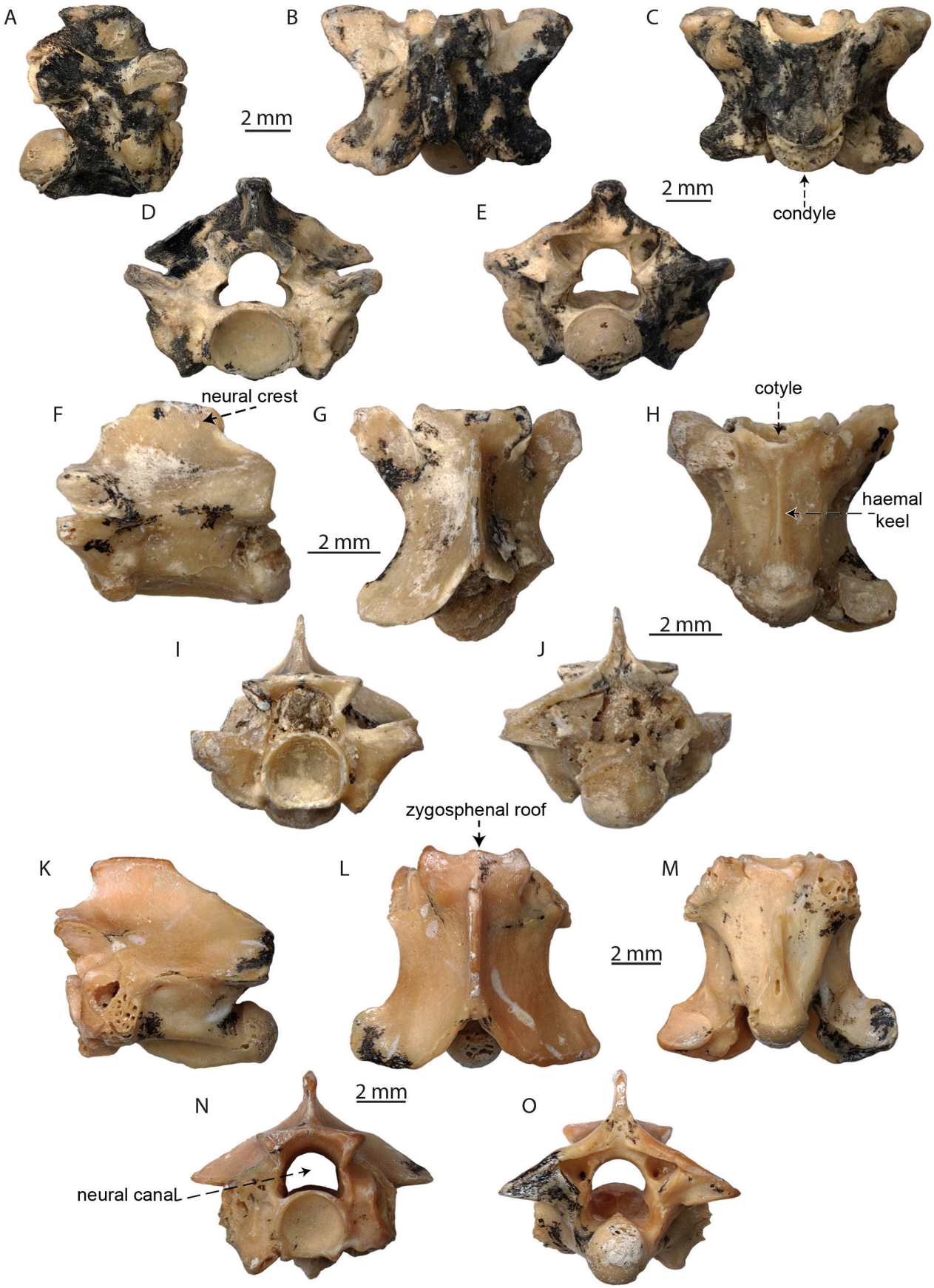

Figure 18. Snakes from the Echzell. **A–E.** *Bavarioboa* cf. *hermi* (HLMD-Ez 2148), middle trunk vertebra; **F–J.** "Colubrinae" indet. (HLMD-Ez 2159), middle trunk vertebra; **K, L.** *Naja* cf. *romani* (HLMD-Ez 2151), middle trunk vertebra. All vertebrae in (**A, F, K**) lateral, (**B, G, L**) dorsal, (**C, H, M**) ventral, (**D, I, N**) anterior and (**E, J, O**) posterior views.

width equals 0.8. The interzygapophyseal constriction, especially in larger vertebrae, is weakly expressed. The centrum is subtriangular in shape. The haemal keel is prominent, broad and slightly broadening posteriorly. In a few vertebrae, however, the keel looks like a biconcave lens owing to the presence of a distinct constriction, located at the level of the subcentral foramina, and prominent broadenings at the anterior and posterior ends. The subcentral grooves and subcentral ridges are prominent. The neural arch is moderately depressed. The neural spine is very low (approximately three times longer than high), thick, and widening posteriorly (Fig. 18A). It occupies more than one half the length of the neural arch and begins immediately behind the zygosphenal articular facets. The zygosphenal roof is slightly convex or roughly straight in dorsal view. The prezygapophyseal and postzygapophyseal articular facets are usually subsquare in shape. The prezygapophyseal processes (if preserved) are very short and hardly visible dorsally. The paradiapophyses are subsquare in outline, higher than long, with indistinct subdivision into para- and diapophyseal portions. The cotyle and condyle are slightly flattened. The subcentral and lateral foramina are large. The paracotylar foramina are absent (Fig. 18D).

In the sole anterior trunk vertebra HLMD-Ez 2146, the haemal keel is replaced by a ventrally directed hypapophysis (its distal portion is broken). The neural spine of this vertebra is very short and relatively high in lateral view. Apart from these characteristics, the anterior trunk vertebra does not differ significantly from the middle trunk vertebrae.

Cloacal vertebra: One cloacal vertebra HLMD-Ez 2149, as characteristic for the sacral portion of the column, is provided with paired lymphapophyses (their distal ends are broken). The centrum length measures 3.4 mm, centrum width – 4.1 mm, centrum length / centrum width equals 0.8. Surprisingly, located on the ventral side of the centrum, minute but distinct paired haemapophyses are present, thus far the trait unknown in the genus *Bavarioboa* (see below).

Caudal vertebrae: Four caudal vertebrae are provided with paired pleurapophyses (missing or partly missing in some vertebrae). In the largest caudal vertebra HLMD-Ez 2150, the centrum length is 4.0 mm, centrum width 4.5 mm, centrum length / centrum width 0.9. Situated on the ventral side of the centrum, are short but distinct paired haemapophyses (partly broken).

Remarks. The constrictor from Echzell displays clearly diagnostic features of the genus *Bavarioboa*, so among others: mid-trunk vertebrae distinctly wider than long; the interzygapophyseal constriction well expressed; the neural arch moderately depressed; the neural spine approximately as high as long, occupying one half the length of the neural arch; the haemal keel prominent; the zygosphene usually roughly straight; the prezygapophyses located clearly above the floor of the neural canal; the long axis of prezygapophyseal facets oblique in dorsal view; the prezygapophyseal processes weakly developed; the paradiapophyses subsquare in shape, with indistinct subdivision into para- and diapophyseal portions (Szyndlar and Rage 2003). By their morphological characteristics and also relatively large size, the vertebrae are similar to those of the type species, *Bavarioboa hermi*, occurring in the German and Czech late early Miocene (Szyndlar and Schleich 1993; Szyndlar and Rage 2003; Ivanov et al. 2020). However, the peculiar hourglass-shaped haemal keels observed in a few trunk vertebrae suggest affinities with *Bavarioboa crocheti* from the French late Oligocene. Interestingly, the sole mid-trunk vertebra of *Bavarioboa* reported from Turkey by Szyndlar and Hoşgör (2012) was provided with a similar (i.e., *crocheti*-like) keel. Nonetheless, other morphological traits of the vertebrae from Echzell suggest that the snake represented *Bavarioboa hermi* or a closely related form.

There is yet another strange anatomical peculiarity observed in the sole cloacal vertebra of *Bavarioboa* from Echzell, namely the presence of the paired haemapophyses. This is surprising, because, in virtually all recent genera of the Boinae, haemapophyses are absent in the sacral region of the column as well as they are absent in the anterior caudals. Exactly the same morphological pattern was observed in some species of *Bavarioboa*, whose vertebrae coming from the sacral / anterior caudal portion of the column of which were available (Szyndlar and Rage 2003). However, there is at last one exception from this tendency in the Boinae, namely, the presence of haemapophyses was confirmed in the posterior cloacal vertebrae (as well in the anterior caudals) in the living boine *Epicrates cenchria* (Szyndlar, unpublished observation).

Colubridae Oppel, 1811
Natrix Laurenti, 1768

Natrix longivertebrata Szyndlar, 1984

Fig. 19

Material. One basisphenoid HLMD-Ez 2158.

Description. The basiphenoid is fragmentary. Its anterior portion, at the level of the anterior orifices of the Vidian canals approximately, is missing. The maximum width of the bone, measured between distal tips of the basipterygoid processes, is 3.7 mm. In ventral view, the basisphenoid crest is absent (Fig. 18A, B). The basipterygoid processes are distinct. Their posterior margins are strongly extended posteriorly covering the recess housing the posterior foramina of the Vidian canals. However, a tiny proximal fragment of the left basipterygoid process is broken off, owing to which the posterior orifice of the Vidian canal as well as the cerebral foramen (for palatine branch of facial nerve, VII) are clearly visible in ventral view.

In dorsal view, several foramina are visible, distributed typically of higher snakes (Fig. 18C, D). The paired largest foramina, located at the midway between

the posterior border of the bone itself and the posterior border of the pituitary fossa (sella turcica), are posterior openings for the abducens nerves (VI). The anterior openings for these nerves are situated near the postero-lateral corners of the pituitary fossa. The sympathetic nerve foramina (not visible on the right side) are located directly anterior to the pituitary fossa. The paired openings piercing the basipterygoid processes, laterally to the abducens nerve foramina, are tentatively interpreted as the deep petrosal nerve foramina (both visible on the left side only).

Seen in left lateral view, an opening located directly above the posterior orifice of the Vidian canal and partly hidden beneath the basipterygoid process, is interpreted as a foramen for re-entry of the constrictor internus dorsalis branch (cid) of the trigeminal nerve (V_4) on its way from the prootic (Fig. 19E, F). The location of the exit of the latter nerve (either within the basisphenoid or in a suture between the basisphenoid and parietal) remains unknown owing to the damage of the bone anterior to the basipterygoid processes.

Remarks. Apart from the basisphenoid, the available snake material from Echzell does not contain any other elements, in particular vertebrae, identifiable as belonging to natricine snakes. This absence of any vertebrae is astonishing, considering that in virtually all fossil sites, if they yield snake cranial remains, the latter are typically accompanied by vertebrae. Unfortunately, this is not the case of the material from Echzell. Theoretically, some vertebral fragments classified here as "Colubroides indet." could belong to natricines, but it cannot be proved on the studied material.

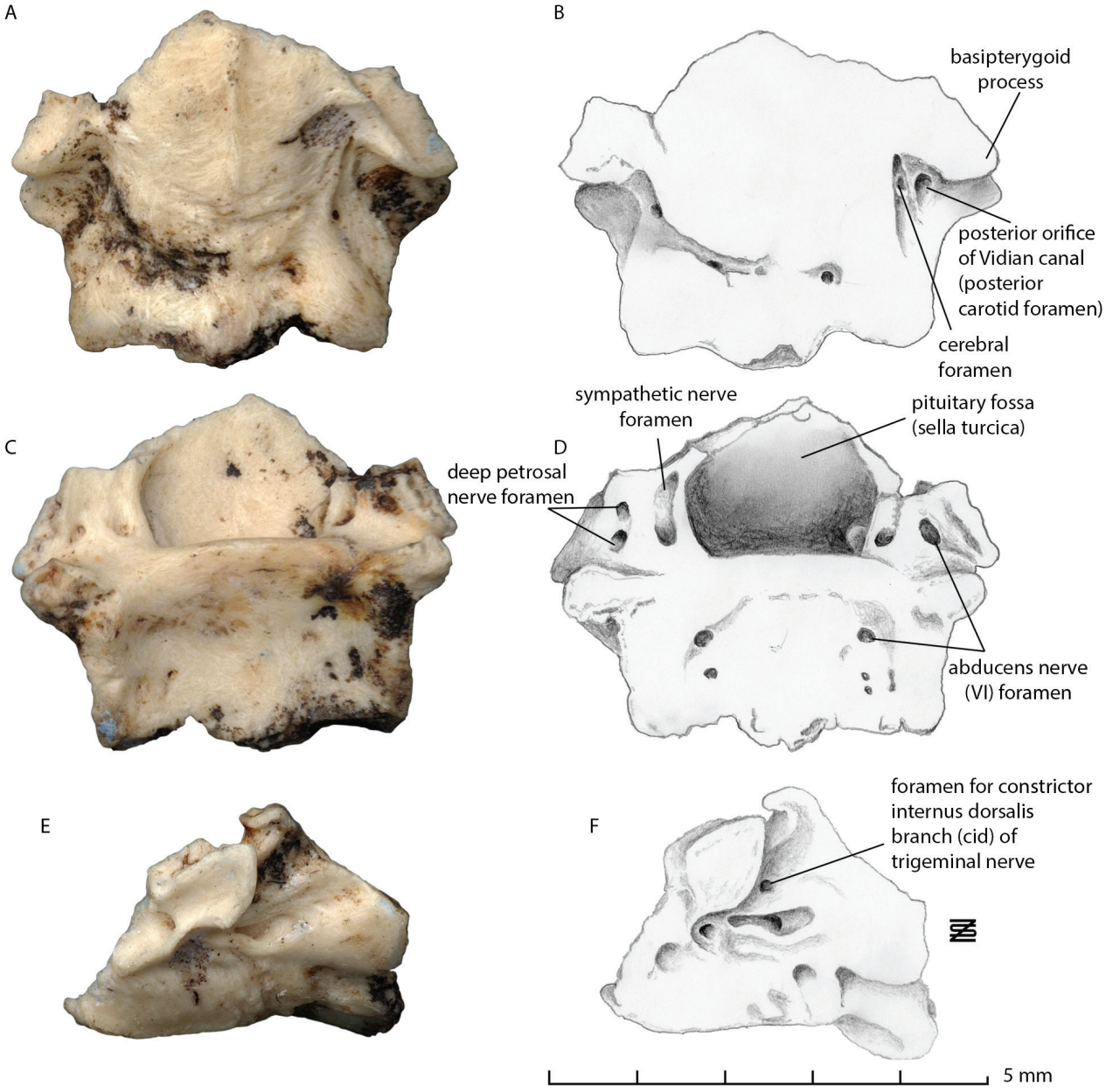

Figure 19. Basisphenoid of *Natrix longivertebrata* (HLMD-Ez 2158) in (**A, B**) dorsal, (**C, D**) ventral and (**E, F**) left lateral views.

The basisphenoid from Echzell is clearly referable to the extinct snake *Natrix longivertebrata*. By its peculiar morphology, it significantly differentiates not only from basisphenoids of other natricines (except for *N. astreptophora*, see below) but also from those belonging to members of other ophidian families (Szyndlar, unpublished observations).

"Colubrinae" indet.

Fig. 18F–J

Material. Seventy trunk vertebrae HLMD-Ez 2159 and HLMD-Ez 2159a.

Description. Vertebrae: All vertebrae classified here as "Colubrinae" are preserved in more or less fragmentary state; most are badly preserved. The largest vertebra, coming from the middle trunk portion of the column HLMD-Ez 2159 (Fig. 18F–J), belonged to a relatively small-sized snake (centrum length measures 4.5 mm, centrum width – 3.6, centrum length / centrum width ratio equals 1.25). It lacks both prezygapophyseal processes and right postzygapophysis. The centrum of most vertebrae is subtriangular in ventral view and slightly longer than wide in the largest vertebrae. In a number of smaller vertebrae, interpreted as posterior trunk vertebrae, the centrum is more elongated. The subcentral ridges are well developed. The haemal keel is distinct and slightly widening before reaching the condyle base. The neural arch is moderately vaulted, not accompanied by any epizygapophyseal spine. The neural spine (partly preserved in few vertebrae only) is twice longer than high approximately. The zygosphenal roof (preserved in few vertebrae) is roughly straight or consisting of three indistinct lobes. The prezygapophyseal articular facets are oval (Fig. 18G), the postzygapophyseal facets are usually subsquare in shape (Fig. 18H). The prezygapophyseal processes are damaged in all vertebrae. Remnants of the processes preserved in one (?posterior) vertebra indicate that the apophyses may have been slender and relatively long (as long or almost as long as the prezygophyseal articular facets). The paradiapophyses (usually eroded) are moderately developed, with the dia- and parapophyseal portions of roughly equal length (Fig. 18I). The cotyle and condyle are slightly depressed dorso-ventrally. The lateral, subcentral and paracotylar foramina are small but distinct.

Remarks. Owing to the bad preservation state of the aforementioned remains, we refrain from identifying the fossil snake to the genus level. The remains resemble roughly those of a number of small "colubrines" (i.e., "Colubridae" devoid of hypapophyses throughout the column) reported from several early Miocene sites (Szyndlar 2012). We cannot exclude the possibility that the fossils belonged to more than one taxon, but it cannot be proved.

Elapidae Boie, 1827
***Naja* Laurenti, 1768**
***Naja romani* (Hoffstetter, 1939)**

Naja* cf. *romani

Fig. 18K–O

Material. Four fangs HLMD-Ez 2157, 50 trunk vertebrae HLMD-Ez 2151–5156.

Description. Fangs: Four isolated teeth are venomous fangs. They are tubular, with acute distal tips. The discharge orifice, located on the anterior surface of each fang, is elongate and gladiate-shaped. The discharge orifice extends, towards the proximal end, in the form of a visible suture. The latter condition is characteristic of elapid snakes, whereas in viperids the anterior surface of the fang is generally smooth. Relatively small dimensions of the fangs suggest that they either belonged to juvenile / subadult individuals or were replacement (non-functional) fangs.

Vertebrae: Most vertebrae come from the middle trunk portion of the column. In the largest (but partly damaged) vertebra (HLMD-Ez 2151, Fig. 18K–O), centrum length measures 7.1 mm, centrum width – 5.7 mm, and centrum length / centrum width ratio equals 1.25. At least in large vertebrae, the centrum is triangular in ventral view, with a flat or slightly concave ventral surface. The subcentral ridges are well developed, especially behind the paradiapophyses. The hypapophysis, preserved partly in few vertebrae, is thick, strongly inclined posteriorly and shows a straight anteroventral margin. The neural arch is rather depressed. The neural spine, preserved partly in few vertebrae, is approximately twice longer than high. Its anterior margin is straight. The shape of the posterior margin is unknown. The paradiapophyses are well developed with short but distinct parapophyseal processes (the latter is preserved only in two vertebrae). The zygosphenal roof is almost straight or slightly convex in dorsal view. The prezygapophyseal and postzygapophyseal articular facets are relatively small and oval-shaped. The prezygapophyseal process (preserved only on the left side of one vertebra) is well developed, somewhat shorter than the articular facet and possesses also a moderately obtuse tip. The cotyle and condyle are suborbicular or slightly depressed. The subcentral, lateral, and paracotylar foramina are distinct (Fig. 18K–M).

A few trunk vertebrae coming from the posterior trunk portion of the vertebral column are more elongated than those from the middle portion. One vertebra (HLMD-Ez 2154; centrum length 4.1 mm, centrum width is 3.0 mm, centrum length / centrum width ratio 1.4) is provided with a completely preserved hypapophysis. The hypapophysis is dagger-shaped and directed posteriorly.

Remarks. Based on the overall vertebral morphology, cobras can be rather easily differentiated from other European fossil snakes. The vertebrae of cobras "mimic" the morphological pattern characteristic of large-sized

"colubrines" but, unlike the latter, they are provided with hypapophyses throughout the trunk portion of the column. The vertebrae described above generally display the anatomical features characteristic (e.g., dagger-shaped and posteriorly directed hypapophysis) of the extinct species *Naja romani* (Szyndlar 2005). Considering the fragmentary state of preservation of the fossils, we prefer to use the species name with the qualifier "cf.".

Colubroides indet.

Material. Fifty-seven caudal vertebrae HLMD-Ez 2160.

Remarks. The caudal vertebrae (all damaged, in most cases badly preserved) belong most likely to small-sized advanced snakes (i.e., different than *Bavarioboa*). Because of the poor preservation, the vertebrae were not identified to the family level.

Serpentes indet.

Material. Fifty-six vertebrae HLMD-Ez 2161.

Remarks. All these elements are minute vertebral fragments (rather than fragmentary vertebrae). They display ophidian characteristics, but besides more precise identification is not realizable.

Discussion

The Echzell fauna consists of one allocaudate – *Albanerpeton inexpectatum*, five salamanders – *Chioglossa* sp., *Mertensiella* sp., *Lissotriton* sp., *Salamandra* sp., *Chelotriton* sp., five frogs – *Latonia*, *Palaeobatrachus robustus*, *Pelophylax* sp., *Rana* sp., *Pelobates sanchizi*, a gecko – Gekkota indet., a chameleon *Chamaeleo andrusovi*, and anguine lizards, also represented by a new genus and species, – *Smithosaurus echzellensis*, a lacertid, a skink – cf. *Calcides* sp., four snakes – *Natrix longivertebrata*, "Colubrinae" indet., *Naja* cf. *romani*, *Bavarioboa* cf. *hermi.* In addition to them, Tobien (1954) mentioned also shell plates of testudinid tortoises which, unfortunately, could not be relocated in the collection of the HLMD and made available for our study. Clearly, the Echzell assemblage does not include the primary paleofauna and thus, a better picture of the fauna as well as our interpretations can be improved by further material collection. For the palaeobiogeographic analysis of the Echzell herpetofauna, we provide an overview of the well-documented amphibian and reptilian assemblages from European localities of the MN3–MN4 zones. The record of amphibians and reptiles follows the references cited in the caption of Table 2. The entire herpetofauna of Echzell is represented by genera very broadly known in the early Miocene of Europe.

The analysis suggests that fossil records of higher taxonomic groups are significantly biased by taphonomic and/or environmental conditions. For instance, the lack of *Latonia* from both localities of Mokrá-Western Quarry is interpreted by Ivanov (2008) to be a result of the depositional environment. Testudinids are entirely missing in e.g. Oberdorf, Austria, whereas for Mokrá-Western Quarry, Czech Republic they have not been studied yet (Table 2). Moreover, many lizard groups, which often occur in other European localities, are missing in Echzell (see below).

We have compared the early Miocene European herpetofauna (Table 2) with the Anatolian one (Vasilyan et al. 2019) as much as the taxonomy of the latter record allows it. The over-regional scale comparison suggests similar frog (*Latonia*, Palaeobatrachidae, Pelobatidae, Bufonidae) and salamander (*Salamandra*) faunas, whereas the lacertids are quite diverse in comparison to Europe. The taxonomic assignment of the anguids from Anatolia does not allow any comparison with the European record. Other groups are missing from the fossil assemblages, or the identification is not as precise as necessary to compare.

Amphibians

The amphibian assemblage of Echzell is represented by characteristic forms commonly known from the (early) Miocene of Europe, e.g. *A. inexpectatum*, *Chioglossa*, *Mertensiella*, *Salamandra*, *Latonia*, *Palaeobatrachus* etc. (Table 2). The remains of *Chelotriton* are the most abundant, whereas *Albanerpeton*, *Chioglossa*, *Mertensiella*, *Salamandra* are less abundant. The genera *Chioglossa* and *Mertensiella*, being phylogenetically sister groups (Pyron and Wiens 2011), have rather synchronous and exclusively European fossil occurrence since the late Oligocene – early Miocene (Böhme and Ilg 2003). Their recent areas are limited to humid forested regions of Western Europe (*Chioglossa*) and Western Asia (*Mertensiella*) (Sparreboom 2014). Surprisingly, in a number of Western and Central European early Miocene localities, they have sympatric occurrences (e.g., see Table 2). Osteologically, the genera can be distinguished by few characters of trunk vertebra, see, e.g. Ivanov (2008), Hodrová (1984). Most probably, Western and Central European early Miocene *Chioglossa* and *Mertensiella* represent the earliest forms of the genera and suggest a European origin of the clade *Chioglossa*+*Mertensiella*. However, due to recent advances in molecular phylogeny (e.g., Wielstra et al. 2010; Recuero and García-París 2011), a better understanding of the diversity of these genera as well as other recent genera, e.g., *Salamandra*, *Lissotriton*, *Triturus* is available. A detailed osteological study (including other skeletal elements than vertebra) of the recent forms, taking into account the current knowledge of molecular studies, will enable more precise identification of the fossil material, for instance, at the species or species-group level.

Among other salamanders, it is interesting to note that the Echzell assemblage includes only one form of *Chelotriton* contrary to, e.g. both localities of Mokrá Western Quarry

(Ivanov 2008). As discussed before, the Echzell *Chelotriton* sp. differs morphologically from all other forms of the genus from MN3–MN4 localities. This has been already observed earlier and interpreted as interspecific variability (Schoch et al. 2015) or uncovered high specific or generic diversity (Vasilyan 2020) for the genus. The second option seems rather probable, considering the present-day biodiversity of the genus *Tylototriton* (Hernandez 2016), a genus most probably related to the European fossil *Chelotriton*.

Two of the five frog taxa, *Latonia* and *Pelobates*, are most abundant in the Echzell assemblage. The species *P. sanchizi* is commonly found in the middle to early late Miocene European localities. So far, the species *P. sanchizi* has been described only from two MN4 localities Mokrá-Western Quarry 1/2001 and 2/2001 and from other younger localities correlated to MN6 and younger zones. A gap in the stratigraphic occurrence at the transition of the early-middle Miocene is "filled" by another species, *P. fahlbuschi* from Sandelzhausen, Germany (Böhme 2010). *P. sanchizi* from Echzell, representing one of the oldest fossil records of the species, extends its geographic occurrence during the early Miocene (MN4) of Europe.

Palaeobatrachus robustus from Echzell extends the stratigraphic occurrence of the species, so far limited to MN2. It was confidently known from the early Miocene (MN2) locality Laugnac, France (Hossini and Rage 2000). Another probable occurrence has been mentioned for the late Oligocene of Germany (loc. Oberleichtersbach; Böhme 2008), where a fragmentary frontoparietal has been identified as *Palaeobatrachus* sp., showing affinities with *P. robustus*. The figured Oberleichtersbach specimen of *Palaeobatrachus* sp. aff. *P. robusutus* in Böhme (2008; plate 3, fig. 7) resembles the morphology of Echzell frontoparietals. The taxonomic identification of the palaeobatrachids both at the generic and species level relies on the frontoparietal morphology (Wuttke et al. 2012; Roček et al. 2015). Unfortunately, this bone has very limited preservation potential in the fossil record, which hinders species-level identification of the material and a better understanding of the stratigraphic occurrence of the species. Nevertheless, the Echzell record of the species suggests a longer presence of the species in Europe during the Miocene.

The other two frog taxa, *Pelophylax* sp. and *Rana* sp., are represented by very few remains. These two genera are also commonly found in all localities of similar age. In general, the comparison of anuran assemblages of MN3–MN4 localities (Table 2) suggests that representatives of the Bufonidae, Hylidae, Pelodytidae families are rarely found. It could be related to the absence of environments, e.g., dry habitats for *Bufotes*, or in general rare occurrences of those clades in the amphibian assemblages.

Lizards

Although the Echzell lizard material is only fragmentarily preserved, it provides essential information on the paleobiodiversity and spatial distribution of lizard taxa in the early Miocene. Several major clades can be recognized: Gekkota, Chamaeleonidae, Anguidae and Scincidae. Overall, the Echzell lizard assemblage is similar to other European localities from MN4, e.g., Dolnice and Mokrá Western-Quarry in the Czech Republic (see Roček 1984; Čerňanský 2010b, 2010c; Ivanov et al. 2020) and Oberdorf in Austria (Čerňanský 2016) (see Table 2). Interestingly, amphisbaenians, varanids, cordylids and the genus *Pseudopus* were not recognized in the material available to us. Lacertids are very limited in Echzell based on the material available to us, although they are very abundant in other localities of this age (Čerňanský 2010c, 2016; Ivanov et al. 2020). The missing group represents large-sized animals, which might point to potential taphonomic and/or sampling biases. However, an environmental bias cannot be excluded since a large size animal (testudinid tortoises) has been reported with one fragment from the locality.

Regarding chameleons, the frontal is partly preserved. The bone described here, although preserved only as a fragment, represents the first described frontal of the extinct species *Chameleo andrusovi* Čerňanský, 2010b.

Regarding the parietal bone, three genera of anguines (where this element can be studied) are recognized in the Neogene of Europe until now: *Pseudopus*, *Anguis* and *Ophisaurus* (including problematic *O. holeci*, see below). Note that these taxa also represent extant lineages. However, the parietals from Echzell and Gratkorn have unique features (plus combination of other character states, see diagnosis) which do not allow to allocate them to any of the currently known genera. Therefore, we have erected a new taxon, *Smithosaurus echzellensis*. The parietal UMJGP 204.749 from Gratkorn was originally allocated to *Ophisaurus spinari* (Böhme and Vasilyan 2014; note that originally three other parietals from Gratkorn were erroneously assigned to anguines) but Klembara and Rummel (2018) recognized its unique morphology in regard to other taxa. The occurrence of a new genus in the Neogene of Europe shows a greater diversity of anguines than previously thought. Besides the clear autapomorhic features typical for this new taxon, it exhibits interestingly a mixture of features of *Ophisaurus*, *Anguis* and *Pseudopus*: (1) a short postfoveal crest – this character state is typical for *Pseudopus* (and present also in the fossil taxon *Ophisaurus holeci*, but absent in *Anguis* and all other *Ophisaurus*; see Klembara 2015; Čerňanský and Klembara 2017; Čerňanský et al. 2019); (2) narrow muscular surface – the large muscular surface is present in *Pseudopus* (a narrow one is developed in some large individuals of *O. holeci* as well, see Klembara et al. 2019); (3) a large occipital shield, its anteroposterior length is longer than the length of the posteriorly located smooth area. This is typical for *Anguis* (Klembara and Rummel 2018; Čerňanský et al. 2020a); (4) the parietal notch present – this can be seen in *Anguis* and *Ophisaurus* (e.g., Čerňanský et al. 2015; Klembara et al. 2019); (5) the supratemporal process with a smooth ventrolateral surface, which fluently continues anteriorly to the muscular surface of the parietal table (a typical character state in *Pseudopus* (see e.g., Klembara

et al. 2017; Klembara and Rummel 2018)); (6) a straight supratemporal process – this is present in *Pseudopus*, but not in *Anguis* and all other *Ophisaurus* species studied except of *O. holeci* (see e.g., Čerňanský and Klembara 2017; Klembara et al. 2019); (7) the anterior end of the ventrolateral ridge of the supratemporal process joining the parietal cranial crest at the level anterior to the posteromedial margin of the floor of the parietal fossa. The parietal crest is sharp in the area of junction. This is in contrast to *O. holeci*, *O. roqueprunensis* and *Pseudopus pannonicus* (Čerňanský and Klembara 2017; Klembara and Rummel 2018; Klembara et al. 2019).

The typical, anteriorly diverging parietal cranial crests in *Smithosaurus* can be seen outside of the Anguinae. It is present, although not developed to such a degree, in e.g., *Elgaria* (Gerrhonotinae; see Bhullar 2011; fig. 35b; Ledesma and Scarpetta 2018; fig. 18b) and in some xenosaurs (Bhullar 2011; fig. 36b).

The results of the phylogenetic analyses, although based only on the limited data, recovered *Smithosaurus echzellensis* as sister to the clade formed by *Ophisaurus* and *Anguis* (or to the larger clade formed by these and *Ophisauriscus quadrupes* + *Ophisaurus holeci*). This reflects the primitive character states of the new taxon in regard to anguines (and/or eventually, the combination of character states is present in the other anguines studied here). Although the position on the tree represents a relative degree of evolutionary relationships rather than reflecting the process of phylogeny (i.e., a sequence of ancestors and descendants), such a result might point to the existence of potentially archaic lineage(s), persisting into the Miocene. Another example in this regard is *Ophisaurus holeci* (see Klembara et al. 2019). As stated above, however, all conclusions are based strictly on the parietal features only and need to be met with caution. Only future studies of complete material can shed light on anguine phylogeny.

Snakes

The genus *Bavarioboa* is an extinct representative of the subfamily Boinae, the group today absent in the Old World continents. *Bavarioboa*, represented by several species, belonged to the commonest European snakes in the second half of the Oligocene. Remains of this snake, of late Oligocene / early Miocene age, were also found in Turkey (Szyndlar and Hoşgör 2012; Syromyatnikova et al. 2019). *Bavarioboa* reappeared in Europe at the end of the early Miocene (Ivanov 2002; Szyndlar and Rage 2003). The geologically youngest remains of *Bavarioboa* were reported from the middle Miocene of Germany (Ivanov and Böhme 2011).

Natrix longivertebrata was described, as a new species, from the late Pliocene of Poland by Szyndlar (1984), based on a large number of diverse bones including several basisphenoids. Later, fossil remains (exclusively vertebrae) referred to this species (usually with qualifiers 'cf.' or 'aff.') were reported from several European sites, dated from late Miocene to late Pliocene, by various authors (see Szyndlar 2005, and references therein). It is doubtful that all these remains belong to *N. longivertebrata*. The turning point in studies on this species was the discovery of several basisphenoids (along with other bones) among ophidian remains coming from the middle Miocene of France (identified as *N.* aff. *longivertebrata*), making *N. longivertebrata* a snake with one of the longest known stratigraphic ranges. *N. longivertebrata* was considered to be morphologically closer to the living *N. natrix* than to any other extant members of the genus *Natrix* and, eventually, it was considered a direct ancestor of *N. natrix* (Rage and Szyndlar 1986; Szyndlar 1991).

The key differences between *N. longivertebrata* and *N. natrix* can be observed in the basicranium, in particular in the posteriormost area of the basisphenoid. In *N. longivertebrata* the posterior margins of the basipterygoid processes of the basisphenoid are strongly extended posteriorly so that the posterior orifices of the Vidian canals are hidden inside bony recesses and hence invisible in ventral aspect. In *N. natrix* (excluding *N. n. astreptophora*, which cranial osteology remained unstudied yet in the early 1990s), the posterior margins of the basipterygoid processes are oriented anteromesially, so that the posterior foramina of the Vidian canals, usually shifted forwards from the posterior border of the bone, are well exposed in ventral view. The former condition was termed "ancient", while the latter was termed "modern" (Szyndlar 1991). The "ancient" pattern is the only condition observed in *N. longivertebrata*, but it occurred very rarely in populations of *N. natrix* from the Polish early and middle Pleistocene: altogether, 3 "ancient" versus 136 "modern" basisphenoids (Szyndlar 1991: table 1). The gradual change in the frequency of the two different basicranial morphological patterns ("ancient" vs. "modern" basisphenoids and also other cranial characteristics) was the basis for Szyndlar (1991) hypothesis of the transformation of the *N. longivertebrata* lineage into *N. natrix*. Clearly, the greatest weakness of the above hypothesis is the lack of any basicranial elements referable to natricine snakes from the long period between the middle Miocene and late Pliocene.

Rage and Szyndlar (1986: 60) mentioned that "in recent snakes, this character [i.e., the "ancient" pattern] has been noted only in one specimen from Spain" (*Natrix natrix*, MNCN 820924). Unfortunately, they did not connect the variability of the basiphenoid with the geographic distribution of different populations (subspecies) of the living grass snake. In 1996, Stefan Müller-Champrenaud (unpublished observations, see Szyndlar 2012 for details) first noticed that the "ancient" pattern of *N. longivertebrata* is also characteristic of a living subspecies of *N. natrix*, namely *N. n. astreptophora*, inhabiting today Iberia and southern France. The taxonomic status of the latter snake was then discussed by Pokrant et al. (2016), who raised *astreptophora*, mainly based on genetic characters, to the species level. Apart from the molecular evidence, these authors presented also some observations on the cranial

osteology of *N. astreptophora* and, eventually, made some comments with reference to *N. longivertebrata*.

Although Pokrant et al. (2016; fig. 2) seemed to appreciate the significance of the basisphenoid morphology, the bone has been missed for *N. astreptophora* when depicting it in ventral aspects for a few subspecies of *Natrix natrix*. Pokrant et al. (2016: 875) argued that Szyndlar (1991) for "contradicting basic phylogenetic principles", without explaining why both "ancient" and "modern" basiphenoid patterns occur together in Pleistocene ophidian assemblages. They claimed (ibidem: 875) that the "re-examination of Szyndlar's material revealed that his only three specimens of *N. natrix* sharing the character state of the fossil *N. longivertebrata* (Szyndlar 1991) belong to [sic!] *N. n. astreptophora*". As mentioned above, these three "ancient" (or *astreptophora*-like) basisphenoids were found in two Polish Pleistocene localities along with more numerous "modern" basisphenoids and, consequently, all remains were identified as belonging to *N. natrix* (Szyndlar 1991; table 1). Such a variability of the skull bone one can interpret as a polymorphism, which has not been considered by Pokrant et al. (2016).

Finally, Pokrant et al.: 885 (2016) observed that "the same character state as in *Natrix longivertebrata* and *N. n. astreptophora* [i.e., the "ancient" basisphenoid pattern] is also found in *N. maura*". The above statement cannot be supported, as the basisphenoid of the latter snake depicted by these authors (ibidem; fig. 2F) represents apparently the "modern" pattern. Similarly, the basisphenoid of another specimen of *N. maura* (MNCN 824272), examined and illustrated by Szyndlar (1984; fig. 28: 7), displays clearly the "modern" pattern, as well. In the light of these facts, Pokrant et al. (2016) conclusions resulting from the osteological observations needs to be critically considered. In particular, the suggestion that homoplasy explains "the occurrence of identical basisphenoid patterns in certain *Natrix* taxa" (ibidem: 884–885) remains unproven.

As mentioned above, based on the cranial osteology (in particular basisphenoids), Rage and Szyndlar (1986) hypothesized that the living species *Natrix natrix* was a direct descendant of the Neogene extinct species *N. longivertebrata*. Based on our current knowledge of the osteology of *N. astreptophora*, we propose to modify this hypothesis and consider *N. natrix* and *N. astreptophora* as descendants of *N. longivertebrata*. If this supposition is correct, the divergence into two extant species must have taken place between the middle Miocene and late Pliocene (indeed, based on molecular data, Kindler et al. (2017; fig. S1) estimated that the split into *N. astreptophora* and *N. natrix* took place between 9.6 and 10.6 Ma, i.e., early late Miocene). Unfortunately, owing to the lack of any fossil record (basisphenoids) from this very long period, more precise dating based on paleontological data is not possible. The proposed hypothesis does not contradict Pokrant et al. (2016; p. 884) conviction "of the unambiguous molecular evidence for the monophyly of *N. natrix* (inclusive of *N. n. astreptophora*)". Last but not least, detailed comparative studies of skulls of *N. natrix* and *N. astreptophora* woud be desired. Concluding, the present discovery of the basisphenoid from Echzell, clearly referable to *Natrix longivertebrata*, extends back the stratigraphic range of this fossil species to the early Miocene.

Naja romani was first described as a member of the extinct genus *Palaeonaja*, from the French middle Miocene (Hoffstetter 1939). Rage and Szyndlar (1990), who revised the entire fossil record of the European cobras, synonymized *Palaeonaja* with the extant genus *Naja*. Remains of *N. romani*, in some cases abundant and perfectly preserved, were reported from several European sites, ranging in age from early to late Miocene (see Szyndlar 2005, and references therein). Additionally, a number of vertebrae identified as *Naja* sp. were reported from some other localities representing the same time span.

Palaeoenvironmental and -climatic implications

The amphibian and reptilian assemblage of Echzell is rich in forms living in humid and warm environments. Thus, the presence of amphibian genera such as *Chioglossa*, *Mertensiella*, *Lissotriton*, *Latonia*, *Pelobates*, and the reptile *Chamaelaeo* suggest in general humid and warm forested environments, whereas *Palaeobatrachus*, *Pelophylax*, *Natrix* indicate the presence of permanent water bodies. Other taxa, including the genus *Rana*, skinks and the remaining snake taxa, allows also concluding about open habitats. The presence of Chamaeleonidae in Echzell allows to reconstruct palaeotemperature. Haller-Probst (1997) suggested that the chamaeleonid occurrence indicates a range of the mean annual temperature of 17.4–28.8 °C, minimal warm month temperature 18–28.3 °C, minimal cold month temperature 8–22.2 °C (Haller-Probst 1997). This is also supported by the presence of the clade Gekkota, which are distributed worldwide in warm temperate to tropical areas (Bauer 2013; Meiri 2020). The mean annual precipitation (MAP) value has been estimated using the bioclimatic analysis of the amphibian and reptilian assemblage of Böhme et al. (2006). The analysis suggests a MAP value of 791±254 mm (Table 2) for Echzell, which is 126% wetter than the present-day value (Table 2).

Sample availability the studied fossils are deposited at the Hessisches Landesmuseum, Darmstadt (HLMD), Germany.

Author contribution

DV and TM designed the project and all authors carried it out. All authors prepared the manuscript with contributions from all co-authors. DV edited the text. All authors read and approved the text.

Competing interests

The authors declare that they have no conflict of interest.

Acknowledgements

The authors thank Oliver Sandrock (Hessisches Landesmuseum Darmstadt) for making the material available for study. A.Č. acknowledges financial support from the Scientific Grant Agency of the Ministry of Education of the Slovak Republic and Slovak Academy of Sciences, Grant Nr. 1/0191/21. T.M. acknowledges financial support from the Bolin Center for Climate Research, Stockholm University (RA6 grant).

References

Bell T (1839) A History of British Reptiles, John van Voorst, London, 142 pp. https://doi.org/10.5962/bhl.title.10835

Bhullar B-AS (2011) The power and utility of morphological characters in systematics: A fully resolved phylogeny of *Xenosaurus* and its fossil relatives (Squamata: Anguimorpha). Bulletin of the Museum of Comparative Zoology160: 65–181. https://doi.org/10.3099/0027-4100-160.3.65

Blain H-A, Bailon S, Agustí J (2007) Anurans and squamate reptiles from the latest early Pleistocene of Almenara-Casablanca-3 (Castellón, East of Spain). Systematic, climatic and environmental considerations. Geodiversitas 29: 269–295.

Bocage JVB (1864) Note sur un nouveau batracien du Portugal, *Chioglossa lusitanica*, et sur une grenouille nouvelle de l´Afrique occidentale. Revue et Magasin de Zoologie Pure et Appliquée, Serie 2, 16: 248–253.

Böhme G (1977) Zur Bestimmung quartärer Anuren Europas an Hand von Skelettelementen. Wissenschaftliche Zeitschrift der Humboldt-Universität zu Berlin, Mathematisch-Naturwissenschaftliche Reihe 26: 283–299.

Böhme M (2008) Ectothermic vertebrates (Teleostei, Allocaudata, Urodela, Anura, Testudines, Choristodera, Crocodylia, Squamata) from the Upper Oligocene of Oberleichtersbach (Northern Bavaria, Germany). Courier Forschungsinstitut Senckenberg 260: 161–183.

Böhme M (2010) Ectothermic vertebrates (Actinopterygii, Allocaudata, Urodela, Anura, Crocodylia, Squamata) from the Miocene of Sandelzhausen (Germany, Bavaria) and their implications for environment reconstruction and palaeoclimate. Paläontologische Zeitschrift 84: 3–41. https://doi.org/10.1007/s12542-010-0050-4

Böhme M, Ilg A (2003) fosFARbase. [Available at] www.wahre-staerke.com

Böhme M, Vasilyan D (2014) Ectothermic vertebrates from the late Middle Miocene of Gratkorn (Austria, Styria). Palaeobiodiversity and Palaeoenvironments 94: 21–40. https://doi.org/10.1007/s12549-013-0143-7

Böhme M, Ilg A, Ossig A, Küchenhoff H (2006) New method to estimate paleoprecipitation using fossil amphibians and reptiles and the middle and late Miocene precipitation gradients in Europe. Geology 34: 425–428. https://doi.org/10.1130/G22460.1

Böhme W, Roček Z, Špinar ZV (1982) On *Pelobates decheni* Troschel, 1961, and *Zaphrissa eurypelis* Cope, 1866 (Amphibia: Pelobatidae) from the early Miocene of Rott near Bonn West Germany. Journal of Vertebrate Paleontology 2: 1–7. https://doi.org/10.1080/02724634.1982.10011913

Boié F (1827) Bemerkungen über Merrem's Versuch eines Systems der Amphibien: 1ste Lieferung. Isis von Oken, Leipzig, 508–566.

Bonaparte CL (1850) Conspectus systematum. Mastozoölogiae. Ornithologiae. Herpetologiae et Amphibiologiae. Ichthyologiae, E. J. Brill, Lugduni Batavorum.

Bremer K (1994) Branch support and tree stability. Cladistics 10: 295–304. https://doi.org/10.1111/j.1096-0031.1994.tb00179.x

Caputo V (2004) The cranial osteology and dentition in the scincid lizards of the genus *Chalcides* (Reptilia, Scincidae). Italian Journal of Zoology 71: 35–45. https://doi.org/10.1080/11250000409356604

Čerňanský A (2011) A revision of the chameleon species *Chamaeleo pfeili* Schleich (Squamata; Chamaeleonidae) with description of a new material of chamaeleonids from the Miocene deposits of southern Germany. Bulletin of Geosciences 86: 275–282. https://doi.org/10.3140/bull.geosci.1259

Čerňanský A (2010a) Albanerpetontid amphibian (Lissamphibia: Albanerpetontidae) from the Early Miocene of the locality Merkur–North (north-west of the Czech Republic): data and a description of a new material. Acta Geologica Slovaka 2: 113–116.

Čerňanský A (2010b) A revision of chamaeleonids from the Lower Miocene of the Czech Republic with description of a new species of *Chamaeleo* (Squamata, Chamaeleonidae). Geobios 43: 605–613. https://doi.org/10.1016/j.geobios.2010.04.001

Čerňanský A (2010c) Earliest world record of green lizards (Lacertilia, Lacertidae) from the Lower Miocene of central Europe. Biologia 64: 737–741. https://doi.org/10.2478/s11756-010-0066-y

Čerňanský A (2016) Another piece of the puzzle: The first report on the Early Miocene lizard fauna from Austria (Ottnangian, MN 4; Oberdorf locality). Paläontologische Zeitschrift 90: 723–746. https://doi.org/10.1007/s12542-016-0329-1

Čerňanský A, Bauer AM (2010) *Euleptes gallica* Müller (Squamata: Gekkota: Sphaerodactylidae) from the Lower Miocene of North-West Bohemia, Czech Republic. Folia zoologica 59: 323–328. https://doi.org/10.25225/fozo.v59.i4.a8.2010

Čerňanský A, Klembara J (2017) A skeleton of *Ophisaurus* (Squamata: Anguidae) from the middle Miocene of Germany, with a revision of the partly articulated postcranial material from Slovakia using micro-computed tomography. Journal of Vertebrate Paleontology 37: e1333515. https://doi.org/10.1080/02724634.2017.1333515

Čerňanský A, Syromyatnikova EV (2019) The first Miocene fossils of *Lacerta* cf. *trilineata* (Squamata, Lacertidae) with a comparative study of the main cranial osteological differences in green lizards and their relatives. PLoS ONE 14: e0216191. https://doi.org/10.1371/journal.pone.0216191

Čerňanský A, Syromyatnikova EV (2021) The first pre-Quaternary fossil record of the clade Mabuyidae with a comment on the enclosure of the Meckelian canal in skinks. Papers in Palaeontology 7: 195–215. https://doi.org/10.1002/spp2.1279

Čerňanský A, Daza JD, Bauer AM (2018) Geckos from the middle Miocene of Devínska Nová Ves (Slovakia): new material and a review of the previous record. Swiss Journal of Geosciences 111: 183–190. https://doi.org/10.1007/s00015-017-0292-1

Čerňanský A, Rage JC, Klembara J (2015) The Early Miocene squamates of Amöneburg (Germany): the first stages of modern squamates in Europe. Journal of Systematic Palaeontology 13: 97–128. https://doi.org/10.1080/14772019.2014.897266

Čerňanský A, Szyndlar Z, Mörs T (2017) Fossil squamate faunas from the Neogene of Hambach (northwestern Germany). Palaeobiodiversity and Palaeoenvironments 97: 329–354. https://doi.org/10.1007/s12549-016-0252-1

Čerňanský A, Herrel A, Kibii JM, Anderson CV, Boistel R, Lehmann T (2020a) The only complete articulated early Miocene chameleon skull (Rusinga Island, Kenya) suggests an African origin for Madagascar's endemic chameleons. Scientific Reports 10: e109. https://doi.org/10.1038/s41598-019-57014-5

Čerňanský A, Syromyatnikova EV, Kovalenko ES, Podurets KM, Kaloyan AA (2020b) The Key to Understanding the European Miocene *Chalcides* (Squamata, Scincidae) Comes from Asia: The Lizards of the East Siberian Tagay Locality (Baikal Lake) in Russia. The Anatomical Record 303: 1901–1934. https://doi.org/10.1002/ar.24289

Čerňanský A, Yaryhin O, Ciceková J, Werneburg I, Hain M, Klembara J (2019) Vertebral Comparative Anatomy and Morphological Differences in Anguine Lizards With a Special Reference to *Pseudopus apodus*. The Anatomical Record 302: 232–257. https://doi.org/10.1002/ar.23944

Cope ED (1865) Sketch of the primary groups of Batrachia Salientia. Natural history review 5: 97–120.

Cuvier G (1816–1817) Le Règne Animal distribué d'après son organisation pour servir de base à l'histoire naturelle des animaux et d'introduction à l'anatomie comparée. Avec Figures, dessinées d'après nature, Contenant Les reptiles, les poissons, les mollusques et les annélides., Deterville, Paris, [i–xviii +] 532 pp.

Daza JD, Bauer AM, Snively ED (2014) On the Fossil Record of the Gekkota. The Anatomical Record 297: 433–462. https://doi.org/10.1002/ar.22856

Digimorph.org (2002–2012): Digital morphology: a national science foundation digital library at the University of Texas at Austin. http://www.digimorph.org/index.phtml

Duellman WE, Trueb L (1994) Biology of Amphibia. The Johns Hopkins University Press, Baltimor-London, 670 pp.

Duméril AMC (1806) Zoologie analytique, ou méthode naturelle de classification des animaux, rendue plus facile à l'aide de tableaux synoptiques. H. L. Perronneau, Paris, 344 pp. https://doi.org/10.5962/bhl.title.44835

Estes R, Hoffstetter R (1976) Les Urodèles du Miocène de la Grive-Saint-Alban (Isère, France). Bulletin du Muséum National d'Histoire Naturelle, 3e Série, Science de la Terre 57: 297–343.

Estes R, Queiroz K, Gauthier J (1988) Phylogenetic relationships within Squamata. In: Estes R, Pregill G (Eds) Phylogenetic relationships of the lizard families. Stanford University Press, Stanford, California, 119–281.

Evans SE (2008) The skull of lizards and tuatara. In: Gans C (Ed.) The skull of Lepidosauria. Society for the Study of Amphibians and Reptiles, Ithaca, 1–347.

Fejfar O (1999) Subfamily Platacanthomyinae. In: Rössner G, Heissig K (Eds) The Miocene Land Mammals of Europe. Dr. Friedrich Pfeil, München, 389–394.

Fejfar O, Kalthoff D (1999) Aberrant cricetids (Platacanthomyines, Rodentia, Mammalia) from the Miocene of Eurasia. Berliner geowissenschaftliche Abhandlungen E 30: 191–206.

Fejfar O, Roček Z (1986) The Lower Micoene vertebrate fauna of Dolnice, Cheb Basin (Western Bohemia, Czechoslovakie). Acta Universitatis Carolinae – Geologica 2: 233–249.

Fischer G (1813) Zoognosia. Tabulis Synopticis Illustrata, in Usum Prælectionum Academiæ Imperialis Medico-Chirurgicæ Mosquensis Edita, 3rd ed., 1. Typis Nicolai Sergeidis Vsevolozsky, Moscow, 465 pp.

Fitzinger L (1843) Systema Reptilium. Fasciculus Primus, Braumüller et Seidel, Wien, 106 pp. https://doi.org/10.5962/bhl.title.4694

Fox RC, Naylor BG (1982) A reconsideration of the relationships of the fossil amphibian *Albanerpeton*. Canadian Journal of Earth Sciences 33: 1–107. https://doi.org/10.1139/e82-009

Fürbinger M (1900) Zur Vergleichenden Anatomie des Brustschulterapparates und der Schultermuskeln. Jenaische Zeitschrift für Naturwissenschaft 34: 215–718. https://doi.org/10.5962/bhl.title.52377

Garsault FAd, Defehrt AJ, Prévost BL, Duflos P, Martinet FN, Geoffroy ÉF (1764) Les figures des plantes et animaux d'usage en medecine décrits dans La matiere medicale de Mr. Geoffroy medecin, Chez l'auteur rue St. Dominique porte St. Jacques, Paris, 644–729. https://doi.org/10.5962/bhl.title.49481

Gauthier JA, Kearney M, Maisano JA, Rieppel O, Behlke AD (2012) Assembling the squamate tree of life: perspectives from the phenotype and the fossil record. Bulletin of the Peabody Museum of Natural History 53: 3–308. https://doi.org/10.3374/014.053.0101

Georgalis GL, Villa A, Delfino M (2016) First description of a fossil chamaeleonid from Greece and its relevance for the European biogeographic history of the group. Die Naturwissenschaften 103: e12. https://doi.org/10.1007/s00114-016-1336-5

Georgalis G, Villa A, Ivanov M, Vasilyan D, Delfino M (2019) Fossil amphibians and reptiles from the Neogene locality of Maramena (Greece), the most diverse European herpetofauna at the Miocene/Pliocene transition boundary. Palaeontologia Electronica 22(3): 1–99. https://doi.org/10.26879/908

Goldfuss GA (1820) Handbuch der Zoologie. Bd. 2. J. L. Schrag, Nürnberg, 510 pp.

Goloboff PA, Farris JS, Nixon KC (2008) TNT, a free program for phylogenetic analysis. Cladistics 24: 774–786. https://doi.org/10.1111/j.1096-0031.2008.00217.x

Gómez RO, Turazzini GF (2015) An overview of the ilium of anurans (Lissamphibia, Salientia), with a critical appraisal of the terminology and primary homology of main ilial features. Journal of Vertebrate Paleontology 36(1): e1030023. https://doi.org/10.1080/02724634.2015.1030023

Gray JE (1825) A synopsis of the genera of reptiles and Amphibia, with a description of some new species. Annals of Philosophy London 10: 193–217.

Greer AE (1970) A subfamilial classification of scincid lizards. Bulletin of the Museum of Comparative Zoology 139(3): 151–183.

Greer AE (1974) The genetic relationships of the Scincid lizard genus *Leiolopisma* and its relatives. Australian Journal of Zoology Supplementary Series 22(31): 1–67. https://doi.org/10.1071/AJZS031

Haeckel E (1866) Generelle Morphologie der Organismen. Georg Reimer, Berlin, 574 pp. https://doi.org/10.1515/9783110848281

Haller-Probst MS (1997) Die Verbreitung der Reptilia in den Klimazonen der Erde: Unter Berücksichtigung Känozoischer Vorkommen Europas. Courier Forschungsinstitut Senckenberg 203: 1–147.

Hedges SB (2014) The high-level classification of skinks (Reptilia, Squamata, Scincomorpha). Zootaxa 3765: 317–338. https://doi.org/10.11646/zootaxa.3765.4.2

Hernandez A (2016) Crocodile newts: The primitive Salamandridae of Asia (genera *Echinotriton* and *Tylototriton*). Frankfurter Beiträge zur Naturkunde 62: 1–415.

Hodrová M (1984) Salamandridae of the Upper Pliocene Ivanovce locality (Czechoslovakia). Acta Universitatis Carolinae – Geologica 4: 331–352.

Hoffstetter R (1939) Contribution à l'étude des Elapidae actuels et fossiles et de l'ostéologie des Ophidiens. Archives du Muséum d'Histoire Naturelle de Lyon 15: 1–78. https://doi.org/10.3406/mhnly.1939.980

Hoffstetter R, Gasc JP (1969) Vertebrae and rips of modern reptiles. In: Gans C (Ed.) Biology of the Reptilia Morphology A. Academic Press, London, New York, 201–310.

Hossini S, Rage JC (2000) Palaeobatrachid frogs from the earliest Miocene (Agenian) of France, with description of a new species. Geobios 33: 223–231. https://doi.org/10.1016/S0016-6995(00)80019-4

Hutchinson MN, Scanlon JD (2009) New and Unusual Plio-Pleistocene Lizard (Reptilia: Scincidae) from Wellington Caves, New South Wales, Australia. Journal of Herpetology 43: 139–147. https://doi.org/10.1670/08-126R.1

Ivanov M (2001) Changes in the composition of the European snake fauna during the Early Miocene and at the Early / Middle Miocene transition. Palaeontologische Zeitschrift 74: 563–573. https://doi.org/10.1007/BF02988162

Ivanov M (2002) The oldest known Miocene snake fauna from Central Europe: Merkur–North locality, Czech Republic. Acta Palaeontologica Polonica 47: 513–534.

Ivanov M (2008) Early Miocene Amphibians (Caudata, Salientia) from the Mokrá-Western Quarry (Czech Republic) with comments on the evolution of Early Miocene amphibian assemblages in Central Europe. Geobios 41: 465–492. https://doi.org/10.1016/j.geobios.2007.11.004

Ivanov M, Böhme M (2011) Snakes from Griesbeckerzell (Langhian, Early Badenian), North Alpine Foreland Basin (Germany), with comments on the evolution of snake faunas in Central Europe during the Miocene Climatic Optimum. Geodiversitas 33: 411–449. https://doi.org/10.5252/g2011n3a2

Ivanov M, Čerňanský A, Bonilla-Salomón I, Luján ÀH (2020) Early Miocene squamate assemblage from the Mokrá-Western Quarry (Czech Republic) and its palaeobiogeographical and palaeoenvironmental implications. Geodiversitas 42: 343–376. https://doi.org/10.5252/geodiversitas2020v42a20

Jovells Vaqué S, Mörs T (2022) The aberrant hamster Melissiodon (Cricetidae, Rodentia) from the early Miocene of Echzell and other German and French localities. Historical Biology. https://doi.org/10.1080/08912963.2022.2067758

Khozatskiy LI (1985) A new species of *Pelobates* from the Pliocene of Moldova. In: Negadaev-Nikonov KN (Ed.) Fauna and flora of Late Cenozoic of Moldova. Shtiintsa, Kishinev, 59–72.

Kindler C, Chèvre M, Ursenbacher S, Böhme W, Hille A, Jablonski D, Vamberger M, Fritz U (2017) Hybridization patterns in two contact zones of grass snakes reveal a new Central European snake species. Scientific Reports 7: e7378. https://doi.org/10.1038/s41598-017-07847-9

Klembara J (2015) New finds of anguines (Squamata, Anguidae) from the Early Miocene of Northwest Bohemia (Czech Republic). Paläontologische Zeitschrift 89: 171–195. https://doi.org/10.1007/s12542-014-0226-4

Klembara J, Čerňanský A (2020) Revision of the cranial anatomy of *Ophisaurus acuminatus* Jörg, 1965 Anguimorpha, Anguidae) from the late Miocene of Germany. Geodiversitas 42: 539–557. https://doi.org/10.5252/geodiversitas2020v42a28

Klembara J, Rummel M (2018) New material of *Ophisaurus*, *Anguis* and *Pseudopus* (Squamata, Anguidae, Anguinae) from the Miocene of the Czech Republic and Germany and systematic revision and palaeobiogeography of the Cenozoic Anguinae. Geological Magazine 155: 20–44. https://doi.org/10.1017/S0016756816000753

Klembara J, Dobiašová K, Hain M, Yaryhin O (2017) Skull Anatomy and Ontogeny of Legless Lizard *Pseudopus apodus* (Pallas, 1775): Heterochronic Influences on Form. The Anatomical Record 300: 460–502. https://doi.org/10.1002/ar.23532

Klembara J, Böhme M, Rummel M (2010) Revision of the Anguine Lizard *Pseudopus laurillardi* (Squamata, Anguidae) from the Miocene of Europe, with Comments on Paleoecology Journal of Paleontology 84: 159–196. https://doi.org/10.1666/09-033R1.1

Klembara J, Hain M, Čerňanský A (2019) The first record of anguine lizards (Anguimorpha, Anguidae) from the early Miocene locality Ulm – Westtangente in Germany. Historical Biology 31: 1016–1027. https://doi.org/10.1080/08912963.2017.1416469

Klembara J, Hain M, Dobiašová K (2014) Comparative anatomy of the lower jaw and dentition of *Pseudopus apodus* and the interrelationships of species of subfamily Anguinae (Anguimorpha, Anguidae). The Anatomical Record 297: 516–544. https://doi.org/10.1002/ar.22854

Laurenti JN (1768) Specimen medicum, exhibens synopsin reptilium emendatum cum experimentis circa venena et antidota Reptilium Austriacorum. Typ. Joan. Thom. nob. de Trattnern, Viennae, 214 pp. https://doi.org/10.5962/bhl.title.5108

Ledesma DT, Scarpetta SG (2018) The skull of the gerrhonotine lizard *Elgaria panamintina* (Squamata: Anguidae). PLoS ONE 13: e0199584. https://doi.org/10.1371/journal.pone.0199584

Linnaeus C (1758) Systema naturae per regna tria naturae, secundum classes, ordines, genera, species, cum characteribus, differentiis, synonymis, locis. L. Salvi, Stockholm, 823 pp. https://doi.org/10.5962/bhl.title.542

Maddison WP, Maddison DR (2011) Mesquite: a modular system for evolutionary analysis.

Marjanović D, Witzmann F (2015) An Extremely Peramorphic Newt (Urodela: Salamandridae: Pleurodelini) from the Latest Oligocene of Germany, and a New Phylogenetic Analysis of Extant and Extinct Salamandrids. PLoS ONE 10: e0137068. https://doi.org/10.1371/journal.pone.0137068

Meyer von H (1843) Mittheilung an Professor Bronn gerichtet. Neues Jahrbuch für Geologie und Paläontologie, Geognasie, Geologie und Petrefactenkunde, 579–590.

Moody S (1978) The phylogenetic relationships of taxa within the lizards family Agamidae. PhD thesis, University of Michigan at Ann Arbor, Michigan, USA.

Mörs T (2010) Wirbeltiere aus dem Miozän von Homberg/Ohm (Vogelsberg, Hessen). Geologisches Jahrbuch Hessen 136: 109–119.

Mörs T, Flink T (2018) Large apeomyine rodents (Mammalia, Eomyidae) from the early Miocene of Echzell, Germany. Historical Biology 30: 1102–1111. https://doi.org/10.1080/08912963.2017.1338695

Mörs T, Reguero M, Vasilyan D (2020) First fossil frog from Antarctica: implications for Eocene high latitude climate conditions and Gondwanan cosmopolitanism of Australobatrachia. Scientific Reports 10: e5051. https://doi.org/10.1038/s41598-020-61973-5

Oppel M (1811) Die Ordnungen, Familien und Gattungen der Reptilien als Prodrom einer Naturgeschichte derselben. Joseph Lindauer, München, 87 pp. https://doi.org/10.5962/bhl.title.4911

Pineker P, Mörs T (2011) *Neocometes* (Rodentia, Platacanthomyinae) from the early Miocene of Echzell, Germany. Geobios 44: 279–287. https://doi.org/10.1016/j.geobios.2010.12.001

Pokrant F, Kindler C, Ivanov M, Cheylan M, Geniez P, Böhme W, Fritz U (2016) Integrative taxonomy provides evidence for the species status of the Ibero-Maghrebian grass snake *Natrix astreptophora*. Biological Journal of the Linnean Society 118: 873–888. https://doi.org/10.1111/bij.12782

Pomel A (1853) Catalogue méthodique et descriptif des vertébrés fossiles découverts dans le bassin hydrographique supérieur de la Loire. J. B. Baillières, Paris, 193 pp.

Pyron AR, Wiens JJ (2011) A large-scale phylogeny of Amphibia including over 2800 species, and a revised classification of extant frogs, salamanders, and caecilians. Molecular Phylogenetics and Evolution 61: 543–583. https://doi.org/10.1016/j.ympev.2011.06.012

Rafinesque CS (1815) Analyse de Nature, ou Tableau de l'Universe et des Corps Organisés. Jean Barravecchia, Palermo, 224 pp. https://doi.org/10.5962/bhl.title.106607

Rage JC, Augé ML (2010) Squamate reptiles from the middle Eocene of Lissieu (France). A landmark in the middle Eocene of Europe. Geobios 43: 253–268. https://doi.org/10.1016/j.geobios.2009.08.002

Rage JC, Bailon S (2005) Amphibians and squamate reptiles from the late early Miocene (MN 4) of Béon 1 (Montréal-du-Gers, southwestern France). Geodiversitas 27: 413–441.

Rage JC, Szyndlar Z (1986) *Natrix longivertebrata* from the European Neogene, a snake with one of the longest known stratigraphic ranges. Neues Jahrbuch für Geologie und Paläontologie - Monatshefte 1986: 56–64. https://doi.org/10.1127/njgpm/1986/1986/56

Rage JC, Szyndlar Z (1990) West Palearctic cobras of the genus *Naja* (Serpentes: Elapidae): interrelationships among extinct and extant species. Amphibia-Reptilia 11: 385–400. https://doi.org/10.1163/156853890X00078

Recuero E, García-París M (2011) Evolutionary history of *Lissotriton helveticus*: multilocus assessment of ancestral vs. recent colonization of the Iberian Peninsula. Molecular Phylogenetics and Evolution 60: 170–182. https://doi.org/10.1016/j.ympev.2011.04.006

Roček Z (1984) Lizards (Reptili: Sauria) from the Lower Miocene locality Dolnice (Bohemia, Czechoslovakia). Řada matematických a přirodních věd 94: 4–69.

Roček Z (1994) A Review of the fossil Caudata of Europe. Abhandlungen und Berichte für Naturkunde 17: 51–56.

Roček Z (2005) Late Miocene Amphibia from Rudabánya. Palaeontographia Italica 90: 11–29.

Roček Z, Wuttke M (2010) Amphibia of Enspel (Late Oligocene, Germany). Palaeobiodiversity and Palaeoenvironments 90: 321–340. https://doi.org/10.1007/s12549-010-0042-0

Roček Z, Boistel R, Lenoir N, Mazurier A, Pierce SE, Rage JC, Smirnov SV, Schwermann AH, Valentin X, Venczel M, Wuttke M, Zikmund T (2015) Frontoparietal Bone in Extinct Palaeobatrachidae (Anura): Its Variation and Taxonomic Value. The Anatomical Record: Advances in Integrative Anatomy and Evolutionary Biology 298: 1848–1863. https://doi.org/10.1002/ar.23203

Roček Z, Böttcher R, Wassersug R (2006) Gigantism in tadpoles of the Neogene frog *Palaeobatrachus*. Paleobiology 32: 666–675. https://doi.org/10.1666/05073.1

Roček Z, Wuttke M, Gardner J, Singh Bhullar BA (2014) The Euro-American genus *Eopelobates*, and a re-definition of the family Pelobatidae (Amphibia, Anura). Palaeobiodiversity and Palaeoenvironments 94: 529–567. https://doi.org/10.1007/s12549-014-0169-5

Rössner G, Heissig K (1999) The Miocene Land Mammals of Europe. Dr. Friedrich Pfeil, München, 516 pp.

Sanchíz B (1998) Vertebrates from the Early Miocene lignite deposits of the opencast mine Oberdorf (Western Styrian Basin, Austria). Annalen des Naturhistorischen Museums in Wien 99A: 13–29.

Sanchíz B, Młynarski M (1979) Pliocene salamandrids (Amphibia, Caudata) from Poland. Acta zoologica cracoviensia 24: 175–188.

Schleich HH (1987) Neue Reptilienfunde aus dem Tertiär Deutschlands 7. Erstnachweis von Geckos aus dem Mittelmiozän Süddeutschlands: *Palaeogekko risgoviensis* nov. gen., nov. spec. (Reptilia, Sauria, Gekkonidae)[1]). Mitteilungen der Bayerischen Staatssammlung für Paläontologie und historische Geologie 27: 67–96.

Schoch RR, Poschmann M, Kupfer A (2015) The salamandrid *Chelotriton paradoxus* from Enspel and Randeck Maars (Oligocene–Miocene, Germany). Palaeobiodiversity and Palaeoenvironments 95: 77–86. https://doi.org/10.1007/s12549-014-0182-8

Scopoli GA (1777) Introductio ad historiam naturalem, sistens genera lapidum, plantarum et animalium hactenus detecta, caracteribus essentialibus donata, in tribus divisa, subinde ad leges naturae. Apud Wolfgangum Gerle, Prague, 506 pp. https://doi.org/10.5962/bhl.title.10827

Sparreboom M (2014) Salamanders of the Old World: The salamanders of Europe, Asia and northern Africa, First edition. KNNV Publishing, Zeist, 431 pp. https://doi.org/10.1163/9789004285620

Steinthorsdottir M, Coxall HK, Boer AM, Huber M, Barbolini N, Bradshaw CD, Burls NJ, Feakins SJ, Gasson E, Henderiks J, Holbourn AE, Kiel S, Kohn MJ, Knorr G, Kürschner WM, Lear CH, Liebrand D, Lunt DJ, Mörs T, Pearson PN, Pound MJ, Stoll H, Strömberg CAE (2021) The Miocene: The Future of the Past. Paleoceanographica and Paleoclimatology 36: e2020PA004037. https://doi.org/10.1029/2020PA004037

Syromyatnikova E, Georgalis GL, Mayda S, Kaya T, Saraç G (2019) A new early Miocene herpetofauna from Kilçak, Turkey. Russian Journal of Herpetology 26: 205. https://doi.org/10.30906/1026-2296-2019-26-4-205-224

Szentesi Z, Pazonyi P, Mészáros L (2015) Albanerpetonidae from the late Pliocene (MN 16A) Csarnóta 3 locality (Villany Hills, South Hungary) in the collection of the Hungarian Natural History Museum. Fragmenta Palaeontologica Hungarica 32: 49–66. https://doi.org/10.17111/FragmPalHung.2015.32.49

Szyndlar Z (1984) Fossil snakes from Poland. Acta zoologica cracoviensia 28: 1–156.

Szyndlar Z (1987) Snakes from the Lower Miocene Locality of Dolnice (Czechoslovakia). Journal of Vertebrate Paleontology 7: 55–71. https://doi.org/10.1080/02724634.1987.10011637

Szyndlar Z (1991) Ancestry of the Grass Snake (*Natrix natrix*): Paleontological Evidence. Journal of Herpetology 25: 412–418. https://doi.org/10.2307/1564762

Szyndlar Z (1998) Vertebrates from the Early Miocene lignite deposits of the opencast mine Oberdorf (Western Styrian Basin, Austria). 3. Reptilia, 2: Serpentes. Annalen des Naturhistorischen Museums in Wien, Series A 99A: 31–38.

Szyndlar Z (2005) Snake fauna from the Late Micoene of Rudabánya. Palaeontographia Italica 90: 31–52.

Szyndlar Z (2012) Early Oligocene to Pliocene Colubridae of Europe: a review. Bulletin de la Société Géologique de France 183: 661–681. https://doi.org/10.2113/gssgfbull.183.6.661

Szyndlar Z, Hoşgör I (2012) *Bavarioboa* sp. (Serpentes, Boidae) from the Oligocene / Miocene of eastern Turkey with comments on connections between European and Asiatic snake faunas. Acta Palaeontologica Polonica 57: 667–671. https://doi.org/10.4202/app.2011.0075

Szyndlar Z, Rage JC (2002) Fossil record of the true vipers. In: Schütt GW, Höggren M, Douglas ME, Greene HW (Eds) Biology of the Vipers. Eagle Mountain Publishing, Eagle Mountain, 419–444.

Szyndlar Z, Rage JC (2003) Non-erycine Booidea from the Oligocene and Miocene of Europe. Institute of Systematics and Evolution of Animals Polish Academy of Sciences, Kraków, 109 pp.

Szyndlar Z, Schleich HH (1993) Description of Miocene Snakes from Petersbuch 2 with Comments on the Lower and Middle Miocene

Ophidian Faunas of Southern Germany. Stuttgarter Beiträge zur Naturkunde. Serie B (Geologie und Paläontologie) 192: 1–47.

Tissier J, Rage JC, Boistel R, Fernandez V, Pollet N, Garcia G, Laurin M (2015) Synchrotron analysis of a 'mummified' salamander (Vertebrata: Caudata) from the Eocene of Quercy, France. Zoological Journal of the Linnean Society 171(1): 147–164. https://doi.org/10.1111/zoj.12341

Tobien H (1954) Eine miozäne Säugerfauna aus vulkanischen Tuffen des Vogelsberges (Vortragsbericht). Zeitschrift der deutschen geologischen Geselschaft 105: 588–588. https://doi.org/10.1127/zdgg/105/1955/588

Tobien H (1982) 1200 Jahre Echzell: 782 - 1982; Ursprung, Epochen u. Strukturen e. Dörfergemeinschaft, Ahnert, Echzell, 400 pp.

Tschudi JJ (1838) Classification der Batrachier, Mit Berucksichtigung der fossilen Thiere dieser Abtheilung der Reptilien. Petitpierre, Neuchâtel, 100 pp. https://doi.org/10.5962/bhl.title.4883

Vasilyan D (2020) Fish, amphibian and reptilian assemblage from the middle Miocene locality Gračanica—Bugojno palaeolake, Bosnia and Herzegovina. Palaeobiodiversity and Palaeoenvironments 100: 437–455. https://doi.org/10.1007/s12549-019-00381-8

Vasilyan D, Roček Z, Ayvazyan A, Claessens LPAM (2019) Fish, amphibian and reptilian faunas from latest Oligocene to middle Miocene localities from Central Turkey. Palaeobiodiversity and Palaeoenvironments 99: 723–757. https://doi.org/10.1007/s12549-019-00405-3

Vasilyan D, Zazhigin VS, Böhme M (2017) Neogene amphibians and reptiles (Caudata, Anura, Gekkota, Lacertilia, Testudines) from south of Western Siberia, Russia and Northeastern Kazakhstan. PeerJ 5: e3025. https://doi.org/10.7717/peerj.3025

Venczel M (2004) Middle Miocene anurans from the Carpathian Basin. Palaeontographica Abteilung A 271: 151–174. https://doi.org/10.1127/pala/271/2004/151

Venczel M, Gardner JD (2005) The geologically youngest Albanerpetontid Amphibian, from the Lower Pliocene of Hungary. Palaeontology 48: 1273–1300. https://doi.org/10.1111/j.1475-4983.2005.00512.x

Venczel M, Hír J (2013) Amphibians and Squamates from the Miocene of Felsötárkány Basin, N-Hungary, Palaeontographica Abteilung A 300: 117–147. https://doi.org/10.1127/pala/300/2013/117

Vidal N, Hedges SB (2005) The phylogeny of squamate reptiles (lizards, snakes, and amphisbaenians) inferred from nine nuclear protein-coding genes. Comptes rendus biologies 328: 1000–1008. https://doi.org/10.1016/j.crvi.2005.10.001

Villa A, Delfino M (2019a) Fossil lizards and worm lizards (Reptilia, Squamata) from the Neogene and Quaternary of Europe: an overview. Swiss Journal of Palaeontology 138: 177–211. https://doi.org/10.1007/s13358-018-0172-y

Villa A, Delfino M (2019b) A comparative atlas of the skull osteology of European lizards (Reptilia: Squamata). Zoological Journal of the Linnean Society 187: 829–928. https://doi.org/10.1093/zoolinnean/zlz035

Villa A, Gobbi S, Delfino M (2021) Additions to the early Miocene herpetofauna of Weisenau (Germany): urodeles and squamates from a rediscovered historical collection in Italy. Paläontologische Zeitschrift 96: 113–127. https://doi.org/10.1007/s12542-021-00571-w

Villa A, Kosma R, Čerňanský A, Delfino M (2018) Taxonomic assessment of '*Bavaricordylus*' Kosma, 2004 (Reptilia, Squamata). Journal of Vertebrate Paleontology 38: 1–4. https://doi.org/10.1080/02724634.2018.1487844

Villa A, Roček Z, Tschopp E, Van den Hoek Ostende LW, Delfino M (2016) *Palaeobatrachus eurydices* sp. nov. (Amphibia, Anura), the last western European palaeobatrachid. Journal of Vertebrate Paleontology 36: e1211664. https://doi.org/10.1080/02724634.2016.1211664

Wagler JG (1830) Natürliches System der Amphibien, mit vorangehender Classification der Säugethiere und Vögel Ein Beitrag zur vergleichenden Zoologie. J.G. Cotta, München-Stuttgart-Tübingen, 354 pp. https://doi.org/10.5962/bhl.title.58730

Wetter und Klima (undated) Wetter und Klima - Deutscher Wetterdienst. https://www.dwd.de/

Wielstra B, Themudo GE, Güçlü O, Olgun K, Poyarkov NA, Arntzen JW (2010) Cryptic crested newt diversity at the Eurasian transition: the mitochondrial DNA phylogeography of Near Eastern *Triturus* newts. Molecular Phylogenetics and Evolution 56: 888–896. https://doi.org/10.1016/j.ympev.2010.04.030

Wolterstorff W (1925) Katalog der Amphibien-Sammlung im Museum für Natur- und Heimkunde zu Magdeburg: Erster Teil, Apoda, Caudata. Abhandlungen und Berichte für Naturkunde aus dem Museum für Natur- und Heimkunde 4: 231–310.

Wuttke M, Přikryl T, Ratnikov VY, Dvořák Z, Roček Z (2012) Generic diversity and distributional dynamics of the Palaeobatrachidae (Amphibia: Anura). Palaeobiodiversity and Palaeoenvironments 92: 367–395. https://doi.org/10.1007/s12549-012-0071-y

Supplementary material 1

Appendix S1

Authors: Davit Vasilyan, Andrej Čerňanský, Zbigniew Szyndlar, Thomas Mörs

Data type: nexus file of the phylogenetic analysis

Explanation note: Updated phylogenetic matrices in TNT. file format used for the phylogenetic analyses in this study.

Link: https://doi.org/10.3897/fr.25.83781.suppl1

Supplementary material 2

Appendix S2

Authors: Davit Vasilyan, Andrej Čerňanský, Zbigniew Szyndlar, Thomas Mörs

Data type: list of characters

Explanation note: List of characters used for analysis.

Link: https://doi.org/10.3897/fr.25.83781.suppl2